NASA CR-145064 54

THE EFFECT OF ADHESIVE LAYER ON CRACK PROPAGATION IN LAMINATES

by

M. Rusen Gecit

and

F. Erdogan

(NASA-CR-145064) THE EFFECT OF ADHESIVE LAYER ON CRACK PROPAGATION IN LAMINATES (Lehigh Univ.) 135 p HC $6.00 CSCL 13M

N76-30299

Unclas
G3/24 50404

March 1976

Department of Mechanical Engineering
and Mechanics
Lehigh University
Bethlehem, Pennsylvania 18015

National Aeronautics and Space Administration
Grant NGR-39-007-011

TABLE OF CONTENTS

LIST OF FIGURES

NOMENCLATURE

a, b	Half lengths of cracks in laminates and buffer strips
E	Young's modulus of elasticity
G_i	Crack surface displacement derivatives
h_1, h_2, h_3	Half widths of laminates, buffer strips and adhesive layers
k_a, k_b	Stress intensity factors
$p_n^{(a,b)}(x)$	Jacobi polynomials
p_1, p_2	Crack surface tractions
r, s	Fourier transform variables
u_i, v_i	Displacement components in x- and y- directions
x_i, y, z	Rectangular Cartesian coordinates
α, β, γ	Power of singularity at the crack tip
$\varepsilon_{ij}, \gamma_{ij}$	Components of strain tensor
κ	$3-4\nu$ for plane strain, $(3-\nu)/(1+\nu)$ for generalized plane stress
λ, λ_i	Ratios of elastic material parameters
μ	Shear modulus of elasticity
ν	Poisson's ratio
∇^2	Laplacian operator
σ_{ij}, τ_{ij}	Components of stress tensor
ϕ_i	Bounded multiplicative part of G_i
θ_i	Normalized ϕ_i
$(\tilde{\ })$	Fourier cosine transform
$(\tilde{\ })$	Fourier sine transform

ABSTRACT

The effect of the adhesive layer on crack propagation in composite materials is investigated. The composite medium consists of parallel load carrying laminates and buffer strips arranged periodically and bonded with thin adhesive layers. The system is assumed to approximate boron-epoxy composites. The strips, which are assumed to be isotropic and linearly elastic, contain symmetric cracks of arbitrary lengths located normal to the interfaces. Two problems are solved for both plane strain and plane stress cases. In the first problem, thin adhesive layers are approximated by uncoupled tension and shear springs distributed along the interfaces of the strips for which only the case of internal cracks can be treated rigorously. The second problem is introduced in order to study the case of broken laminates and tc detect the true singular behavior in the presence of the adhesive layer. In this case the adhesive is treated as an isotropic, linearly elastic continuum. General expressions for field quantities are obtained in terms of infinite Fourier integrals. These expressions, with relevant boundary and continuity conditions, give a system of singular integral equations in terms of the crack surface displacement derivatives. By using appropriate quadrature formulas, the integral equations reduce to a system of linear algebraic equations which is solved numerically.

Then, stress intensity factors and some significant stress components are calculated. The results are compared to those obtained by neglecting the adhesive layer (perfect bonding assumption). Results are presented in graphical form.

I. INTRODUCTION

Fracture mechanics is the study of the strength of a structural member that contains a crack. A normally ductile member may behave in a brittle manner if it contains cracks or other flaws which are sufficiently large. Adhesive-bonded composites tend to have flaws due to the complexity of shape, chemical dissimilarities, and assembly procedures. These flaws, under load, may develop into cracks with a resulting brittle failure. In applying fracture mechanics, it is assumed that all real structures have initial flaws or cracks, and that failure is caused by the propagation of the largest of these. The techniques of fracture mechanics can measure the intrinsic toughness of the material, which determines the load-carrying capacity of the structure in the presence of flaws. Therefore, if the size of the largest flaw in a particular structure is known, minimum toughness standards can be established for the materials in the structure. One has to adopt a proper fracture criterion and decide on the type of "load factor" to be evaluated. Usually the fracture criterion consists of a simple comparison between a calculated load factor and a material constant which is determined from certain standard experiments.

In most fracture analyses, two basic (essentially equivalent) approaches have been used with variations. With one

approach, due originally to Griffith (1920), the energy required to propagate a crack of a given size is considered. A crack will propagate if the rate of release of the stored energy per unit growth of the crack exceeds the rate of change of the surface energy required by the new surfaces. According to Irwin [1], the stress field in the vicinity of a crack tip can be adequately defined for studies of crack extension by a single parameter, proportional to the stress intensity factor. Since this parameter is a function of the applied load and crack size (it increases with load), when the intensity of the local tensile stresses at the crack tip attains a critical value, a previously stationary or slow-moving crack propagates rapidly. This critical value defines the "fracture toughness" and it is a constant for a particular material, since cracking always occurs at a given value of local stress intensity regardless of the structure in which the material has been used. Fracture toughness has the same relationship to brittle design that yield strength has to ductile design. Variations of these theories also have been useful. When a significant degree of plasticity takes place in the structural member, the usefulness of the elastic stress intensity factor as a correlating parameter becomes questionable. For cases where large-scale yielding can be expected, there are other correlating parameters that have been suggested in recent

years such as the J-integral, crack opening displacement, plastic stress and strain intensity factors, etc.

In the fatigue of bulky structures with no high stress concentrations, the major portion of the fatigue life is elapsed before the formation of macrocracks. The remaining portion of the fatigue life is relatively very short. On the other hand, in composite structures the formation of a dominant macrocrack may take place relatively early in the fatigue life. Hence in such cases the propagation phase, i.e., the number of load cycles necessary for the fatigue crack to reach a critical length at which the structure may fail statically, represents the major portion of the total fatigue life. Therefore in composite structures propagation and arrest of fatigue cracks is a major subject. Since the stress intensity factor is the simplest and the most appropriate single variable used in studying the fatigue crack propagation, its evaluation attracts considerable attention.

Because of the ever-increasing use of modern composite materials in a wide variety of structural applications, the mechanics of multi-phased materials has attracted considerable attention, particularly within the last ten or fifteen years. A great amount of work in this area has been concerned with the influence of the localized imperfections on the overall response of the medium regarding its failure.

The primary interest is mostly in the initiation and propagation of fracture in the composite material. The fracture process may start as the initiation of a fatigue crack at a local imperfection in the composite material. This crack then propagates with the cyclic effect of applied loads resulting in structural failure at stress levels considered moderate in relation to the theoretical strength of the material. There are two types of failure: (1) due to a controlled rate of cracking, arising from a steady rate of stressing; (2) due to catastrophically fast crack growth. The latter one needs more attention since the growth cannot be controlled easily. The main reason for the use of relatively low stiffness and high toughness buffer strips parallel to main load-carrying laminates in designing with high strength composite materials, is to improve the fatigue crack propagation and arrest characteristics of the structure.

The use of very strong epoxy type adhesives has been very common in joints of flight and space vehicle structures in which lightweight and high fatigue strength are dominant requirements. Epoxy based adhesives are also being used increasingly in stiffening, joining, and repairing precast prestressed concrete and other structures.

The adhesive layers, which serve as the bonding agent in composites, have not been treated adequately in

literature (see [2]). In the past some of the problems, particularly the problems relating to the traction-free boundaries, have presented considerable analytical difficulties. There are some finite element solutions which are good to the extent that they are reliable. However, these solutions miss the correct singular behavior near the corners and hence, from the viewpoint of fracture studies, they are of limited value. In recent years, with the introduction of the concept of generalized Cauchy kernel and the development of the related numerical techniques (see [3], [4]) it seems that some of these problems can now be treated in an analytically correct manner. For example, the problem of a composite isotropic plate which consists of parallel load-carrying laminates and buffer strips has been solved by Erdogan and Bakioglu [5]. In this study the effect of the adhesive layers has not been taken into account. Eisenmann and Kaminski [6] had considered this problem before. They concluded that crack arrest could be achieved through the use of buffer strips in the primary load-carrying laminates. However, their analytical work in evaluating the quantities which are useful in design considerations is not complete. The same problem has recently been considered by Delale and Erdogan [7] for orthotropic materials again neglecting the adhesive layers. Erdogan and Civelek [8] have treated the thin adhesive layer as a shear spring in the contact problem for a thin

elastic reinforcement bonded to an elastic plate. In the stress analysis of a metal base plate stiffened by a fiber-reinforced composite layer Erdogan and Arin [9] assumed that the two materials are bonded through an adhesive which is treated as a two-dimensional shear spring. The problem of an elastic plate bonded to a rigid horizontal substrate through an adhesive layer has been considered by Williams [10]. In this work, the adhesive layer has been assumed to react as a Winkler elastic foundation. It should be noted that the essential assumption introduced by Winkler allows for vertical motion and dilatation stress only. In one of the most recent works, Updike [11] has investigated the effect of adhesive layer elasticity on debonding of a blister test specimen. The adhesive layer has been treated as a distributed spring or elastic foundation which transmits normal and shear stresses between plate and support.

The objective of this work is to investigate the effect of adhesive layer on crack propagation in composite materials. A composite medium, which is generated by parallel main load-carrying laminates and buffer strips bonded through thin adhesive layers, is considered. Materials of main laminates and buffer strips are assumed to be isotropic and linearly elastic. Main laminates and buffer strips are arranged periodically and they are assumed to contain symmetric fatigue cracks of arbitrary lengths and

traction-free surfaces normal to their longitudinal direction. The composite medium is loaded in y-direction considerably far from crack region (see Figure 1). The solution to this problem can be obtained by superposition of solutions for the following two problems: (1) A strip having no crack loaded in y-direction, and (2) a strip having a crack whose surface is subjected to the negative of the stress distribution obtained at the same location in the first problem resulting from the applied loads. Solution of the first problem is relatively simple and straightforward hence one pays more attention to the second problem (see Figure 2). Therefore we solve the perturbation problem in which crack surfaces are subjected to prescribed tractions.

Thin adhesive layers are approximated by distributed uncoupled tension and shear springs. As it can be seen in the relevant references mentioned above, short of considering the adhesive as an elastic continuum, this is the most sophisticated model for adhesives in literature. A formulation is given for both plane strain and plane stress cases. General expressions for displacement and stress components are obtained by solving field equations using Fourier transform technique. Applying boundary conditions and the continuity conditions at the interfaces a system of singular integral equations in terms of crack surface

displacement derivatives is derived. By using appropriate quadrature formulas, these integral equations are converted to a system of linear algebraic equations which is solved numerically. Stress intensity factors and stress components for imbedded cracks are computed and results are given in Figures 3-16. The results are compared to those obtained without taking thickness of the adhesive layer into account. Then the case of broken laminates is considered. It is observed that the spring model approximation is not suitable under these circumstances when the crack touches interface. Therefore, in order to be able to examine the singular behavior of the cleavage stress, we introduced the problem described in Chapter III. In this problem, the adhesive is treated as an isotropic and linearly elastic medium. All laminates are of the same material and thickness but the cracks are of different lengths (see Figure 17). The problem is solved for imbedded cracks in order to determine limitations for the spring model approximation in the first problem. Comparison of two solutions can be seen in Figures 18-23. The case of broken laminates can now satisfactorily be solved. The power of singularity at the crack tip is determined from the characteristic equation obtained by following Muskhelishvili [12]. The integral equation is replaced again by a system of linear algebraic equations and this system is solved to calculate the stress intensity

factor and stresses. These results are given in Figures 24-37. Discussion of numerical results and conclusions can be found in Sections 2.5, 3.6. and Chapter IV.

II. SPRING MODEL PROBLEM

2.1 Formulation of the Problem

Consider a medium consisting of infinitely many number of linearly elastic and isotropic strips bonded together. These strips constitute periodically arranged load carrying laminates and buffer strips which are of different thicknesses and material properties. There are fatigue cracks in laminates and buffer strips normal to the interfaces. Main laminates and buffer strips are bonded through thin layers of adhesive. Loads are applied away from the crack region and in a direction parallel to the strips (see Figure 1). Solution for a strip having a crack of traction-free surface and loaded sufficiently far from the crack region can be obtained by superposing the solutions of (i) a loaded and uncracked strip, and (ii) a strip having a crack whose surface is subjected to the negative of the stress distribution acting on the image of the crack in the uncracked strip due to remotely applied loads. Therefore in solving the abovementioned elastostatic plane problem, one should first solve the problem of a strip having a crack whose surface is subjected to a prescribed traction. In this work we will consider the singular part of the problem in which the self-equilibrating crack surface tractions are the only external loads (see Figure 2).

First, we will establish the forms of the field quantities for a strip having a crack. Forms of the exp essions for the field quantities for a strip having a crack and which is loaded sufficiently far from the crack region can be obtained by superposing the general expressions of these quantities for: (1) an uncracked strip, and;(2) an infinitely large medium having a crack.

The basic equations for a linearly elastic, isotropic medium in plane problems can be written as (see [13]):

Strain-displacement relations:

$$\varepsilon_{xx} = \frac{\partial u}{\partial x} ,$$

$$\varepsilon_{yy} = \frac{\partial v}{\partial y} , \qquad (2.1a\text{-}c)$$

$$\gamma_{xy} = \frac{\partial u}{\partial y} + \frac{\partial v}{\partial x} ,$$

where ε_{xx}, ε_{yy}, γ_{xy} are components of the strain tensor, u, v are displacements in x- and y-directions in a Cartesian coordinate system.

Stress-displacement relations:

$$\frac{1}{2\mu}\sigma_{xx} = \frac{\kappa+1}{2(\kappa-1)} \frac{\partial u}{\partial x} + \frac{3-\kappa}{2(\kappa-1)} \frac{\partial v}{\partial y} ,$$

$$\frac{1}{2\mu}\sigma_{yy} = \frac{3-\kappa}{2(\kappa-1)} \frac{\partial u}{\partial x} + \frac{\kappa+1}{2(\kappa-1)} \frac{\partial v}{\partial y} \qquad (2.2a\text{-}c)$$

$$\frac{1}{2\mu}\tau_{xy} = \frac{1}{2} \left(\frac{\partial u}{\partial y} + \frac{\partial v}{\partial x}\right) ,$$

where σ_{xx}, σ_{yy}, τ_{xy} are components of the stress tensor, μ is the shear modulus, $\kappa=3-4\nu$ for plane strain case, and $\kappa=(3-\nu)/(1+\nu)$ for generalized plane stress case, ν being the Poisson's ratio.

Equilibrium equations, in the absence of body forces:

$$\nabla^2 u + \frac{2}{\kappa-1}\frac{\partial}{\partial x}\left(\frac{\partial u}{\partial x}+\frac{\partial v}{\partial y}\right) = 0 \,, \qquad (2.3a,b)$$

$$\frac{2}{\kappa-1}\frac{\partial}{\partial y}\left(\frac{\partial u}{\partial x}+\frac{\partial v}{\partial y}\right) + \nabla^2 v = 0 \,,$$

where $\nabla^2 = \frac{\partial^2}{\partial x^2} + \frac{\partial^2}{\partial y^2}$.

2.1.1 *Strip Having no Crack*

Taking the Fourier cosine transform of Eq. (2.3a) and sine transform of Eq. (2.3b) in y-direction, and combining the resulting equations, we obtain:

$$\frac{d^4\tilde{v}}{dx^4} - 2s^2\frac{d^2\tilde{v}}{dx^2} + s^4\tilde{v} = 0 \,, \qquad (2.4)$$

where $(\tilde{})$ stands for the sine transform and s is the transform variable. Note that the strip is symmetric about both x- and y-axes. The solution of Eq. (2.4) is:

$$\tilde{v} = [f(s) + \tfrac{\kappa+1}{2} g(s)]s^{-1}\cosh(sx) + g(s)x\sinh(sx) \,, \qquad (2.5a)$$

where f(s) and g(s) are unknown functions. Similarly,

$$\tilde{u} = -[f(s) - \tfrac{\kappa-1}{2} g(s)]s^{-1}\sinh(sx) - g(s)x\cosh(sx) \,, \qquad (2.5b)$$

where ($\tilde{}$) implies the cosine transform. Taking the inverse transform of Eqs. (2.5), displacement components are found to be

$$u(x,y) = -\frac{2}{\pi}\int_0^\infty \{[f(s)-\frac{\kappa-1}{2}g(s)]s^{-1}\sinh(sx) + g(s)x\cosh(sx)\}\cos(sy)ds\,,$$

$$v(x,y) = \frac{2}{\pi}\int_0^\infty \{[f(s)+\frac{\kappa+1}{2}g(s)]s^{-1}\cosh(sx) + g(s)x\sinh(sx)\}\sin(sy)ds\,. \qquad (2.6a,b)$$

Substituting Eqs. (2.6) into Eqs. (2.2) one obtains the following expressions for the stress components:

$$\frac{1}{2\mu}\sigma_{xx}(x,y) = -\frac{2}{\pi}\int_0^\infty [f(s)\cosh(sx)+ g(s)sx\sinh(sx)]\cos(sy)ds\,,$$

$$\frac{1}{2\mu}\sigma_{yy}(x,y) = \frac{2}{\pi}\int_0^\infty \{[f(s)+2g(s)]\cosh(sx) + g(s)sx\sinh(sx)\}\cos(sy)ds\,, \qquad (2.7a\text{-}c)$$

$$\frac{1}{2\mu}\tau_{xy}(x,y) = \frac{2}{\pi}\int_0^\infty \{[f(s)+g(s)]\sinh(sx)+g(s)sx\cosh(sx)\}\sin(sy)ds\,.$$

2.1.2 *Elastic Solid Having a Crack*

Taking now the Fourier sine transform of Eq. (2.3a) and cosine transform of Eq. (2.3b) in x-direction and combining again the resulting equations, one obtains

$$\frac{d^4\tilde{u}}{dy^4} - 2r^2\frac{d^2\tilde{u}}{dy^2} + r^4\tilde{u} = 0 \ , \qquad (2.8)$$

in which r is the transform variable. Note again that the medium is symmetric about both x- and y-axes. Solution to Eq. (2.8) vanishing when $y\to\infty$ becomes then

$$\tilde{u} = -\, m(r)r^{-1}\left(\frac{\kappa-1}{2} - ry\right)e^{-ry} \ , \qquad (2.9a)$$

where m(r) is an unknown function. Similarly,

$$\tilde{v} = m(r)r^{-1}\left(\frac{\kappa+1}{2} + ry\right)e^{-ry} \ . \qquad (2.9b)$$

Taking the inverse transforms of Eqs. (2.9), we get

$$u(x,y) = -\frac{2}{\pi}\int_0^\infty m(r)r^{-1}\left(\frac{\kappa-1}{2} - ry\right)e^{-ry}\sin(rx)dr \ , \qquad (2.10a,b)$$

$$v(x,y) = \frac{2}{\pi}\int_0^\infty m(r)r^{-1}\left(\frac{\kappa+1}{2} + ry\right)e^{-ry}\cos(rx)dr \ .$$

Substituting Eqs. (2.10) into (2.2) one obtains the stress components as follows:

$$\frac{1}{2\mu}\sigma_{xx}(x,y) = -\frac{2}{\pi}\int_0^\infty m(r)(1-ry)e^{-ry}\cos(rx)dr \ ,$$

$$\frac{1}{2\mu}\sigma_{yy}(x,y) = -\frac{2}{\pi}\int_0^\infty m(r)(1+ry)e^{-ry}\cos(rx)dr \ , \qquad (2.11a\text{-}c)$$

$$\frac{1}{2\mu}\tau_{xy}(x,y) = -\frac{2}{\pi}\int_0^\infty m(r)rye^{-ry}\sin(rx)dr \ .$$

2.1.3 *Superposition*

Now consider a strip which has a crack on which there

are prescribed tractions as the only external loads. General forms of displacement and stress components are established by superposing those for an uncracked strip, and a cracked space as mentioned before. Hence we obtain:

$$u_i(x_i,y) = -\frac{2}{\pi}\int_0^\infty \{s^{-1}[f_i(s) - \frac{\kappa_i-1}{2} g_i(s)]\sinh(x_i s) + x_i g_i(s)\cosh(x_i s)\}\cos(ys)ds$$

$$- \frac{2}{\pi}\int_0^\infty r^{-1} m_i(r)(\frac{\kappa_i-1}{2} - ry)e^{-ry}\sin(x_i r)dr \,, \qquad (2.12a,b)$$

$$v_i(x_i,y) = \frac{2}{\pi}\int_0^\infty \{s^{-1}[f_i(s) + \frac{\kappa_i+1}{2} g_i(s)]\cosh(x_i s) + x_i g_i(s)\sinh(x_i s)\}\sin(ys)ds$$

$$+ \frac{2}{\pi}\int_0^\infty r^{-1} m_i(r)(\frac{\kappa_i+1}{2} + ry)e^{-ry}\cos(x_i r)dr \,,$$

as the general expressions for displacement components for the i-th strip where i=1 for the main load carrying laminates and i=2 for buffer strips. Similarly, general expressions for the stresses become:

$$\frac{1}{2\mu_i}\sigma_{ixx}(x_i,y) = -\frac{2}{\pi}\int_0^\infty [f_i(s)\cosh(x_i s)+sx_i g_i(s)\sinh(x_i s)]\cos(ys)ds$$

$$- \frac{2}{\pi}\int_0^\infty m_i(r)(1-ry)e^{-ry}\cos(x_i r)dr \,,$$

$$\frac{1}{2\mu_i}\sigma_{iyy}(x_i,y) = \frac{2}{\pi}\int_0^\infty \{[f_i(s)+2g_i(s)]\cosh(x_i s) + sx_i g_i(s)\sinh(x_i s)\}\cos(ys)ds - \frac{2}{\pi}\int_0^\infty m_i(r)(1+ry)e^{-ry}\cos(x_i r)dr \,, \qquad (2.13a\text{-}c)$$

$$\frac{1}{2\mu_i}\tau_{ixy}(x_i,y) = \frac{2}{\pi}\int_0^\infty \{[f_i(s)+g_i(s)]\sinh(x_i s) + sx_i g_i(s)\cosh(x_i s)\}\sin(ys)ds - \frac{2}{\pi}\int_0^\infty m_i(r)rye^{-ry}\sin(x_i r)dr \,.$$

The unknown functions $f_i(s)$, $g_i(s)$ and $m_i(r)$, $(i=1,2)$ can be determined by using appropriate boundary and continuity conditions.

2.1.4 *Continuity Conditions*

Consider the elastostatic plane problem shown in Figure 2. Load carrying laminates (①) having thickness of $2h_1$ are bonded to buffer strips (②) of thickness $2h_2$ by means of thin adhesive layers (③) of thickness $2h_3$. Main laminates and buffer strips contain symmetrical cracks of lengths 2a and 2b respectively located on the line y=0, normal to y-axis. Thin adhesive layers are approximated by distributed tension and shear springs. That is, the x

component of normal stresses and the x-y component of shear stresses in the adhesive layer are assumed to be constant through the thickness $2h_3$. Then the continuity conditions may be written as:

$$\sigma_{1xx}(h_1,y) = \sigma_{2xx}(-h_2,y) \quad , \quad 0\leq y<\infty$$
$$\tau_{1xy}(h_1,y) = \tau_{2xy}(-h_2,y) \quad , \quad 0\leq y<\infty \qquad (2.14a,b)$$

$$u_1(h_1,y) - u_2(-h_2,y) = -\frac{h_o}{E_o}\sigma_{1xx}(h_1,y) \quad , \quad 0\leq y<\infty$$
$$v_1(h_1,y) - v_2(-h_2,y) = -\frac{h_o}{\mu_o}\tau_{1xy}(h_1,y) \quad , \quad 0\leq y<\infty \qquad (2.15a,b)$$

where $h_o=2h_3$, $\mu_o=\mu_3$, $E_o=E_3/(1-\nu_3^2)$ for generalized plane stress case [$\varepsilon_{3yy}=0$, $(\sigma_{3zz})_{av.}=0$] and $E_o=E_3(1-\nu_3)/(1+\nu_3)(1-2\nu_3)$ for plane strain case ($\varepsilon_{3yy}=0$, $\varepsilon_{3zz}=0$) where E is the Young's modulus and the subscript $(_3)$ stands for the adhesive layer.

Substituting Eqs. (2.12), (2.13) into Eqs. (2.14), (2.15), taking Fourier sine and cosine transforms of the resulting equations in y, and making use of the integral formulas given by (A.1) in Appendix A we obtain the following four equations:

$$(\alpha_1+2\lambda_4 sh_o\alpha_2)f_1(s)+\alpha_3 f_2(s)+(-\frac{\kappa_1-1}{2}\alpha_1+sh_1\alpha_2+2\lambda_4 s^2h_oh_1\alpha_1)g_1(s)$$
$$+(-\frac{\kappa_2-1}{2}\alpha_3+sh_2\alpha_4)g_2(s) = -F_{11}(s)-2\lambda_4 sh_oF_{13}(s)-F_{21}(s) \ ,$$

$$(\alpha_2+2\lambda_3 sh_0\alpha_1)f_1(s)-\alpha_4 f_2(s)+(\frac{\kappa_1+1}{2}\alpha_2+sh_1\alpha_1+2\lambda_3 s^2h_0h_1\alpha_2+2\lambda_3 sh_0\alpha_1)g_1(s)$$

$$-(\frac{\kappa_2+1}{2}\alpha_4+sh_2\alpha_3)g_2(s) = -F_{12}(s)+2\lambda_3 sh_0F_{14}(s)+F_{22}(s) ,$$

$$-\alpha_2 f_1(s)+\lambda_2\alpha_4 f_2(s)-sh_1\alpha_1 g_1(s)+\lambda_2 sh_2\alpha_3 g_2(s) = F_{13}(s)-\lambda_2 F_{23}(s) ,$$

(2.16a-d)

$$\alpha_1 f_1(s)+\lambda_2\alpha_3 f_2(s)+(\alpha_1+sh_1\alpha_2)g_1(s)$$

$$+\lambda_2(\alpha_3+sh_2\alpha_4)g_2(s) = F_{14}(s)+\lambda_2 F_{24}(s) ,$$

where

$$\alpha_1 = \sinh(sh_1) ,$$

$$\alpha_2 = \cosh(sh_1) ,$$

$$\alpha_3 = \sinh(sh_2) ,$$

$$\alpha_4 = \cosh(sh_2) ,$$

and

$$\lambda_1 = \mu_1/\mu_2 \quad , \quad \lambda_2 = \mu_2/\mu_1 \quad ,$$

$$\lambda_3 = \mu_1/\mu_0 \quad , \quad \lambda_4 = \mu_1/E_0 \quad .$$

The functions $F_{ij}(s)$, $(i=1,2;j=1-4)$ are defined by (B.1) in Appendix B. Solving Eqs. (2.16) simultaneously we obtain the unknown functions $f_i(s)$, $g_i(s)$, $(i=1,2)$ in terms of

infinite integrals of the other unknown functions $m_i(r)$, $(i=1,2)$ as follows:

$$f_i(s) = \sum_{j=1}^{4} [a_{ij}F_{1j}(s)+b_{ij}F_{2j}(s)]e^{-sh_i} ,$$

$$g_i(s) = \sum_{j=1}^{4} [c_{ij}F_{1j}(s)+d_{ij}F_{2j}(s)]e^{-sh_i} , \ (i=1,2) . \qquad (2.17a,b)$$

Known functions a_{ij}, b_{ij}, c_{ij}, d_{ij} $(i=1,2;j=1-4)$ are given in Appendix B by (B.2).

2.1.5 *Boundary Conditions*

The boundary conditions related to symmetry about x- and y-axes have already been used in deriving the general expressions for displacement and stress components. The remaining boundary conditions are used to determine the two unknown functions $m_i(r)$,$(i=1,2)$. These boundary conditions may be stated as follows:

$$v_1(x_1,0) = 0 \quad , \quad a<|x_1|<h_1$$

$$v_2(x_2,0) = 0 \quad , \quad b<|x_2|<h_2 \qquad (2.18a,b)$$

$$\sigma_{1yy}(x_1,0) = -p_1(x_1) \quad , \quad 0<|x_1|<a$$

$$\sigma_{2yy}(x_2,0) = -p_2(x_2) \quad , \quad 0<|x_2|<b \qquad (2.19a,b)$$

Eqs. (2.18) can be replaced by:

$$\frac{\partial}{\partial x_i} v_i(x_i,0) = 0 \ , \ a_i<|x_i|<h_i \ , \ (a_1=a,a_2=b) \qquad (2.20)$$

and

$$\int_{-a_i}^{a_i} \frac{\partial}{\partial x_i} v_i(x_i,0)dx_i = 0 \quad , \quad (i=1,2) \ . \tag{2.21}$$

The unknown functions $m_i(r)$, $(i=1,2)$ are determined from the mixed boundary conditions (2.19) and (2.20).

2.2 Derivation of Integral Equations

Substituting Eqs. (2.12b), (2.13b), and (2.17) into Eqs. (2.19) and (2.20) we could obtain two sets of dual integral equations for $m_i(r)$, $(i=1,2)$. However, we will follow a more direct procedure to solve the problem by defining new unknown functions, $G_i(x_i)$, as

$$G_i(x_i) = \frac{\partial}{\partial x_i} v_i(x_i,0) \ , \ (i=1,2) \ ; \ 0<|x_i|<h_i \ . \tag{2.22}$$

From Eqs. (2.12b) and (2.22),

$$G_i(x_i) = (-\frac{\kappa_i+1}{2}) \frac{2}{\pi} \int_0^\infty m_i(r)\sin(x_i r)dr \ . \tag{2.23}$$

Taking the Fourier sine transform of Eq. (2.23) in x_i and using Eq. (2.20),

$$m_i(r) = -\frac{2}{\kappa_i+1} \int_0^{a_i} G_i(t)\sin(rt)dt \tag{2.24}$$

is obtained.

Now using Eq. (2.24) and the integral formulas given by (A.2) in Appendix A, the functions defined by (B.1) may be expressed as:

$$F_{ij}(s) = \frac{1}{\kappa_i+1}\int_0^{a_j}[M_{ij}(s,t)-M_{ij}(s,-t)]G_j(t)dt \ , \qquad (2.25)$$

where

$$M_{ij}(s,t) = N_{ij}(s,t)e^{-s(h_j-t)} \ , \qquad (2.26)$$

and

$$N_{i1}(s,t) = -s(h_j-t) + \frac{1-\kappa_i}{2} \ ,$$

$$N_{i2}(s,t) = s(h_j-t) - \frac{1+\kappa_i}{2}$$

$$N_{i3}(s,t) = s(h_j-t) \ , \qquad (2.27a\text{-}d)$$

$$N_{i4}(s.t) = s(h_j-t) - 1 \ , \ (i=1,2) \ .$$

From Eq. (2.13b) we can write,

$$\frac{1}{2\mu_i}\sigma_{iyy}(x_i,0) = \frac{2}{\pi}\int_0^{\infty}\{[f_i(s)+2g_i(s)]\cosh(x_is)+sx_ig_i(s)\sinh(x_is)\}ds$$

$$- \lim_{y\to 0^+}[\frac{2}{\pi}\int_0^{\infty}m_i(r)/1+ry)e^{-ry}\cos(x_ir)dr] \ . \qquad (2.28)$$

With $m_i(r)$ as defined in Eq. (2.24), the second integral in Eq. (2.28) becomes;

$$\lim_{y\to 0^+}[\frac{2}{\pi}\int_0^{\infty}m_i(r)(1+ry)e^{-ry}\cos(x_ir)dr] = -\frac{2}{\pi(\kappa_i+1)}\int_0^{a_j}(\frac{1}{t-x_i}+\frac{1}{t+x_i})G_j(t)dt,$$

$$(i=1,2) \ . \qquad (2.29)$$

Note that,

$$G_i(x_i) = - G_i(-x_i) \ , \ (i=1,2) \ , \tag{2.30}$$

due to symmetry of $v_i(x_i,y)$ about y-axis.

Substituting Eqs. (2.17), (2.25), and (2.29) into Eq. (2.28) and using Eq. (2.30)

$$\begin{aligned}\sigma_{iyy}(x_i,0) = \sum_{j=1}^{4} \{ & \frac{4\mu_i}{\pi(\kappa_1+1)} \int_{-a}^{a} G_1(t)dt \int_0^{\infty} M_{1j}(s,t)[(a_{ij}+2c_{ij})\cosh(x_i s) \\ & + c_{ij} s x_i \sinh(x_i s)] \\ & e^{-sh_i} ds + \frac{4\mu_i}{\pi(\kappa_2+1)} \int_{-b}^{b} G_2(t)dt \int_0^{\infty} M_{2j}(s,t)[(b_{ij}+2d_{ij})\cosh(x_i s) \\ & + d_{ij} s x_i \sinh(x_i s)] e^{-sh_i} ds \} + \frac{4\mu_i}{\pi(\kappa_i+1)} \int_{a_i}^{a_i} \frac{G_i(t)}{t-x_i} dt, (i=1,2)\end{aligned} \tag{2.31}$$

is obtained. Now Eqs. (2.19) with Eq. (2.31) give,

$$\begin{aligned}\frac{1}{\pi} \int_{-a}^{a} \frac{G_1(t)}{t-x_1} dt + \int_{-a}^{a} k_{11}(x_1,t)G_1(t)dt + \frac{1+\kappa_1}{1+\kappa_2} \int_{-b}^{b} k_{12}(x_1,t)G_2(t)dt = \\ - \frac{1+\kappa_1}{4\mu_1} p_1(x_1) \ , \ -a<x_1<a \ ,\end{aligned} \tag{2.32a,b}$$

$$\begin{aligned}\frac{1}{\pi} \int_{-b}^{b} \frac{G_2(t)}{t-x_2} dt + \frac{1+\kappa_2}{1+\kappa_1} \int_{-a}^{a} k_{21}(x_2,t)G_1(t)dt + \int_{-b}^{b} k_{22}(x_2,t)G_2(t)dt = \\ - \frac{1+\kappa_2}{4\mu_2} p_2(x_2) \ , \ -b<x_2<b \ ,\end{aligned}$$

as the integral equations for the new unknown functions $G_i(t),(i=1,2)$ where the kernels $k_{ij}(x_i,t)$, $(i,j=1,2)$ are given by

$$k_{ij}(x_i,t) = \int_0^\infty K_{ij}(x_i,t,s)e^{-s(h_j-t)}ds \ . \qquad (2.33)$$

The expressions for the functions $K_{ij}(x_i,t,s)$ are given in Appendix B by (B.5).

The dominant parts of the integral equations (2.32) have a simple Cauchy type singularity for $a<h_1$ and $b<h_2$. However, it is worthwhile to take a closer look at the Fredholm type kernels $k_{ij}(x_i,t)$. The integrands of the kernels vanish as $s\to\infty$ and are bounded everywhere except for $s=0$. From (B.5) it can be seen that as $s\to 0$ the functions $L_{ij}(x_i,t,s) = K_{ij}(x_i,t,s)e^{-s(h_i-t)}$ behave as s^{-1}. That is, for small values of s,

$$L_{ij}(x_i,t,s) = \frac{\alpha_{ij}}{s} + \mathcal{O}(1) \ , \qquad (2.34)$$

where $i,j=1,2$, and α_{ij} are constants independent of t. We can write,

$$\int_0^\infty L_{ij}(x_i,t,s)ds = \int_0^\varepsilon L_{ij}(x_i,t,s)ds + \int_\varepsilon^\infty L_{ij}(x_i,t,s)ds \qquad (2.35)$$

for any $0\leq\varepsilon<\infty$. Choosing a very small ε, and hence replacing $L_{ij}(x_i,t,s)$ in $[0,\varepsilon]$ by its asymptotic expansion around $s=0$ [see Eq. (2.34)], we can rewrite Eq. (2.35) as

$$\int_0^\infty L_{ij}(x_i,t,s)ds = \int_0^\varepsilon [\frac{\alpha_{ij}}{s} + \mathcal{O}(1)]ds + \int_\varepsilon^\infty L_{ij}(x_i,t,s)ds \ . \qquad (2.36)$$

Now consider the last equation and, for example, the following integral appearing in Eq. (2.32a):

$$\int_{-a}^{a} k_{11}(x_1,t)G_1(t)dt = \int_{-a}^{a} G_1(t)dt\{ \int_0^{\varepsilon}[\frac{\alpha_{11}}{s}+\mathcal{O}(1)]ds + \int_{\varepsilon}^{\infty} K_{11}(x_1,t,s)e^{-s(h_1-t)}ds\}$$

$$= \int_{-a}^{a}[\int_0^{\varepsilon}\mathcal{O}(1)ds + \int_{\varepsilon}^{\infty} K_{11}(x_1,t,s)e^{-s(h_1-t)}ds]G_1(t)dt + \int_{-a}^{a} G_1(t)dt \cdot \int_0^{\varepsilon} \frac{\alpha_{11}}{s}\,ds. \qquad (2.37)$$

Using the single-valuedness condition, Eq. (2.21), we can see that the last integral in Eq. (2.37) vanishes. The remaining integrals are all bounded and they can be evaluated numerically. One can show similarly that the singularity around s=0 is removable for all kernels.

All the known special cases may be recovered from Eqs. (2.32) by letting a, b, h_1, h_2, and h_0 (or E_0, μ_0) go to proper limits. For example, for $h_0 \neq 0$ Eqs. (2.32) become identical to those found in [5]. Note that making h_0 very small has the same effect as making E_0, μ_0 very large due to spring model assumption. That is, a very small h_0 corresponds to a very stiff adhesive and as h_0 increases the adhesive becomes less stiff. Hence the case of direct adhesion of laminates to buffer strips [5] can be achieved

by letting $E_0, \mu_0 \to \infty$ too. An infinitely large h_0 will then imply that there is almost no bond between laminates and buffer strips. Therefore, letting $h_0 \to \infty$ (or $E_0, \mu_0 \to 0$) we recover the case of a center-notched strip having traction-free straight boundaries [14]. By letting $h_0 \to 0$ (or $E_0, \mu_0 \to \infty$) and making laminates and buffer strips be identical ($a=b$, $h_1=h_2$, $\mu_1=\mu_2$, $\nu_1=\nu_2$) we can obtain the solution for the case of colinear cracks in a homogeneous medium [15]. If we let $b=0$, $h_0=0$ (or $E_0, \mu_0 \to \infty$), and $h_2 \to \infty$, the integral equations (2.32) reduce to an integral equation in $G_1(t)$ for the problem of two half planes bonded through a center-notched strip [16].

2.3 Solution of Integral Equations

2.3.1 *No Crack in Buffer Strips* ($a<h_1, b=0$)

In this case the integral equations (2.32) reduce to:

$$\frac{1}{\pi}\int_{-a}^{a} \frac{G_1(t)}{t-x_1}\,dt + \int_{-a}^{a} k_{11}(x_1,t)G_1(t)dt = -\frac{1+\kappa_1}{4\mu_1}\,p_1(x_1)\ ,\quad -a<x_1<a \tag{2.38}$$

where $G_1(t)$ is unknown, and $p_1(x_1)$ and $k_{11}(x_1,t)$ are known functions which are Hölder-continuous in the closed interval $[-a,a]$. A function $f(x)$ is said to be Hölder-continuous in $[-a,a]$, if for any two points x_1, x_2 in $[-a,a]$ the following condition is satisfied:

$$|f(x_2) - f(x_1)| < A|x_2 - x_1|^{\mu} \ , \ -a \leq x \leq a \tag{2.39}$$

where A and μ are positive constants, and $0<\mu<1$.

$G_1(t)$ and $k_{11}(x_1,t)$ being Hölder-continuous, the second integral in Eq. (2.38) gives a bounded function of x_1. Hence, the singular behavior of $G_1(t)$ may be obtained by studying the dominant part of Eq. (2.38) only:

$$\frac{1}{\pi}\int_{-a}^{a} \frac{G_1(t)}{t-x_1}\,dt = F_1(x_1) \ , \ -a<x_1<a \tag{2.40}$$

where $F_1(x_1)$ contains all the bounded terms in Eq. (2.38).

Define the sectionally holomorphic function,

$$\psi_1(z) = \frac{1}{2\pi i}\int_{-a}^{a} \frac{G_1(t)}{t-z}\,dt \ . \tag{2.41}$$

Assume that the unknown function $G_1(t)$ has the following form:

$$G_1(t) = \phi_1(t)(t+a)^{\beta}(-t+a)^{\alpha} \sim \begin{cases} (t+a)^{\beta} \text{ near } t=-a \ , \\ (-t+a)^{\alpha} \text{ near } t=a \ , \end{cases} \tag{2.42}$$

where $\phi_1(t)$ is a bounded continuous function in the closed interval $[-a,a]$, and α,β are yet unknown constants restricted by $-1<\alpha,\beta<0$, which implies that the unknown function $G_1(t)$ has an integrable singularity at the end points $t=\pm a$.

Following [12] and using Plemelj formulas [17] given below

$$\psi_1^+(x_1) - \psi_1^-(x_1) = G_1(x_1) \ ,$$
$$\psi_1^+(x_1) + \psi_1^-(x_1) = \frac{1}{\pi i}\int_a^a \frac{G_1(t)}{t-x_1}\,dt \ , \qquad (2.43)$$

the value of $\psi_1(x_1)$ around $x_1 = -a$ and $x_1 = a$ can be found as

$$\psi_1(x_1) = \begin{cases} -(2a)^{\alpha}\frac{\cot\pi\beta}{2i}\,\phi_1(-a)(x_1+a)^{\beta}+\phi_1(-a)\psi_{11}(x_1)+\psi_{12}(x_1) \text{ around } x_1=-a, \\ (2a)^{\beta}\frac{\cot\pi\alpha}{2i}\,\phi_1(a)(-x_1+a)^{\alpha}+\phi_1(a)\psi_{13}(x_1)+\psi_{14}(x_1) \text{ around } x_1=a \ , \end{cases} \qquad (2.44)$$

where $\psi_{1i}(x_1)$, (i=1-4) are bounded in [-a,a]. From Eqs. (2.40), (2.41), and (2.44)

$$-(2a)^{\alpha}\cot\pi\beta\,\phi_1(-a)(x_1+a)^{\beta}+(2a)^{\beta}\cot\pi\alpha\,\phi_1(a)(-x_1+a)^{\alpha} = F_{11} \ , \ -a\le x_1\le a \ , \qquad (2.45)$$

where $F_{11}(x_1)$ contains all the bounded terms. Multiplying Eq. (2.45) first by $(-x_1+a)^{-\alpha}$ and letting $x_1\to a$, and then by $(x_1+a)^{-\beta}$ and letting $x_1\to -a$

$$\cot\pi\alpha = 0 \ , \qquad (2.46a,b)$$
$$\cot\pi\beta = 0 \ ,$$

are obtained for $-1<\alpha,\beta<0$ since $\phi_1(-a),\phi_1(a)\neq 0$. Eqs. (2.46) give

$$\alpha = \beta = -1/2 \ . \qquad (2.47)$$

The index of the problem which is defined by

$$\kappa = -(\alpha+\beta) , \tag{2.48}$$

is related to the physical nature of the problem. In this problem, $G_1(t)$ has integrable singularities at both ends and $\kappa = +1$. From Eqs. (2.42) and (2.47) we obtain

$$G_1(t) = \frac{\phi_1(t)}{\sqrt{a^2-t^2}} , \quad -a<t<a . \tag{2.49}$$

The solution of the problem will contain one arbitrary constant [12]. Theoretically this constant is determined by using the single-valuedness condition, Eq. (2.21). However, due to symmetry, Eq. (2.21) will be automatically satisfied if one considers a solution satisfying Eq. (2.30).

Now substituting Eq. (2.49) into Eq. (2.38) we obtain

$$\frac{1}{\pi}\int_{-a}^{a} \frac{\phi_1(t)}{\sqrt{a^2-t^2}} \left[\frac{1}{t-x_1} + \pi k_{11}(x_1,t)\right]dt = -\frac{1+\kappa_1}{4\mu_1} p_1(x_1) , \quad -a<x_1<a . \tag{2.50}$$

Define non-dimensional variables ω,τ by

$$x_1 = a\omega , \quad t = a\tau , \quad -a\leq x_1, t\leq a . \tag{2.51}$$

Then Eq. (2.50) takes the form

$$\frac{1}{\pi}\int_{-1}^{1} \frac{\theta_1(\tau)}{\sqrt{1-\tau^2}} \left[\frac{1}{\tau-\omega} + \pi a k_{11}(a\omega,a\tau)\right]d\tau = -1 , \quad -1<\omega<1 , \tag{2.52}$$

where

$$\theta_1(\tau) = \frac{4\mu_1}{1+\kappa_1} \cdot \frac{\phi_1(a\tau)}{a p_1} \tag{2.53}$$

and $p_1(x_1)$ is assumed to be $p_1(x_1) = p_1 = \text{constant}$. Actually, this is not an assumption. The self-equilibrating pressure acting on the crack surface is $p_1 = \text{constant}$ when the strips are subjected to uniformly distributed normal loads in y-direction. The integral in Eq. (2.52) can be evaluated by using the Gauss-Chebyshev integration formula given in [17]. Hence, Eq. (2.52) becomes

$$\sum_{i=1}^{N} \theta_1(\tau_i)\left[\frac{1}{\tau_i-\omega_j} + \pi a k_{11}(a\omega_j, a\tau_i)\right] = -N \quad , \qquad (2.54)$$

where

$$\tau_i = \cos[(2i-1)\pi/2N] \quad , \quad (i=1,\ldots,N) \quad ,$$

$$\omega_j = \cos(j\pi/N) \quad , \quad (j=1,\ldots,N-1) \quad , \qquad (2.55a,b)$$

are the roots of related Chebyshev polynomials. Eq. (2.54) provides (N-1) linear algebraic equations for (N) unknowns, $\theta_1(\tau_i)$, $(i=1,\ldots,N)$. The single-valuedness condition, Eq. (2.21), which can now be written as

$$\sum_{i=1}^{N} \theta_1(\tau_i) = 0 \qquad (2.56)$$

completes the system of (N) equations for (N) unknowns. However, one can take advantage of symmetry and can deal with less number of equations. Using Eq. (2.30) we can write Eq. (2.52) in the following form:

$$\frac{1}{\pi}\int_0^1 \frac{\theta_1(\tau)}{\sqrt{1-\tau^2}}\left[\frac{1}{\tau-\omega}+\frac{1}{\tau+\omega}+\pi\bar{k}_{11}(\omega,\tau)\right]d\tau = -1 \quad , \quad 0<\omega<1 \quad , \tag{2.57}$$

where

$$\bar{k}_{11}(\omega,\tau) = a[k_{11}(a\omega,a\tau) - k_{11}(a\omega,-a\tau)] \quad . \tag{2.58}$$

Now Eq. (2.57) can be replaced by

$$\sum_{i=1}^{n} \theta_1(\tau_i)\left[\frac{1}{\tau_i-\omega_j}+\frac{1}{\tau_i+\omega_j}+\pi\bar{k}_{11}(\omega_j,\tau_i)\right] = -N \quad , \quad (j=1,\ldots,n) \quad , \tag{2.59}$$

in which τ_i and ω_j are the same as in Eqs. (2.55) and $2n=N$. Eq. (2.59) constitutes a system of (n) linear algebraic equations in (n) unknowns, $\theta_1(\tau_i)$, $(i=1,\ldots,n)$. The single-valuedness condition, Eq. (2.21), is automatically satisfied by the solution obtained from Eq. (2.59).

After determining $\theta_1(\tau)$ at discrete colocation points, the field quantities can be computed numerically. In fracture problems, one is interested mostly in the so-called "stress intensity factor". The stress intensity factor may be defined in terms of cleavage stress, $\sigma_{1yy}(x_1,0)$, and may be expressed in terms of $\theta_1(\tau)$ as follows (see Appendix C):

$$k_a = \lim_{x_1 \to a} \sqrt{2(x_1-a)}\,\sigma_{1yy}(x_1,0) = -\sqrt{a}\,p_1\theta_1(1) \quad , \quad a<h_1 \quad . \tag{2.60}$$

2.3.2 *No Crack in Main Laminates* $(a=0, b<h_2)$

The integral equations (2.32) reduce to

$$\frac{1}{\pi}\int_{-b}^{b}\frac{G_2(t)}{t-x_2}\,dt + \int_{-b}^{b}k_{22}(x_2,t)G_2(t)dt = -\frac{1+\kappa_2}{4\mu_2}p_2(x_2)\ ,\ -b<x_2<b\ . \tag{2.61}$$

Following a procedure similar to the one followed in section 2.3.1, we determine the behavior of the unknown function $G_2(t)$ as

$$G_2(t) = \frac{\phi_2(t)}{\sqrt{b^2-t^2}}\ ,\quad -b<t<b \tag{2.62}$$

where $\phi_2(t)$ is a bounded continuous function in the closed interval $[-b,b]$.

Substituting Eq. (2.62) into Eq. (2.61) one obtains

$$\frac{1}{\pi}\int_{-b}^{b}\frac{\phi_2(t)}{\sqrt{b^2-t^2}}\left[\frac{1}{t-x_2}+\pi k_{22}(x_2,t)\right]dt = -\frac{1+\kappa_2}{4\mu_2}p_2(x_2)\ ,\ -b<x_2<b\ . \tag{2.63}$$

Defining non-dimensional variables η,τ by

$$x_2 = b\eta\ ,\quad t = b\tau\ ,\quad -b\leq x_2,t\leq b \tag{2.64}$$

Eq. (2.63) takes the following form

$$\frac{1}{\pi}\int_{-1}^{1}\frac{\theta_2(\tau)}{\sqrt{1-\tau^2}}\left[\frac{1}{\tau-\eta}+\pi b k_{22}(b\eta,b\tau)\right]d\tau = -1\ ,\quad -1<\eta<1\ , \tag{2.65}$$

where

$$\theta_2(\tau) = \frac{4\mu_2}{1+\kappa_2} \cdot \frac{\psi_2(b\tau)}{pb_2} \tag{2.66}$$

and $p_2(x_2) = p_2 = \text{constant}$. Using the Gauss-Chebyshev integration formula given in [17], Eq. (2.65) becomes

$$\sum_{i=1}^{N} \theta_2(\tau_i)\left[\frac{1}{\tau_i - \eta_j} + \pi b k_{22}(b\eta_j, b\tau_i)\right] = -N \ . \tag{2.67}$$

Note that

$$\eta_j = \omega_j \quad , \quad (j=1,\ldots,N-1) \ , \tag{2.68}$$

τ_i, ω_j being defined in Eqs. (2.55), and hence Eq. (2.67) can be written as

$$\sum_{i=1}^{N} \theta_2(\tau_i)\left[\frac{1}{\tau_i - \omega_j} + \pi b k_{22}(b\omega_j, b\tau_i)\right] = -N \ . \tag{2.69}$$

The single-valuedness condition, Eq. (2.21), in this case, becomes

$$\sum_{i=1}^{N} \theta_2(\tau_i) = 0 \ . \tag{2.70}$$

Eqs. (2.69) and (2.70) constitute again a system of (N) linear algebraic equations for (N) unknowns, $\theta_2(\tau_i)$, $(i=1,\ldots,N)$. Taking again the advantage of symmetry, namely using Eq. (2.30), Eqs. (2.69) and (2.70) can be replaced by

$$\sum_{i=1}^{n} \theta_2(\tau_i)\left[\frac{1}{\tau_i - \omega_j} + \frac{1}{\tau_i + \omega_j} + \pi \bar{k}_{22}(\omega_j, \tau_i)\right] = -N \ , \ (j=1,\ldots,n) \ , \tag{2.71}$$

where

$$\bar{k}_{22}(\omega_j,\tau_i) = b[k_{22}(b\omega_j,b\tau_i) - k_{22}(b\omega_j,-b\tau_i)] \quad , \tag{2.72}$$

and $2n = N$. Eq. (2.71) give (n) linear algebraic equations for (n) unknowns, $\theta_2(\tau_i)$, $(i=1,\ldots,n)$. θ_2 obtained from Eq. (2.71) will satisfy the single-valuedness condition, Eq. (2.21), automatically.

The stress intensity factor, in this case, may be expressed as (see again Appendix C):

$$k_b = \lim_{x_2\to b} \sqrt{2(x_2-b)}\ \sigma_{2yy}(x_2,0) = -\sqrt{b}\ p_2\theta_2(1) \ , \ b<h_2 \ . \tag{2.73}$$

2.3.3 *Cracks in Laminates and Buffer Strips* $(a<h_1, b<h_2)$

The singular behaviors of $G_1(t)$ and $G_2(t)$ at the end points $t = -a,a$ and $t = -b,b$ respectively will be the same as in the cases where there are cracks in one type of strips only. Now substituting Eqs. (2.49) and (2.62) into Eqs. (2.32) we obtain

$$\frac{1}{\pi}\int_{-a}^{a} \frac{\phi_1(t)}{\sqrt{a^2-t^2}}\left[\frac{1}{t-x_1}+\pi k_{11}(x_1,t)\right]dt + \frac{1+\kappa_1}{1+\kappa_2}\int_{-b}^{b} \frac{\phi_2(t)}{\sqrt{b^2-t^2}}\,k_{12}(x_1,t)dt$$

$$= -\frac{1+\kappa_1}{4\mu_1}\,p_1(x_1) \ , \ -a<x_1<a \ ,$$

$$\frac{1+\kappa_2}{1+\kappa_1}\int_{-a}^{a} \frac{\phi_1(t)}{\sqrt{a^2-t^2}}\,k_{21}(x_2,t)dt + \frac{1}{\pi}\int_{-b}^{b} \frac{\phi_2(t)}{\sqrt{b^2-t^2}}\left[\frac{1}{t-x_2}+\pi k_{22}(x_2,t)\right]dt \tag{2.74a,b}$$

$$= -\frac{1+\kappa_2}{4\mu_2}\,p_2(x_2) \ , \ -b<x_2<b$$

Using the non-dimensional variables defined by Eqs. (2.51) and (2.64), Eqs. (2.74) and (2.21) become

$$\frac{1}{\pi}\int_{-1}^{1}\frac{1}{\sqrt{1-\tau^2}}\{\theta_1(\tau)[\frac{1}{\tau-\omega}+\pi a k_{11}(a\omega,a\tau)]+\theta_2(\tau)\frac{p_2}{p_1}\lambda_1\pi b k_{12}(a\omega,b\tau)\}d\tau$$

$$= -1\ ,\ -1<\omega<1\ ,$$

(2.75a,b)

$$\frac{1}{\pi}\int_{-1}^{1}\frac{1}{\sqrt{1-\tau^2}}\{\theta_1(\tau)\frac{p_1}{p_2}\lambda_2\pi a k_{21}(b\eta,a\tau)+\theta_2(\tau)[\frac{1}{\tau-\eta}+\pi b k_{22}(b\eta,b\tau)]\}d\tau$$

$$= -1,\ -1<\eta<1\ ,$$

and

$$\int_{-1}^{1}\theta_k(\tau)d\tau = 0\ ,\ (k=1,2)\ . \tag{2.76}$$

Use of Gauss-Chebyshev integration formula for the evaluation of integrals in Eqs. (2.75) and (2.76) leads us to

$$\sum_{i=1}^{N}\{\theta_1(\tau_i)[\frac{1}{\tau_i-\omega_j}+\pi a k_{11}(a\omega_j,a\tau_i)]+\theta_2(\tau_i)\frac{p_2}{p_1}\lambda_1\pi b k_{12}(a\omega_j,b\tau_i)\} = -N\ ,$$

(2.77a,b)

$$\sum_{i=1}^{N}\{\theta_1(\tau_i)\frac{p_1}{p_2}\lambda_2\pi a k_{21}(b\omega_j,a\tau_i)+\theta_2(\tau_i)[\frac{1}{\tau_i-\omega_j}+\pi b k_{22}(b\omega_j,b\tau_i)]\} = -N\ ,$$

$$(j=1,\ldots,N-1)$$

and

$$\sum_{i=1}^{N}\theta_k(\tau_i) = 0\ ,\ (k=1,2)\ , \tag{2.78}$$

which constitute a system of (2N) linear algebraic equations

for (2N) unknowns, $\theta_k(\tau_i)$, (k=1,2;i=1,...,N). We can use Eq. (2.30) with Eqs. (2.75) to obtain

$$\sum_{i=1}^{n}\{\theta_1(\tau_i)[\frac{1}{\tau_i-\omega_j}+\frac{1}{\tau_i+\omega_j}+\pi\bar{k}_{11}(\omega_j,\tau_i)]+\theta_2(\tau_i)\frac{p_2}{p_1}\lambda_1\pi\bar{k}_{12}(\omega_j,\tau_i)\}=-N\ ,$$

$$\sum_{i=1}^{n}\{\theta_1(\tau_i)\frac{p_1}{p_2}\lambda_2\pi\bar{k}_{21}(\omega_j,\tau_i)+\theta_2(\tau_i)[\frac{1}{\tau_i-\omega_j}+\frac{1}{\tau_i+\omega_j}+\pi\bar{k}_{22}(\omega_j,\tau_i)]\}=-N\ , \quad (j=1,\ldots,n) \qquad (2.79a,b)$$

where

$$\bar{k}_{12}(\omega_j,\tau_i)=b[k_{12}(a\omega_j,b\tau_i)-k_{12}(a\omega_j,-b\tau_i)]\ ,$$

$$\bar{k}_{21}(\omega_j,\tau_i)=a[k_{21}(b\omega_j,a\tau_i)-k_{21}(b\omega_j,-a\tau_i)]\ . \qquad (2.80a,b)$$

Eqs. (2.79) give an (NxN) system.

Definitions of the stress intensity factors will be the same as those in Eqs. (2.60) and (2.73) since the singular behaviors of the functions $G_i(t)$, (i=1,2), at the end points are not affected by the cracks in the other strips for $a<h_1$ and $b<h_2$.

In these numerical solutions we cannot determine the values of the unknown functions θ_1,θ_2 at the end points directly from the system of linear equations, since we are not allowed to choose the end points as colocation points, as it can easily be seen in Eq. (2.55a). Nevertheless, using an appropriate summation formula [18], which is based

on the properties of Chebyshev polynomials, we can determine $\theta_1(1),\theta_2(1)$ in terms of the values of θ_1,θ_2 at collocation points. From [18], we can write

$$\theta_k(1) \cong \frac{1}{n} \sum_{i=1}^{n} \frac{\sin[\frac{2n-1}{4n}(2i-1)\pi]}{\sin[\frac{2i-1}{4n}\pi]} \theta_k(\tau_i) \ , \ (k=1,2) \ . \qquad (2.81)$$

One should keep in mind that the above approximate formula can be used for $\alpha=\beta=-1/2$ only.

2.4 Stresses at the Interfaces

We consider the stresses at the interfaces for the case in which there are cracks in main laminates ($a<h_1, b=0$) only. The other cases can be treated similarly. Since the shear stresses, τ_{ixy}, and the normal stress in x-direction, σ_{ixx}, are assumed to be the same for both strips at the interfaces, for the sake of simplicity we consider the stresses in the buffer strips when there are cracks in the main laminates.

Now, from Eqs. (2.13) we can write

$$\frac{1}{2\mu_2}\sigma_{2xx}(-h_2,y) = -\frac{2}{\pi}\int_0^\infty [f_2(s)\cosh(h_2s) + sh_2g_2(s)\sinh(h_2s)]\cos(ys)ds \ ,$$

$$\frac{1}{2\mu_2}\sigma_{2yy}(-h_2,y) = \frac{2}{\pi}\int_0^\infty \{[f_2(s)+2g_2(s)]\cosh(h_2s) + sh_2g_2(s)\sinh(h_2s)\}$$
$$\cos(ys)ds \ ,$$

$$\frac{1}{2\mu_2}\tau_{2xy}(-h_2,y) = -\frac{2}{\pi}\int_0^\infty \{[f_2(s)+g_2(s)]\sinh(h_2s)+sh_2g_2(s)\cosh(h_2s)\}$$

$$\sin(ys)ds\ , \qquad (2.82a\text{-}c)$$

since $m_2(r)$ is zero by definition, Eq. (2.24), for b=0. Using Eqs. (2.17) with Eq. (2.25)

$$f_2(s) = \sum_{j=1}^{4}\frac{a_{2j}}{1+\kappa_1}e^{-sh_2}\int_0^a [M_{1j}(s,t)-M_{1j}(s,-t)]G_1(t)dt\ ,$$

$$g_2(s) = \sum_{j=1}^{4}\frac{c_{2j}}{1+\kappa_1}e^{-sh_2}\int_0^a [M_{1j}(s,t)-M_{1j}(s,-t)]G_1(t)dt\ , \qquad (2.83a,b)$$

are obtained. Then substituting Eqs. (2.83) into Eqs. (2.82), the stress expressions become

$$\frac{1}{2\mu_2}\sigma_{2xx}(-h_2,y) = -\frac{2}{\pi(1+\kappa_1)}\int_0^a [h_{21}(y,t)-h_{21}(y,-t)]G_1(t)dt\ ,$$

$$\frac{1}{2\mu_2}\sigma_{2yy}(-h_2,y) = \frac{2}{\pi(1+\kappa_1)}\int_0^a [h_{22}(y,t)-h_{22}(y,-t)]G_1(t)dt\ ,$$

$$\frac{1}{2\mu_2}\tau_{2xy}(-h_2,y) = -\frac{2}{\pi(1+\kappa_1)}\int_0^a [h_{23}(y,t)-h_{23}(y,-t)]G_1(t)dt\ , \qquad (2.84a\text{-}c)$$

where

$$h_{2k}(y,t) = \int_0^\infty H_{2k}(y,t,s)e^{-s(h_1-t)}ds\ ,\ (k=1\text{-}3) \qquad (2.85)$$

and

$$H_{21}(y,t,s) = \sum_{j=1}^{4}N_{1j}(s,t)[a_{2j}\cosh(h_2s)+c_{2j}sh_2\sinh(h_2s)]e^{-sh_2}\cos(ys)\ ,$$

$$H_{22}(y,t,s) = \sum_{j=1}^{4} N_{1j}(s,t)[(a_{2j}+2c_{2j})\cosh(h_2 s)+c_{2j}sh_2\sinh(h_2 s)]e^{-sh_2} \cos(ys) ,$$

$$H_{23}(y,t,s) = \sum_{j=1}^{4} N_{1j}(s,t)[(a_{2j}+c_{2j})\sinh(h_2 s)+c_{2j}sh_2\cosh(h_2 s)]e^{-sh_2} \sin(ys) . \quad (2.86a\text{-}c)$$

Now using Eqs. (2.49) and (2.53) with the non-dimensional variables ω,τ defined by Eq. (2.51), and defining ρ by

$$y = h_1\rho , \quad (2.87)$$

we obtain

$$\sigma_{2xx}(-h_2,y)/p_1 = -\lambda_2 \frac{1}{\pi}\int_0^1 \frac{\theta_1(\tau)}{\sqrt{1-\tau^2}}\bar{h}_{21}(\rho,\tau)d\tau ,$$

$$\sigma_{2yy}(-h_2,y)/p_1 = \lambda_2 \frac{1}{\pi}\int_0^1 \frac{\theta_1(\tau)}{\sqrt{1-\tau^2}}\bar{h}_{22}(\rho,\tau)d\tau , \quad (2.88a\text{-}c)$$

$$\tau_{2xy}(-h_2,y)/p_1 = -\lambda_2 \frac{1}{\pi}\int_0^1 \frac{\theta_1(\tau)}{\sqrt{1-\tau^2}}\bar{h}_{23}(\rho,\tau)d\tau ,$$

where

$$\bar{h}_{2k}(\rho,\tau) = a[h_{2k}(h_1\rho,a\tau) - h_{2k}(h_1\rho,-a\tau)] , \quad (k=1\text{-}3) . \quad (2.89)$$

The Gauss-Chebyshev integration formula given in [17] again can be used to evaluate the integrals in Eqs. (2.88). Hence

$$\sigma_{2xx}(-h_2,y)/p_1 = -\frac{\lambda_2}{N}\sum_{i=1}^{n}\theta_1(\tau_i)\bar{h}_{21}(\rho,\tau_i) ,$$

$$\sigma_{2yy}(-h_2,y)/p_1 = \frac{\lambda_2}{N} \sum_{i=1}^{n} \theta_1(\tau_i)\bar{h}_{22}(\rho,\tau_i) \quad , \qquad (2.90a\text{-}c)$$

$$\tau_{2xy}(-h_2,y)/p_1 = -\frac{\lambda_2}{N} \sum_{i=1}^{n} \theta_1(\tau_i)\bar{h}_{23}(\rho,\tau_i) \quad .$$

2.5 Numerical Results

The analysis carried out is valid for both plane strain and generalized plane stress cases. The systems of equations (2.59), (2.71), and (2.79) are solved numerically for $\theta_k(\tau_i)$, $(k=1,2;i=1,\ldots,n)$. In computing the kernels, the infinite integrals are evaluated by using the approximate Laguerre quadrature formula [19] since the integrands have exponentially decaying behavior. Once $\theta_k(\tau_i)$ are determined, the stress intensity factors and the stresses at the interfaces can then be computed easily. Note that the stresses are computed for the perturbation problem whose configuration and loading conditions are shown in Figure 2. Assuming that there is no constraint in x-direction, and the composite medium shown in Figure 1 is loaded in y-direction sufficiently far from the crack region (i.e., the dimension of the medium in y-direction is large compared to that in x-direction), the crack surface tractions in Figure 2 satisfy the following conditions:

$$p_1/p_2 = E_1/E_2 \quad \text{for plane stress case,} \qquad (2.91a,b)$$

$$p_1/p_2 = E_1(1-\nu_2^2)/E_2(1-\nu_1^2) \quad \text{for plane strain case.}$$

Here E_1 and E_2 are the Young's moduli for the strips ① and ② respectively. The problem is solved for three combinations of materials:

Combination I:

$\mu_1 = 6.65\mu_2$, $\mu_3 = 0.167\mu_2$; $\nu_1 = \nu_3 = 0.35$, $\nu_2 = 0.45$.

$E_1 = 12.38 \times 10^{10} N/m^2$ $(17.955 \times 10^6 psi)$,

$E_2 = 2.0 \times 10^{10} N/m^2$ $(2.9 \times 10^6 psi)$,

$E_3 = 0.31 \times 10^{10} N/m^2$ $(0.45 \times 10^6 psi)$.

Combination II:

$\mu_2 = \mu_1$, $\mu_3 = 0.025\mu_1$; $\nu_1 = \nu_2 = \nu_3 = 0.35$.

$E_1 = E_2 = 12.38 \times 10^{10} N/m^2$ $(17.955 \times 10^6 psi)$,

$E_3 = 0.31 \times 10^{10} N/m^2$ $(0.45 \times 10^6 psi)$.

Combination III:

$\mu_1 = \mu_2$, $\mu_3 = 0.167\mu_2$; $\nu_1 = \nu_2 = 0.45$, $\nu_3 = 0.35$.

$E_1 = E_2 = 2.0 \times 10^{10} N/m^2$ $(2.9 \times 10^6 psi)$,

$E_3 = 0.31 \times 10^{10} N/m^2$ $(0.45 \times 10^6 psi)$.

Among these, Combination I is the most significant one which is assumed to approximate boron-epoxy composites

having buffer strips of the same material with different stiffness. In this combination, the first strip is the stiffest one and the adhesive layer is the softest one. Figures 3-16 show the results obtained for material Combination I. Figure 3 shows the variation of the normalized stress intensity factor, $K_1 = k_a/\sqrt{a}\ p_1$, with a/h_1 for $h_2 = h_1$(*), $b = 0$ (section 2.3.1), $h_3/h_1 = .00$, .05, and .10; for plane strain and generalized plane stress cases. It may be observed that: (a) K_1 increases with increasing h_3/h_1; (b) K_1 is larger in generalized plane stress case; (c) K_1 increases with increasing a/h_1. Figure 4 is the plot of $K_2 = k_b/\sqrt{b}\ p_2$ vs. b/h_2 for $h_1 = h_2$, $a = 0$ (section 2.3.2), $h_3/h_2 = .00$, .05, and .10; for plane strain and generalized plane stress cases again. One can conclude that: (a) K_2 increases as h_3/h_2 increases; (b) K_2 is larger again in generalized plane stress case; (c) The trend in variation of K_2 with b/h_2 depends on the ratio h_3/h_2. For small values of h_3/h_2 (up to ~.04) K_2 decreases with increasing b/h_2. For larger h_3/h_2 ratios K_2 increases with increasing b/h_2. It is well known that the stress intensity factor at the tip of a crack approaching the interface of two different materials increases if the crack is in the stiffer material and decreases if the crack is in the softer

(*) Problem is formulated in such a way that the ratio h_2/h_1 can vary. But the results are shown for $h_2/h_1 = 1$ to conform with the experimental programs carried out elsewhere.

material. When h_3/h_2 is small, it seems as if the crack in buffer strip approaches the main laminate, which is stiffer than buffer strip, when b/h_2 increases. But when h_3/h_2 is large, the adhesive layer, which is softer than buffer strip, seems to dominate. One should also keep in mind that increase in h_3/h_2 is equivalent to relative decrease in E_3, μ_3 due to spring model approximation. Figures 5-8 show the variation of K_1 and K_2 with a/h_1 and b/h_2 for $h_2 = h_1$, $h_3/h_1 = .00$, .05, and .10. Main laminates and buffer strips both contain cracks (section 2.3.3). We can observe and state similar conclusions as in Figures 3 and 4. In Figures 9 and 10, variation of K_1 with h_3/h_1 is shown for $h_2 = h_1$, $a/h_1 = 0.8$, $b/h_1 = 0.0$, 0.8, and $h_3/h_1 = 0 - 100$. As h_3/h_1 increases, K_1 also increases tending to the asymptotic value for $h_3 \to \infty$ which corresponds to the case of center-notched infinite strip having traction-free straight boundaries, since $h_3 \to \infty$ is equivalent to $E_3, \mu_3 \to 0$. Figures 11 and 12 show similarly the variation of K_2 with h_3/h_2 for $h_1 = h_2$, $a/h_2 = 0.0$, 0.8, $b/h_2 = 0.8$, and $h_3/h_2 = 0 - 100$. K_1 and K_2 become equal to each other when $h_3 \to \infty$ (or $E_3, \mu_3 \to 0$). Note that the solution (stress intensity factor) for a center-notched single strip is independent of the material. All the results obtained for $h_3 = 0$ are exactly the same as those in [5].

In Figures 13,14 distributions of the stress components σ_{2yy} and τ_{2xy} along $x_2 = -h_2$ boundary for generalized plane stress case with $h_2 = h_1$, $h_3 = 0.05h_1$, $b = 0$ are shown. As the crack propagates, the stresses at the interface increase. Note that $\sigma_{1xx}(h_1,y) = \sigma_{2xx}(-h_2,y)$, $\tau_{1xy}(h_1,y) = \tau_{2xy}(-h_2,y)$ and σ_{xx},σ_{yy} are symmetric whereas τ_{xy} is antisymmetric about the x-axis. Figures 15 and 16 show the variations of $\sigma_{2yy}(-h_2,0)$ and $\tau_{2xy}(-h_2,h_1)$ with h_3/h_1 again for generalized plane stress case in which $h_2 = h_1$, $b = 0$. Beginning at $h_3 = 0$, σ_{2yy} first increases (up to $h_3 \approx .012h_1$) and then decreases as h_3/h_1 increases, limiting value being zero for $h_3 \to \infty$, whereas τ_{2xy} decreases continuously, vanishing for $h_3 \to \infty$. This is expected since $h_3 \to \infty$ (or equivalently $E_3, \mu_3 \to 0$) relieves the constraints on the boundaries.

We attempted to solve the problem for $a = h_1$, $b = 0$. But some unavoidable troubles arose. For example, a singularity power of -1/2 is found from a characteristic equation which does not contain any material constants. It is now obvious that the spring model used to approximate the adhesive layers is not suitable for this case. The model is valid for cases where crack tip is away from the adhesive layer. So we introduced the problem described in the next chapter in order to be able to examine the effect of the adhesive on the solution of the problem when $a = h_1$. In this problem, the adhesive is treated as an elastic continuum.

III. CONTINUUM MODEL PROBLEM

3.1 Formulation of the Problem

Consider the following problem: Infinite number of strips of the same material and the same thickness of $2h_1$ are bonded through adhesive layers of thickness $2h_3$. The main laminates contain periodically arranged symmetric cracks of lengths 2a and 2b on the line $y=0$ perpendicular to y-direction (see Figure 17). The strips ① and ② are symmetric about x- and y-axes. Therefore the general expressions derived in Section 2.1.3 for displacement and stress components are still valid for the main laminates in this problem. But the adhesive layers are symmetric with respect to x-axis only. Therefore we have to derive displacement and stress expressions for the adhesive layer.

3.1.1 *Displacement and Stress Expressions for the Adhesive Layer*

Now let us consider Eq. (2.4). The adhesive layer is symmetric about x-axis only. The solution to Eq. (2.4) for a strip with no symmetry about y-axis becomes

$$\tilde{v}_3 = \frac{1}{s}\left[\frac{\kappa_3+1}{2} f_4(s) + g_4(s) + sx_3 g_3(s)\right] \sinh(sx_3) + \frac{1}{s}\left[f_3(s) + \frac{\kappa_3+1}{2} g_3(s) + sx_3 f_4(s)\right] \cosh(sx_3) , \tag{3.1a}$$

where $f_i(s), g_i(s), (i=3,4)$ are unknown functions. We can get

$$\tilde{u}_3 = -\frac{1}{s}\left[f_3(s) - \frac{\kappa_3-1}{2} g_3(s) + sx_3 f_4(s)\right] \sinh(sx_3)$$

$$-\frac{1}{s}\left[g_4(s) - \frac{\kappa_3-1}{2} f_4(s) + sx_3 g_3(s)\right] \cosh(sx_3) \ , \qquad (3.1b)$$

in a similar way. Taking the inverse transforms of Eqs. (3.1), the displacement components are found as,

$$u_3(x_3,y) = -\frac{2}{\pi}\int_0^\infty \frac{1}{s}\left\{\left[f_3(s) - \frac{\kappa_3-1}{2} g_3(s) + sx_3 f_4(s)\right] \sinh(sx_3)\right.$$

$$\left. + \left[g_4(s) - \frac{\kappa_3-1}{2} f_4(s) + sx_3 g_3(s)\right] \cosh(sx_3)\right\}\cos(sy)ds \ ,$$

$$v_3(x_3,y) = \frac{2}{\pi}\int_0^\infty \frac{1}{s}\left\{\left[\frac{\kappa_3+1}{2} f_4(s) + g_4(s) + sx_3 g_3(s)\right] \sinh(sx_3)\right. \qquad (3.2a,b)$$

$$\left. + \left[f_3(s) + \frac{\kappa_3+1}{2} g_3(s) + sx_3 f_4(s)\right] \cosh(sx_3)\right\}\sin(sy)ds \ .$$

Substituting Eqs. (3.2) into Eqs. (2.2) we obtain,

$$\frac{1}{2\mu_3}\sigma_{3xx}(x_3,y) = -\frac{2}{\pi}\int_0^\infty \left\{\left[f_3(s) + sx_3 f_4(s)\right] \cosh(sx_3)\right.$$

$$\left. + \left[g_4(s) + sx_3 g_3(s)\right] \sinh(sx_3)\right\}\cos(sy)ds \ ,$$

$$\frac{1}{2\mu_3}\sigma_{3yy}(x_3,y) = \frac{2}{\pi}\int_0^\infty \left\{\left[f_3(s) + 2g_3(s) + sx_3 f_4(s)\right] \cosh(sx_3)\right.$$

$$\left. + \left[g_4(s) + 2f_4(s) + sx_3 g_3(s)\right] \sinh(sx_3)\right\}\cos(sy)ds \ ,$$

$$\frac{1}{2\mu_3}\tau_{3xy}(x_3,y) = \frac{2}{\pi}\int_0^\infty \{[f_3(s) + g_3(s) + sx_3 f_4(s)]\sinh(sx_3) + [f_4(s) + g_4(s) + sx_3 g_3(s)]\cosh(sx_3)\}\sin(sy)ds \qquad (3.3a\text{-}c)$$

for a strip having no crack.

3.1.2 *Boundary and Continuity Conditions*

Boundary conditions on the line $y = 0$ for this problem are the same as those in Eqs. (2.18), (2.19). However, the continuity conditions do change since the adhesive layer is not modeled as distributed springs any more. Taking the adhesive layer as an elastic continuum we can write the following conditions of continuity:

$$\begin{aligned}
&\sigma_{1xx}(h_1,y) = \sigma_{3xx}(-h_3,y) \quad ,\\
&\tau_{1xy}(h_1,y) = \tau_{3xy}(-h_3,y) \quad ,\\
&u_1(h_1,y) = u_3(-h_3,y) \quad ,\\
&v_1(h_1,y) = v_3(-h_3,y) \quad ,\\
&\sigma_{2xx}(-h_1,y) = \sigma_{3xx}(h_3,y) \quad ,\\
&\tau_{2xy}(-h_1,y) = \tau_{3xy}(h_3,y) \quad ,\\
&u_2(-h_1,y) = u_3(h_3,y) \quad ,\\
&v_2(-h_1,y) = v_3(h_3,y) \quad , \quad 0 \le y < \infty \quad .
\end{aligned} \qquad (3.4a\text{-}h)$$

Substituting Eqs. (2.12), (2.13), (i=1,2), and Eqs. (3.2), (3.3) into Eqs. (3.4); then taking the Fourier sine and cosine transforms of the resulting equations in y; and using the integral formulas given by (A.1) in Appendix A we obtain the following eight equations:

$$\lambda\alpha_2 f_1(s)+\lambda sh_1\alpha_1 g_1(s)-\alpha_4 f_2(s)-sh_3\alpha_3 g_3(s)+sh_3\alpha_4 f_4(s)+\alpha_3 g_4(s) = -\lambda F_{13} ,$$

$$\lambda\alpha_1 f_1(s)+\lambda(\alpha_1+sh_1\alpha_2)g_1(s)+\alpha_3 f_3(s)+(\alpha_3+sh_3\alpha_4)g_3(s)-(\alpha_4+sh_3\alpha_3)f_4(s)$$
$$-\alpha_4 g_4(s) = \lambda F_{14} ,$$

$$\alpha_1 f_1(s)+[(1-\kappa_1)\alpha_1/2+sh_1\alpha_2]g_1(s)+\alpha_3 f_3(s)+[(1-\kappa_3)\alpha_3/2+sh_3\alpha_4]g_3(s)$$
$$-[sh_3\alpha_3+(1-\kappa_3)\alpha_4/2]f_4(s)-\alpha_4 g_4(s) = -F_{11} ,$$

$$\alpha_2 f_1(s)+[sh_1\alpha_1+(1+\alpha_1)\alpha_2/2]g_1(s)-\alpha_4 f_3(s)-[sh_3\alpha_3+(1+\kappa_3)\alpha_4/2]g_3(s)$$
$$+[(1+\kappa_3)\alpha_3/2+sh_3\alpha_4]f_4(s)+\alpha_3 g_4(s) = -F_{12} ,$$

$$\lambda\alpha_2 f_2(s)+\lambda sh_1\alpha_1 g_2(s)-\alpha_4 f_3(s)-sh_3\alpha_3 g_3(s)-sh_3\alpha_4 f_4(s)-\alpha_3 g_4(s) = -\lambda F_{23} ,$$

$$\lambda\alpha_1 f_2(s)+\lambda(\alpha_1+sh_1\alpha_2)g_2(s)+\alpha_3 f_3(s)+(\alpha_3+sh_3\alpha_4)g_3(s)+(sh_3\alpha_3+\alpha_4)f_4(s)$$
$$+\alpha_4 g_4(s) = \lambda F_{24} ,$$

$$\alpha_1 f_2(s)+[(1-\kappa_1)\alpha_1/2+sh_1\alpha_2]g_2(s)+\alpha_3 f_3(s)+[(1-\kappa_3)\alpha_3/2+sh_3\alpha_4]g_3(s)$$
$$+[sh_3\alpha_3+(1-\kappa_3)\alpha_4/2]f_4(s)+\alpha_4 g_4(s) = -F_{21} ,$$

$$\alpha_2 f_2(s)+[sh_1\alpha_1+(1+\kappa_1)\alpha_2/2]g_2(s)-\alpha_4 f_3(s)-[sh_3\alpha_3+(1+\kappa_3)\alpha_4/2]g_3(s)$$
$$-[(1+\kappa_3)\alpha_3/2+sh_3\alpha_4]f_4(s)-\alpha_3 g_4(s) = -F_{22} , \qquad (3.5a-h)$$

where

$$\alpha_1 = \sinh(sh_1) ,$$

$$\alpha_2 = \cosh(sh_1) ,$$

$$\alpha_3 = \sinh(sh_3) ,$$

$$\alpha_4 = \cosh(sh_3) ,$$

and $\lambda = \mu_1/\mu_3$. The functions $F_{ij}(s)$, (i=1,2;j=1-4) are defined in Appendix D. After solving Eqs. (3.5) simultaneously, the unknwon functions $f_i(s)$, $g_i(s)$, (i=1-4) are expressed in terms of infinite integrals of $m_i(r)$, (i=1,2) as follows:

$$f_i(s) = \sum_{j=1}^{4} [a_{ij}F_{1j}(s) + b_{ij}F_{2j}(s)]e^{-sh_k} ,$$

$$g_i(s) = \sum_{j=1}^{4} [c_{ij}F_{1j}(s) + d_{ij}F_{2j}(s)]e^{-sh_k} , \quad (i=1-4) , \qquad (3.6a,b)$$

where k = 1 for i = 1,2 and k = 3 for i = 3,4. a_{ij}, b_{ij}, c_{ij}, d_{ij}, (i,j=1-4) are given in Appendix D. The unknown functions $m_i(r)$, (i=1,2) can again be determined from the mixed boundary conditions (2.19) and (2.20).

3.2 Derivation of Integral Equations

Defining $G_i(x_i)$, (i=1,2) as in Eq. (2.22) we can similarly obtain

$$m_i(r) = -\frac{2}{\kappa_1+1}\int_0^{a_i} G_i(t)\sin(rt)dt \quad , \quad (i=1,2) \quad . \tag{3.7}$$

Following a precedure similar to that followed in section 2.2 and using the pertinent equations one can write

$$\sigma_{iyy}(x_i,0) = \frac{4\mu_1}{\kappa_1+1}\sum_{j=1}^{4}\{\frac{1}{\pi}\int_{-a}^{a} G_1(t)dt\int_0^{\infty} M_{1j}(s,t)[(a_{ij}+2c_{ij})\cosh(x_i s)$$

$$+ c_{ij} s x_i \sinh(x_i s)]e^{-sh_1}ds + \frac{1}{\pi}\int_{-b}^{b} G_2(t)dt\int_0^{\infty} M_{1j}(s,t)$$

$$[(b_{ij}+2d_{ij})\cosh(x_i s) + d_{ij} s x_i \sinh(x_i s)]e^{-sh_1}ds\}$$

$$+ \frac{4\mu_1}{\kappa_1+1}\frac{1}{\pi}\int_{-a_i}^{a_i}\frac{G_i(t)}{t-x_i}dt \quad , \quad (i=1,2) \quad . \tag{3.8}$$

Now substituting Eq. (3.8) into stress boundary conditions, Eqs. (2.19), we obtain

$$\frac{1}{\pi}\int_{-a}^{a}[\frac{1}{t-x_1}+\pi k_{11}(x_1,t)]G_1(t)dt + \int_{-b}^{b} k_{12}(x_1,t)G_2(t)dt = -\frac{1+\kappa_1}{4\mu_1}p_1(x_1) \quad ,$$

$$-a<x_1<a$$

$$\int_{-a}^{a} k_{21}(x_2,t)G_1(t)dt + \frac{1}{\pi}\int_{-b}^{b}[\frac{1}{t-x_2}+\pi k_{22}(x_2,t)]G_2(t)dt = -\frac{1+\kappa_1}{4\mu_1}p_1(x_1) \quad ,$$

$$-b<x_2<b \tag{3.9a,b}$$

where the kernels $k_{ij}(x_i,t)$, $(i,j=1,2)$ are given by

$$k_{ij}(x_i,t) = \int_0^{\infty} K_{ij}(x_i,t,s)e^{-s(h_1-t)}ds \quad , \tag{3.10}$$

and $K_{ij}(x_i,t,s)$ are given in Appendix D by (D.5). $k_{ij}(x_i,t)$ behave similar to those used in Section 2.2.

Again some special cases can be recovered from Eqs. (3.9) by letting some length and/or material parameters go to proper limits. For example, for a = b one can obtain the one-crack case in [5]. For a = b and $h_3 = 0$ or $\mu_3 = \mu_1$, $\nu_3 = \nu_1$ we recover the problem of colinear cracks in an elastic solid [15]. If we let $\mu_3 \to 0$ the integral equations (3.9) reduce to an integral equation for the problem of a center-notched strip [14]. By making $h_3 \to \infty$ we obtain the case of two half planes bonded by a center-notched strip [16]. Finally by letting $h_1 \to \infty$ or $h_2 \to \infty$ we recover the case of a crack in an infinite elastic solid.

3.3 Solution of Integral Equations

Following exactly the same procedure as in Section 2.3 we can obtain, for the case of crack in strip (1) only ($a<h_1, b=0$),

$$\sum_{i=1}^{n} \theta_1(\tau_i)\left[\frac{1}{\tau_i-\omega_j} + \frac{1}{\tau_i+\omega_j} + \pi\bar{k}_{11}(\omega_j,\tau_i)\right] = -N \quad , (j=1,\ldots,n) \qquad (2.59)$$

which is to be solved for $\theta_1(\tau_i)$, $(i=1,\ldots,n)$ and $\theta_1(\tau)$ is defined in Eq. (2.53). For the case of crack in strip (2) only ($a=0, b<h_1$), we will have again

$$\sum_{i=1}^{n} \theta_2(\tau_i)\left[\frac{1}{\tau_i-\omega_j} + \frac{1}{\tau_i+\omega_j} + \pi\bar{k}_{22}(\omega_j,\tau_i)\right] = -N \ , \ (j=1,\ldots,n) \quad (2.71)$$

in which

$$\theta_2(\tau) = \frac{4\mu_1}{1+\kappa_1}\cdot\frac{\phi_2(b\tau)}{bp_1} \ . \quad (3.11)$$

In case of crack in both strip ① and strip ② ($a<h_1, b<h_1$),

$$\sum_{i=1}^{n} \{\theta_1(\tau_i)\left[\frac{1}{\tau_i-\omega_j} + \frac{1}{\tau_i+\omega_j} + \pi\bar{k}_{11}(\omega_j,\tau_i)\right] + \theta_2(\tau_i)\pi\bar{k}_{12}(\omega_j,\tau_i)\} = -N,$$

$$\sum_{i=1}^{n} \{\theta_1(\tau_i)\pi\bar{k}_{21}(\omega_j,\tau_i) + \theta_2(\tau_i)\left[\frac{1}{\tau_i-\omega_j} + \frac{1}{\tau_i+\omega_j} + \pi\bar{k}_{22}(\omega_j,\tau_i)\right]\} = -N,$$

$$(j=1,\ldots,n) \quad (3.12a,b)$$

are the equations to be solved for $\theta_k(\tau_i)$, $(k=1,2; i=1,\ldots,n)$. Eqs. (2.60) and (2.73) are still valid for the stress intensity factors for $a<h_1$, $b<h_1$ in this problem.

3.4 Case of Broken Laminates ($a=h_1, b=0$)

3.4.1 *The Integral Equation*

In this case, Eqs. (3.9) reduce to

$$\frac{1}{\pi}\int_{-h_1}^{h_1}\left[\frac{1}{t-x_1} + \pi k_{11}(x_1,t)\right]G_1(t)dt = -\frac{1+\kappa_1}{4\mu_1}p_1(x_1) \ , \ -h_1<x_1<h_1 \ . \quad (3.13)$$

However, $k_{11}(x_1,t)$ is no longer bounded in $-h_1\leq x_1,t\leq h_1$ and it has point singularities at $t = h_1$ and $x_1 = \pm h_1$. Eq. (3.13)

is not an ordinary singular integral equation since it contains generalized Cauchy kernel. Integrand of the infinite integral giving $k_{11}(x_1,t)$ is bounded and continuous everywhere in $0<s<\infty$, and the singularity near $s = 0$ is removable (see Section 2.2). The divergence in the integral is due to the behavior of the integrand as $s\to\infty$. One can separate the asymptotic part of $K_{11}(x_1,t,s)$ by writing

$$K_{11}(x_1,t,s) = K_{11s}(x_1,t,s) + K_{11f}(x,t,s) \quad , \tag{3.14}$$

where

$$K_{11s}(x_1,t,s) = \lim_{s\to\infty} K_{11}(x_1,t,s) \quad , \tag{3.15}$$

and $K_{11f}(x_1,t,s)$ is bounded in $0<s\leq\infty$. Now define

$$k_{11s}(x_1,t) = \int_0^\infty K_{11s}(x_1,t,s)e^{-s(h_1-t)}ds \quad ,$$

$$k_{11f}(x_1,t) = \int_0^\infty K_{11f}(x_1,t,s)e^{-s(h_1-t)}ds \quad , \tag{3.16a,b}$$

so that

$$k_{11}(x_1,t) = k_{11s}(x_1,t) + k_{11f}(x_1,t) \quad , \tag{3.17}$$

$k_{11f}(x_1,t)$ being bounded in $-h_1\leq x_1,t\leq h_1$. After taking limits it is found that

$$\pi K_{11s}(x_1,t,s) = \{[4Q_1h_1(h_1-t)s^2 - Q_1(8h_1-6t)s + 3Q_1 + Q_2]\cosh(x_1s)$$
$$- 2Q_1x_1[2(h_1-t)s^2-s]\sinh(x_1s)\}e^{-sh_1} \quad , \tag{3.18}$$

where

$$Q_1 = (1-\lambda)/(\lambda+\kappa_1) \quad ,$$
$$Q_2 = (\kappa_1-\lambda\kappa_3)/(1+\lambda\kappa_3) \quad . \tag{3.19}$$

Using the following integral formula [20]

$$\int_0^\infty s^n e^{-s(2h_1-t)} \begin{Bmatrix} \sinh(x_1 s) \\ \cosh(x_1 s) \end{Bmatrix} ds = \frac{d^n}{dt^n} \left[\frac{1}{(2h_1-t)^2-x_1^2} \begin{Bmatrix} x_1 \\ 2h_1-t \end{Bmatrix} \right] , \quad (n=1,2,\ldots) \tag{3.20}$$

we can evaluate the integral in Eq. (3.16a) and obtain

$$\pi k_{11s}(x_1,t) = \frac{1}{2} \left[4Q_1(h_1+x_1)^2 \frac{d^2}{dx_1^2} + 12Q_1(h_1+x_1) \frac{d}{dx_1} + 3Q_1 - Q_2 \right]$$
$$\left[\frac{1}{t-(2h_1+x_1)} \right]$$
$$+ \frac{1}{2} \left[4Q_1(h_1-x_1)^2 \frac{d^2}{dx_1^2} - 12Q_1(h_1-x_1) \frac{d}{dx_1} + 3Q_1 - Q_2 \right]$$
$$\left[\frac{1}{t-(2h_1-x_1)} \right] \quad . \tag{3.21}$$

Now substituting Eq. (3.17) into Eq. (3.13)

$$\frac{1}{\pi} \int_{-h_1}^{h_1} \left[\frac{1}{t-x_1} + \pi k_{11s}(x_1,t) \right] G_1(t)dt + \int_{-h_1}^{h_1} k_{11f}(x_1,t) G_1(t)dt$$
$$= - \frac{1+\kappa_1}{4\mu_1} p_1(x_1) \quad , \quad -h_1<x_1<h_1 \tag{3.22}$$

is obtained. The terms in the bracket constitute a typical generalized Cauchy kernel.

3.4.2 *Characteristic Equation*

Assume that $G_1(t)$ has an integrable singularity at $t = \pm h_1$ which can be expressed as

$$G_1 = \frac{\phi_1(t)}{(h_1^2-t^2)^\gamma} = \frac{\phi_1(t)e^{\pi i\gamma}}{(t-h_1)^\gamma(t+h_1)^\gamma} \quad , \quad |t|<h_1 \tag{3.23}$$

where $0<\mathrm{Re}(\gamma)<1$ and $\phi_1(t)$ is Hölder-continuous in the closed interval $-h_1 \leq t \leq h_1$. In order to determine the power of singularity, γ, one should study Eq. (3.22) near $t = \pm h_1$. Consider the following sectionally holomorphic function

$$\psi_1(z) = \frac{1}{\pi}\int_{-h_1}^{h_1} \frac{G_1(t)}{t-z}\, dt \tag{3.24}$$

which becomes

$$\psi_1(z) = \frac{\phi_1(-h_1)}{(2h_1)^\gamma}\,\frac{e^{\pi i\gamma}}{\sin\pi\gamma}\,\frac{1}{(z+h_1)^\gamma} - \frac{\phi_1(h_1)}{(2h_1)^\gamma\sin\pi\gamma}\,\frac{1}{(z-h_1)^\gamma} + \psi_{10}(z) \tag{3.25}$$

by using Eq. (3.23) and following [17]. Here $\psi_{10}(z)$ is bounded everywhere except at the end points $\pm h_1$ where

$$|\psi_{10}(z)| < \frac{A}{|z\pm h_1|^{\gamma_1}} \quad , \quad \mathrm{Re}(\gamma_1)<\mathrm{Re}(\gamma) \quad , \tag{3.26}$$

A is a real constant. From Eq. (3.25), using the Plemelj formulas given by Eq. (2.43) we obtain

$$\psi_1(x_1) = \frac{\phi_1(-h_1)}{(2h_1)^\gamma}\,\frac{\cot\pi\gamma}{(h_1+x_1)^\gamma} - \frac{\phi_1(h_1)}{(2h_1)^\gamma}\,\frac{\cot\pi\gamma}{(h_1-x_1)^\gamma} + \psi_{11}(x_1) \quad , \tag{3.27}$$

where the behavior of ψ_{11} is similar to that of ψ_{10}. We can similarly evaluate

$$\frac{1}{\pi}\int_{-h_1}^{h_1} G_1(t)(h_1 \pm x_1)\,\frac{d}{dx_1}\left[\frac{1}{t-(2h_1 \pm x_1)}\right] dt = \pm\,\frac{\phi_1(h_1)}{(2h_1)^{\gamma}\sin\pi\gamma}\,\frac{\gamma}{(h_1 \pm x_1)^{\gamma}} + (h_1 \pm x_1)\,\frac{d}{dx_1}\psi_{12}(\pm x_1)\ ,$$

$$\frac{1}{\pi}\int_{-h_1}^{h_1} G_1(t)(h_1 \pm x_1)^2\,\frac{d^2}{dx_1^2}\left[\frac{1}{t-(2h_1 \pm x_1)}\right] dt = \frac{-\phi_1(h_1)}{(2h_1)^{\gamma}\sin\pi\gamma}\,\frac{\gamma(\gamma+1)}{(h_1 \pm x_1)^{\gamma}} + (h_1 \pm x_1)^2\,\frac{d^2}{dx_1^2}\psi_{12}(\pm x_1)\ , \qquad (3.28a,b)$$

where the behavior of ψ_{12} is again similar to that of ψ_{10}. Substituting Eqs. (3.27), (3.28) into Eq. (3.22) and noting that $\phi_1(t) = -\phi_1(-t)$ from Eqs. (2.30) and (3.23) we obtain

$$\frac{\phi_1(h_1)}{(2h_1)^{\gamma}\sin\pi\gamma}\left[2\cos\pi\gamma - 4Q_1\gamma(\gamma+1) + 12Q_1\gamma - 3Q_1 + Q_2\right]\left[\frac{1}{(h_1+x_1)^{\gamma}} + \frac{1}{(h_1-x_1)^{\gamma}}\right] = F_1(x_1)\ , \qquad (3.29)$$

where F_1 contains all the bounded terms. Now multiplying Eq. (3.29) by $(h_1+x_1)^{\gamma}$ and letting $x_1 \to -h_1$ or multiplying by $(h_1-x_1)^{\gamma}$ and letting $x_1 \to h_1$, we obtain the following characteristic equation for the unknown constant γ:

$$2\cos\pi\gamma + 4Q_1(\gamma-1)^2 - (Q_1+Q_2) = 0\ . \qquad (3.30)$$

One can see that this equation is the same as those found in [5], [21], [22], [23]. Eq. (3.30) is solved for γ, the power of singularity, which is assumed to be $0<\gamma<1$ to get an integrable singularity. We can find this real value of γ numerically, for example, using Newton's iteration method [24] within the desired accuracy.

3.4.3 *Solution of Integral Equation*

Define now the dimensionless variables ω,τ by

$$x_1 = h_1\omega \quad , \quad t = h_1\tau \quad , \quad -h_1 \leq x_1, t \leq h_1 \quad . \tag{3.31}$$

Then Eq. (3.22), with Eq. (3.23), takes the following form

$$\frac{1}{\pi}\int_{-1}^{1}\left[\frac{1}{\tau-\omega} + \pi h_1 k_{11s}(h_1\omega,h_1\tau) + \pi h_1 k_{11f}(h_1\omega,h_1\tau)\right]\frac{\phi_1(h_1\tau)}{(h_1)^{2\gamma}(1-\tau^2)^{\gamma}}\,d\tau = - \frac{1+\kappa_1}{4\mu_1}\,p_1(h_1\omega) \quad . \tag{3.32}$$

Introducing the new unknown function

$$\theta_1(\tau) = \frac{4\mu_1}{1+\kappa_1}\cdot\frac{\phi_1(h_1\tau)}{(h_1)^{2\gamma}p_1} \quad , \tag{3.33}$$

in which $p_1 = p_1(x_1) = \text{constant}$, one can write

$$\int_{-1}^{1}\left[\frac{1}{\tau-\omega} + \pi h_1 k_{11s}(h_1\omega,h_1\tau) + \pi h_1 k_{11f}(h_1\omega,h_1\tau)\right]\frac{\theta_1(\tau)}{(1-\tau^2)^{\gamma}}\,d\tau = -\pi \quad . \tag{3.34}$$

Note that $(1-\tau^2)^{-\gamma}$ is the weight function of the Jacobi polynomials $P_n^{(-\gamma,-\gamma)}(\tau)$. Thus the integral in Eq. (3.34) can be evaluated by using a Gauss-Jacobi integration formula given in [17]. Hence Eq. (3.34) becomes

$$\sum_{i=1}^{n}\theta_1(\tau_i)W_i\left[\frac{1}{\tau_i-\omega_j}+\pi h_1 k_{11s}(h_1\omega_j,h_1\tau_i)+\pi h_1 k_{11f}(h_1\omega_j,h_1\tau_i)\right]=-\pi\ ,$$

$$(j=1,\ldots,N-1) \qquad (3.35)$$

in which τ_i,ω_j are the roots of the Jacobi polynomials:

$$P_N^{(-\gamma,-\gamma)}(\tau_i)=0\ ,\quad (i=1,\ldots,N)\ ,$$
$$P_{N-1}^{(1-\gamma,1-\gamma)}(\omega_j)=0\ ,\quad (j=1,\ldots,N-1)\ , \qquad (3.36a,b)$$

and $W_i(i=1,\ldots,N)$ are the weights of $P_N^{(-\gamma,-\gamma)}(\tau_i)$. The single-valuedness condition, Eq. (2.21), which can be written as

$$\sum_{i=1}^{N}\theta_1(\tau_i)W_i=0 \qquad (3.37)$$

in this case, completes the system of (N) equations for (N) unknowns, $\theta_1(\tau_i)$. We can replace this system by an (nxn) system by considering the symmetry of the strip about y-axis. Hence

$$\sum_{i=1}^{n}\theta_1(\tau_i)W_i\left[\frac{1}{\tau_i-\omega_j}+\frac{1}{\tau_i+\omega_j}+\pi\bar{k}_{11s}(\omega_j,\tau_i)+\pi\bar{k}_{11f}(\omega_j,\tau_i)\right]=-\pi\ ,$$

$$(j=1,\ldots,n)\ , \qquad (3.38)$$

in which $2n=N$ and

$$\bar{k}_{11s}(\omega_j,\tau_i) = h_1[k_{11s}(h_1\omega_j,h_1\tau_i) - k_{11s}(h_1\omega_j,-h_1\tau_i)] \quad ,$$

$$\bar{k}_{11f}(\omega_j,\tau_i) = h_1[k_{11f}(h_1\omega_j,h_1\tau_i) - k_{11f}(h_1\omega_j,-h_1\tau_i)] \quad ,$$

$$(i,j=1,\ldots,n) \quad , \qquad (3.39a,b)$$

is obtained.

Examination of stress expressions indicates that the stress components are bounded for this case except σ_{3yy} which has a singularity at $x_3 = -h_3$. The definition of the stress intensity factor at the tip of the crack ($x_1=h_1$, $x_3=-h_3$) is no longer the same as those in Eqs. (2.60), (2.73) since the power of the singularity is not 1/2 anymore. Now define

$$k_a = \lim_{x_3 \to -h_3} \sqrt{2}\,(x_3+h_3)^{\gamma}\sigma_{3yy}(x_3,0) \quad , \; a=h_1 \quad , \qquad (3.40)$$

which can be expressed as (Appendix E)

$$k_a = -Q_3(h_1)^{\gamma}p_1\theta_1(1) \quad , \quad a=h_1 \quad , \qquad (3.41)$$

Q_3 being defined by (E.11) in Appendix E. After solving the system given by Eq. (3.38) for $\theta_1(\tau_i)$, (i=1,...,n) we can compute $\theta_1(1)$ using an appropriate extrapolation technique. According to [18]

$$\theta_1(1) \simeq \sum_{j=1}^{m-1} c_j P_j^{(-\gamma,-\gamma)}(1) \quad , \qquad (3.42)$$

$$c_j = \frac{1}{h_j} \sum_{i=1}^{m} \lambda_{im} P_j^{(-\gamma,-\gamma)}(\tau_i)\theta_1(\tau_i) \quad ,$$

$$h_j = \frac{2^{1-2\gamma}}{2j-2\gamma+1} \frac{[\Gamma(j-\gamma+1)]^2}{j!\Gamma(j-2\gamma+1)} \quad , \qquad (3.43a\text{-}c)$$

$$\lambda_{im} = -2^{-2\gamma} \frac{[\Gamma(m-\gamma+1)]^2}{(m+1)!\Gamma(m-2\gamma+2)} \frac{2m-2\gamma+2}{P_m^{(-\gamma,-\gamma)'}(\tau_i) P_{m+1}^{(-\gamma,-\gamma)}(\tau_i)} \quad .$$

Hence $\theta_1(1)$ can be computed after determining γ and computing $\theta_1(\tau_i)$, $(i=1,\ldots n)$.

3.5 Stresses

We consider the stress components which seem to be the most significant ones for $a \leq h_1$, $b=0$. The stresses at $x_2 = -h_1$ can directly be obtained from Eqs. (2.90) as

$$\sigma_{2xx}(-h_1,y)/p_1 = \begin{cases} -\frac{1}{N} \sum_{i=1}^{n} \theta_1(\tau_i)\bar{h}_{21}(\rho,\tau_i) \quad , & a<h_1 \quad , \\ -\frac{1}{\pi} \sum_{i=1}^{n} \theta_1(\tau_i)W_i\bar{h}_{21}(\rho,\tau_i) \quad , & a=h_1 \quad , \end{cases}$$

$$\sigma_{2yy}(-h_1,y)/p_1 = \begin{cases} \frac{1}{N} \sum_{i=1}^{n} \theta_1(\tau_i)\bar{h}_{22}(\rho,\tau_i) \quad , & a<h_1 \quad , \\ \frac{1}{\pi} \sum_{i=1}^{n} \theta_1(\tau_i)W_i\bar{h}_{22}(\rho,\tau_i) \quad , & a=h_1 \quad , \end{cases} \qquad (3.44a\text{-}c)$$

$$\tau_{2xy}(-h_1,y)/p_1 = \begin{cases} -\frac{1}{N} \sum_{i=1}^{n} \theta_1(\tau_i)\bar{h}_{23}(\rho,\tau_i) \quad , & a<h_1 \quad , \\ -\frac{1}{\pi} \sum_{i=1}^{n} \theta_1(\tau_i)W_i\bar{h}_{23}(\rho,\tau_i) \quad , & a=h_1 \quad , \end{cases}$$

where $\tau_i(i=1,\ldots,n)$ are defined in Eq. (2.55a) for $a<h_1$ and in Eq. (3.36a) for $a=h_1$. From Eq. (3.8), by using Eqs.

(3.10) and (D.5), one can write

$$\sigma_{2yy}(x_2,0) = \frac{4\mu_1}{\kappa_1+1}\int_{-a}^{a} k_{21}(x_2,t)G_1(t)dt \quad , \quad a\leq h_1 \tag{3.45}$$

and following a procedure similar to the one followed in section 2.4 he can further write

$$\sigma_{2yy}(x_2,0)/p_1 = \begin{cases} \frac{\pi}{N}\sum_{i=1}^{n}\theta_1(\tau_i)\bar{k}_{21}(\eta,\tau_i) & , \quad a<h_1 \\ \sum_{i=1}^{n}\theta_1(\tau_i)W_i\bar{k}_{21}(\eta,\tau_i) & , \quad a=h_1 \end{cases} \tag{3.46}$$

where τ_i are the same as stated above and $x_2 = h_1\eta$.

From Eqs. (3.3) we obtain

$$\sigma_{3yy}(x_3,0) = \frac{4\mu_3}{\kappa_1+1}\frac{1}{\pi}\int_{-a}^{a} k_{31}(x_3,t)G_1(t)dt \quad ,$$

$$\sigma_{3xx}(-h_3,y) = -\frac{4\mu_3}{\kappa_1+1}\frac{1}{\pi}\int_{-a}^{a} h_{34}(y,t)G_1(t)dt \quad , \tag{3.47a,b}$$

where

$$k_{31}(x_3,t) = \int_0^\infty K_{31}(x_3,t,s)e^{-s(h_1-t)}ds \quad ,$$

$$h_{34}(y,t) = \int_0^\infty H_{34}(y,t,s)e^{-s(h_1-t)}ds \quad , \tag{3.48a,b}$$

and

$$K_{31}(x_3,t,s) = \sum_{k=1}^{4} N_{1k}(s,t)[(a_{3k}+2c_{3k}+a_{4k}sx_3)\cosh(x_3s) + (2a_{4k}+c_{4k}+c_{3k}sx_3)\sinh(x_3s)]e^{-sh_3} \quad ,$$

$$H_{34}(y,t,s) = \sum_{k=1}^{4} N_{1k}(s,t)[(a_{3k}-a_{4k}sh_3)\cosh(h_3 s) - (c_{4k}-c_{3k}sh_3)\sinh(h_3 s)]e^{-sh_3}\cos(ys) \quad . \quad (3.49a,b)$$

Defining $x_3=h_3\xi$, and using Eqs. (2.49), (2.53) for $a<h_1$ and Eqs. (3.23), (3.33) for $a=h_1$, then replacing integrals by appropriate summations, we can rewrite Eqs. (3.47) as

$$\sigma_{3yy}(x_3,0)/p_1 = \begin{cases} \frac{1}{\lambda N} \sum_{i=1}^{n} \theta_1(\tau_i)\bar{k}_{31}(\xi,\tau_i) & , \quad a<h_1 \\ \frac{1}{\lambda\pi} \sum_{i=1}^{n} \theta_1(\tau_i)W_i\bar{k}_{31}(\xi,\tau_i) & , \quad a=h_1 \end{cases}$$

$$\sigma_{3xx}(-h_3,y)/p_1 = \begin{cases} -\frac{1}{\lambda N} \sum_{i=1}^{n} \theta_1(\tau_i)\bar{h}_{34}(\rho,\tau_i) & , \quad a<h_1 \\ -\frac{1}{\lambda\pi} \sum_{i=1}^{n} \theta_1(\tau_i)W_i\bar{h}_{34}(\rho,\tau_i) & , \quad a=h_1 \end{cases} \quad (3.50a,b)$$

where τ_i are given again by Eq. (2.55a) for $a<h_1$, by Eq. (3.36a) for $a=h_1$; $y=h_1\rho$, and

$$\bar{k}_{31}(\xi,\tau_i) = a[k_{31}(h_3\xi,a\tau_i) - k_{31}(h_3\xi,-a\tau_i)] \quad ,$$

$$\bar{h}_{34}(\rho,\tau_i) = a[h_{34}(h_1\rho,a\tau_i) - h_{34}(h_1\rho,-a\tau_i)] \quad . \quad (3,51a,b)$$

3.6 Numerical Results

The problem is solved for both plane strain and generalized plane stress cases since the formulation is carried out with κ, definition of which characterizes plane strain or

plane stress cases in itself (see section 2.1). Numerical results are obtained for material combinations II and III (see section 2.5 for definitions of material combinations). The cases where $a<h_1$ and/or $b<h_1$ are solved in the same way as the former problem. Solutions for these cases are obtained in order to establish limitations of the spring model approximation in the first problem.

Figures 18-23 show comparison of the stress intensity factors for various geometries and material combinations for plane strain and plane stress cases. As one can see in Figures 18-23, the stress intensity factor does not depend on the material properties and plane strain or plane stress cases when $h_3=0$. This is expected since $h_3=0$ corresponds to the case of colinear cracks in an infinite elastic solid. These figures show that the two solutions match very well for practical values of h_3/h_1 ratio ($h_3/h_1 = 0 - 10\%$). Results do not vary for plane strain or plane stress cases. But it is notable that agreement between the two solutions is better for material combination II. As $h_3 \to \infty$ the stress intensity factors for $a,b = 0,0.9h_1$ become the same for material combinations II and III, for plane strain and plane stress cases in the problem where the adhesive layers are approximated by distributed springs. Note that $h_3 \to \infty$ is equivalent to $E_3, \mu_3 \to 0$ which make the problem be the same as a center-notched strip having traction-free boundaries.

However, in the second problem the stress intensity factors depend on the conditions of plane strain or plane stress and the material combination. In Figures 22,23 the stress intensity factors for $a = b = 0.9h_1$ (for plane stress case) first increase as h_3/h_1 increases (up to ~.10), then start decreasing with further increases in h_3/h_1. This, we believe, can be explained as follows: When h_3 is too small the two cracks in adjacent strips are close to each other. As h_3 increases the tips of these cracks will still be close to each other for small values of h_3 whereas we will have the effect of a thin soft layer between main laminates. This will increase the stress intensity factors. But if h_3 continues to increase, the cracks will loose the interacting effect of each other which will make the stress intensity factors decrease. As a result, for small values of h_3, the effect of increasing the thickness of the softer layer is dominant; for larger values of h_3, effect of ceasing interaction between two cracks dominates.

Figures 24 and 25 show the variations of the normal stresses in x-direction on the boundaries of the adhesive layer. The normal stresses in x-direction in the adhesive layer and the adjacent laminate increase as the crack propagates. However, they can be reduced by increasing the thickness of the adhesive layer. In Figures 26 and 27 the normal stresses in y-direction on the line y=0 are shown.

These figures show that the cleavage stress ahead of a crack decreases as the thickness of the adhesive layer increases. This is very important as far as crack arrest in composites is concerned. One can see in Figure 26 that the cleavage stress at a location $x_2 = -h_1$ can be reduced to 1/3 of its value in a homogeneous medium by bonding strips with adhesive layers of thickness $h_3 = 5\%h_1$ for $a = 0.9h_1$. Comparison of Figures 25 and 27 shows that there is a possibility of delamination along the line $x_3 = -h_3$ when the crack approaches this boundary. The normal stress in x-direction is much higher than the normal stress in y-direction at the beginning of the adhesive layer. Therefore, depending on the strength of the bond between adhesive and laminates, a crack approaching the interface may propagate along the boundary (delamination) rather than going through the adhesive layer.

In order to solve the problem for $a=h_1$ we should first determine the power of singularity, γ, from Eq. (3.30). By using Newton's iteration method γ is found for various cases as shown in Table 1(a). Figure 28 and Table 1(b) show the variation of γ with $\lambda = \mu_1/\mu_3$ for plane stress and plane strain cases when $\nu_1 = \nu_3 = 0.35$. From these results one can observe that the power of singularity is higher for plane strain case. The difference is larger for small values of λ and it vanishes as λ becomes larger. One can also observe

that $\gamma = 0.5$ for both plane strain and plane stress cases when $\lambda = 1$ for which the composite medium is equivalent to a homogeneous medium. γ is lower than 0.5 for $\lambda<1$ and it is larger than 0.5 for $\lambda>1$. Figure 29 shows the variation of the normalized stress intensity factor, $K = k_a/p_1 h_1^{\gamma}$, with λ on a logarithmic scale for $h_3 = .05h_1$, $\nu_1 = \nu_3 = 0.35$. For small values of $\lambda(<\sim 1)$ K is larger for plane stress case by an amount of more than 50%, then for larger values of λ it is almost the same for both cases. The value of this normalized factor is much less for $\lambda>1$ than its value for $\lambda<1$ in both plane stress and plane strain cases, vanishing as $\lambda\to\infty$. Variations of K for $a=h_1$ with h_3/h_1 are given in Figures 30,31. Figure 30 shows the results for material combination II whereas Figure 31 does for combination III. One can observe that (a) K is slightly larger for plane strain case, deviation being small (the same trend in γ), (b) K is larger (~4 times) for material combination III, (c) K increases with increasing h_3/h_1 ratio.

Figures 32-37 show some of the calculated results for stress components. In Figure 32, the cleavage stress σ_{2yy} at $x_2 = -h_1$, $y=0$ varies as the crack in main laminate propagates. The stress increases as the crack approaches the adhesive layer. The value of the cleavage stress when the crack touches the interface ($a=h_1$) is unbounded if $h_3=0$ and it is bounded otherwise. Presumably this is the most

important point in this problem. The infinite cleavage stress (for $h_3=0$) at the beginning of the second strip can be made finite by considering even a very thin adhesive layer. This finite value decreases as the thickness of the adhesive layer increases. Figures 33 and 34 show the variations of the stress components σ_{2yy} and τ_{2xy} along $x_2 = -h_1$ line in y-direction. These stresses decrease as y increases and they are slightly larger for plane stress case. σ_{2yy} becomes smoother over $0 \leq y < \infty$ with increasing h_3/h_1 ratio (relaxation). In Figure 35, the variation of σ_{2yy} with x_2/h_1 at $y=0$ is shown for material combination II. σ_{2yy} again decreases with increasing h_3/h_1 ratio. Variation of the cleavage stress σ_{3yy} in the adhesive layer as the crack approaches interface is shown in Figure 36. $\sigma_{3yy}(-h_3,0)$ becomes unbounded when the crack touches the interface. Figure 37 shows the variation of σ_{3yy} with x_3/h_3 on $y=0$ line for $a=h_1$.

IV. CONCLUSIONS AND SUGGESTIONS FOR FUTURE WORK

The effect of the adhesive layers on crack propagation in composites has been examined for both plane stress and plane strain cases. Composite medium consists of main load-carrying laminates and buffer strips bonded periodically through thin adhesive layers. The adhesive layers have been approximated by distributed tension and shear springs. We solved the problem for the cases where the cracks were imbedded in laminates and/or buffer strips. The problem has been reduced to a system of singular integral equations and this system has been replaced by a system of linear algebraic equations which has been solved numerically. The stress intensity factors and some stress components have been computed and presented in Figures 3-16. We saw that the stress intensity factors at the crack tips have increased by taking the adhesive layer into account. They increase as the thickness of the adhesive layer increases (or as Young's and shear moduli of adhesive decrease). However, the presence of the adhesive layer relaxes the constraints at the interfaces so that the cleavage and shear stresses in the strip on the other side of the adhesive layer decrease. This is important from the point of view of crack arrest in composite materials. All the relevant special cases treated in literature can be

recovered from this solution which has been observed to be in good agreement with them.

Then we attempted to solve the case of broken laminates. We observed that the spring model approximation is not mathematically suitable for this case. Hence we introduced the problem described in Chapter III in which the adhesive has been treated as an elastic continuum. We solved the case of imbedded cracks in order to establish limitations of the spring model approximation in the former problem. We concluded that the spring model is good enough within practical ranges. Approximation is not reliable for very large thicknesses of adhesive layer or for comparatively weak adhesives. The case of broken laminates has been solved without any major difficulty. The characteristic equation to be solved for the power of singularity has come out to be the same as those obtained in [5], [21], [22], [23]. Stress intensity factors still increase as the thickness of the adhesive layer increases. However, the cleavage stress at the closer edge of the second strip (first strip is broken) becomes finite in this case whereas it has been found infinite by ignoring the adhesive layer. Special cases can be recovered from this solution too. See detailed numerical results and conclusions in sections 2.5 and 3.6.

The work presented here can be extended in several directions treating the adhesive as an elastic continuum:

(i) The problem can be solved for non-isotropic (e.g., orthotropic) materials which will be more realistic.

(ii) The strips bonded by adhesive can be of different materials.

(iii) Finite number of strips can be studied.

(iv) It may be useful to solve the problem for the cases where crack continues to propagate into the adhesive or along the interface (delamination).

However, one should keep in mind that all these problems will require considerable amount of time and labor. We hope that the present work will contribute to future studies in this field.

Combination	Power of singularity, γ	
	Plane Strain	Plane Stress
II	.8689	.8658
III	.7183	.7060

(a)

$\nu_1=\nu_3=.35$	Power of singularity, γ	
$\lambda=\mu_1/\mu_3$	Plane Strain	Plane Stress
.0	.3203	.2617
.001	.3207	.2623
.01	.3240	.2680
.1	.3538	.3155
1.	.5000	.5000
10.	.7551	.7552
100.	.9160	.9138
1000.	.9732	.9724

(b)

Table 1. Values of the power of singularity, γ, for various material combinations when $a=h_1$.

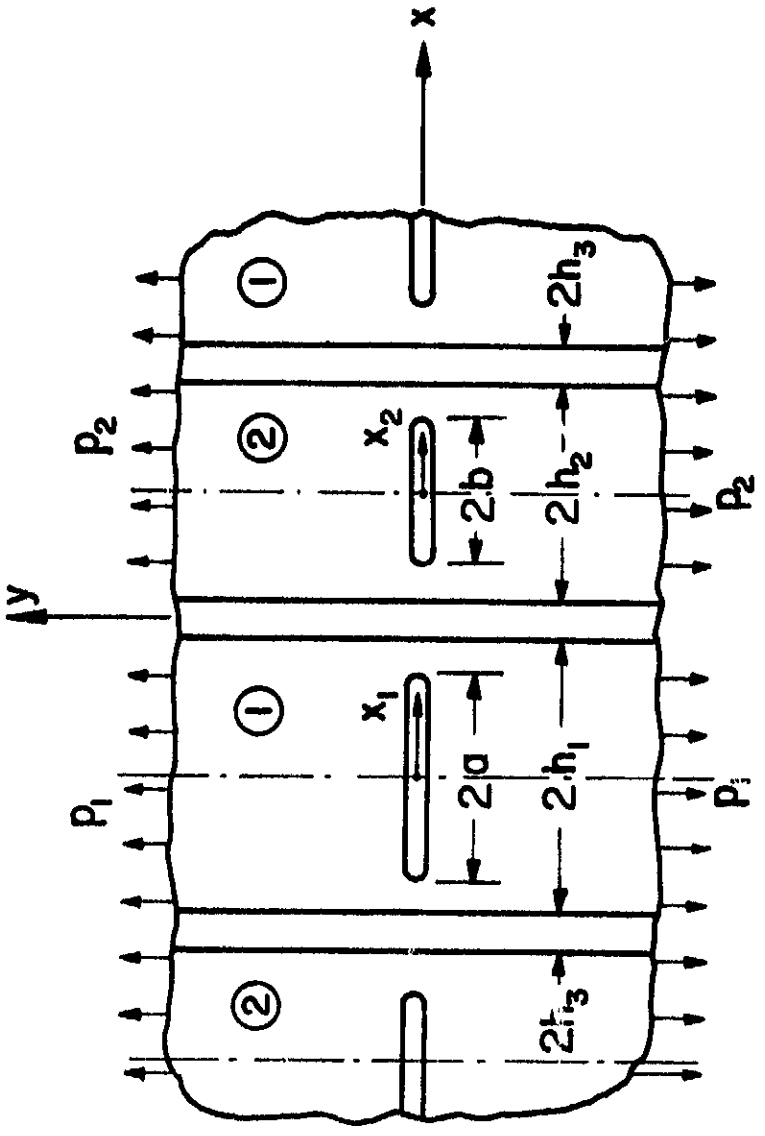

Figure 1. Geometry of the composite medium.

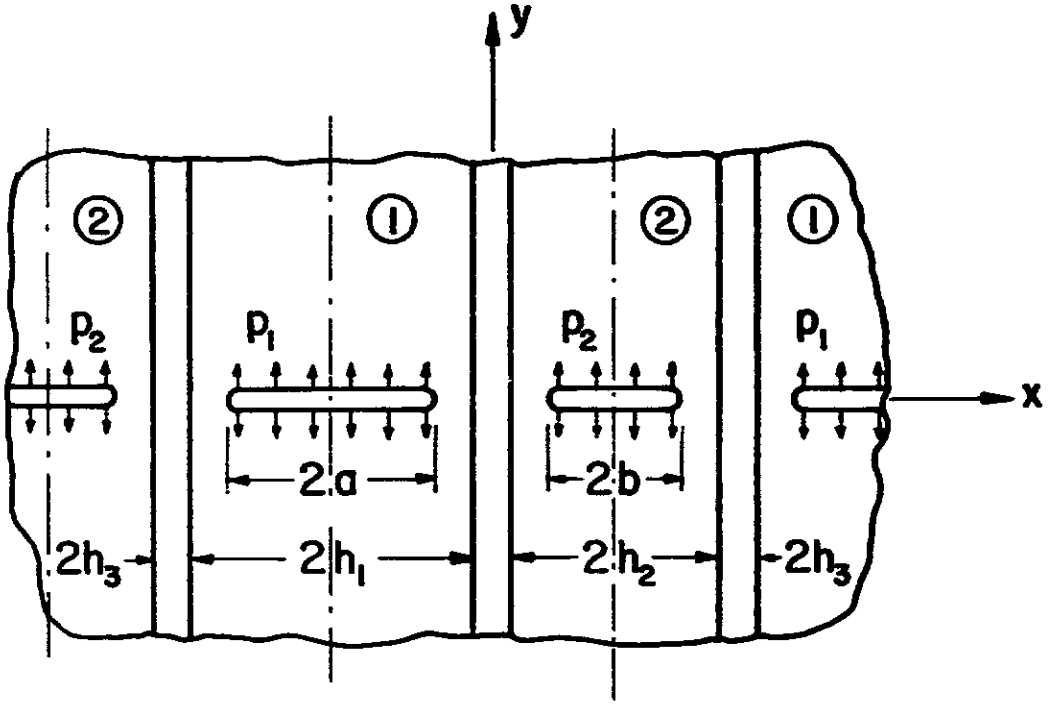

Figure 2. Configuration of the perturbation problem.

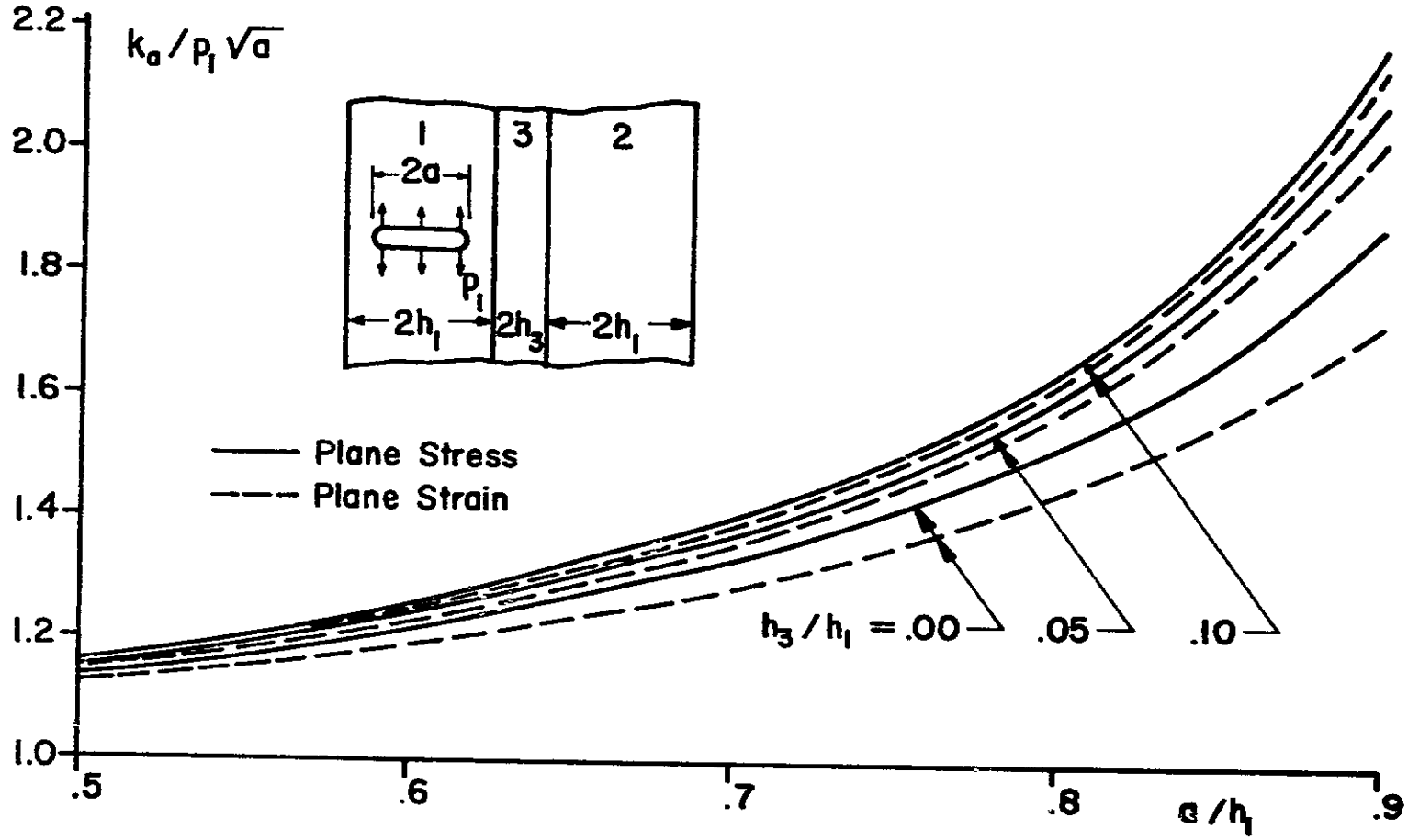

Figure 3. The stress intensity factor k_a vs. a/h_1 for the crack in main laminate (Combination I).

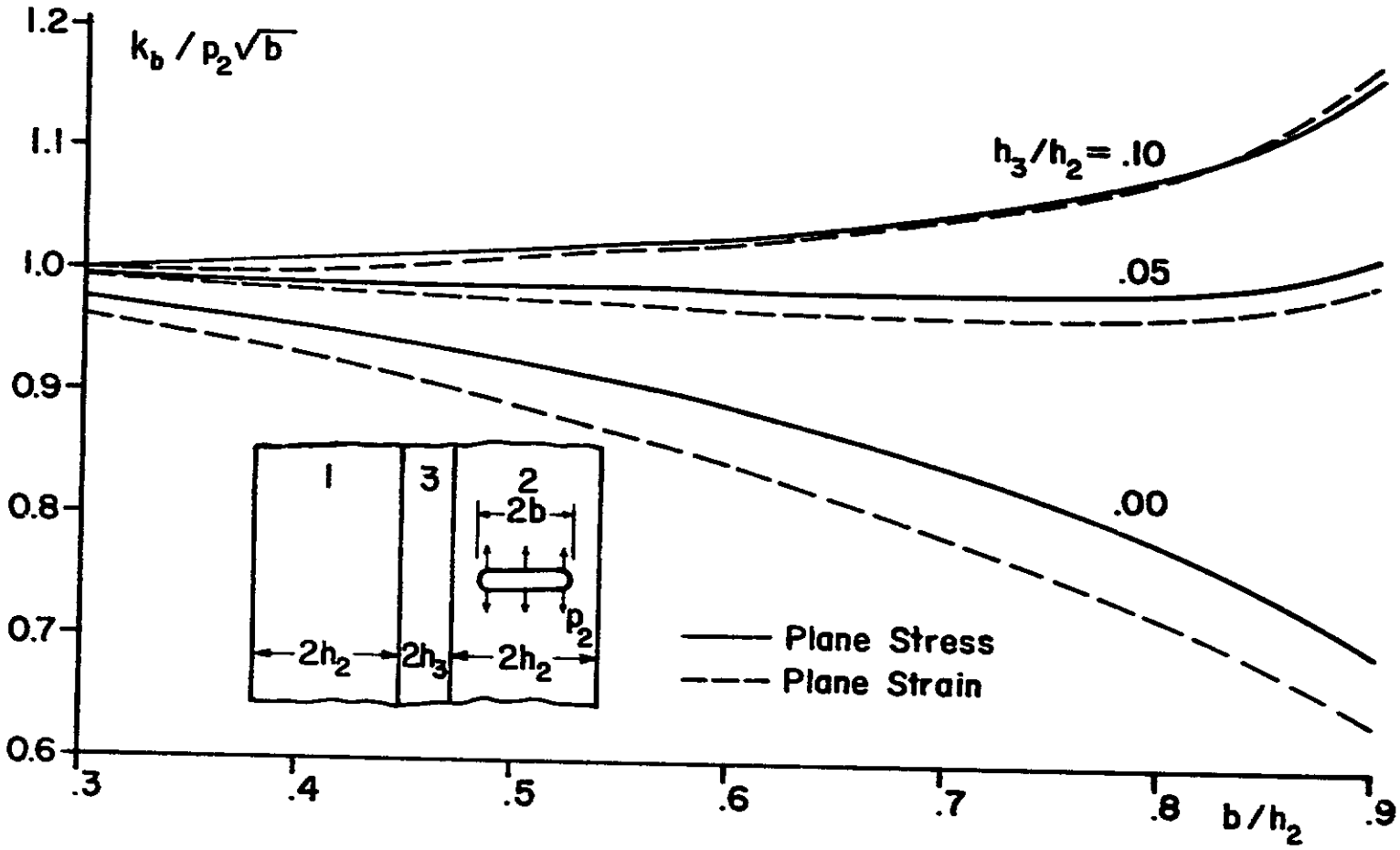

Figure 4. The stress intensity factor k_b vs. b/h_2 for the crack in buffer strip (Combination I).

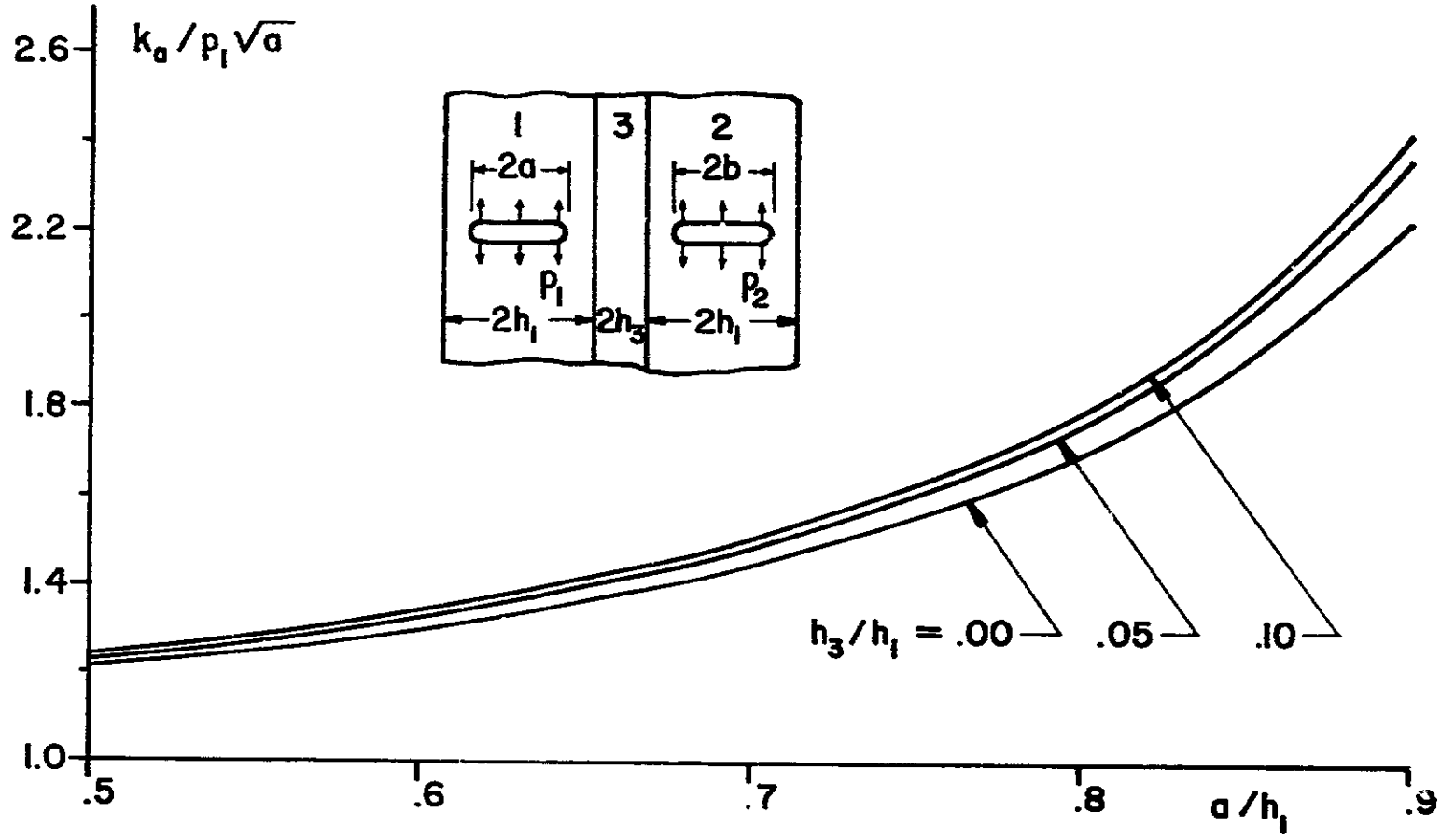

Figure 5. Variation of k_a with respect to a/h_1 for $b=0.3h_1$, plane stress case (Combination I).

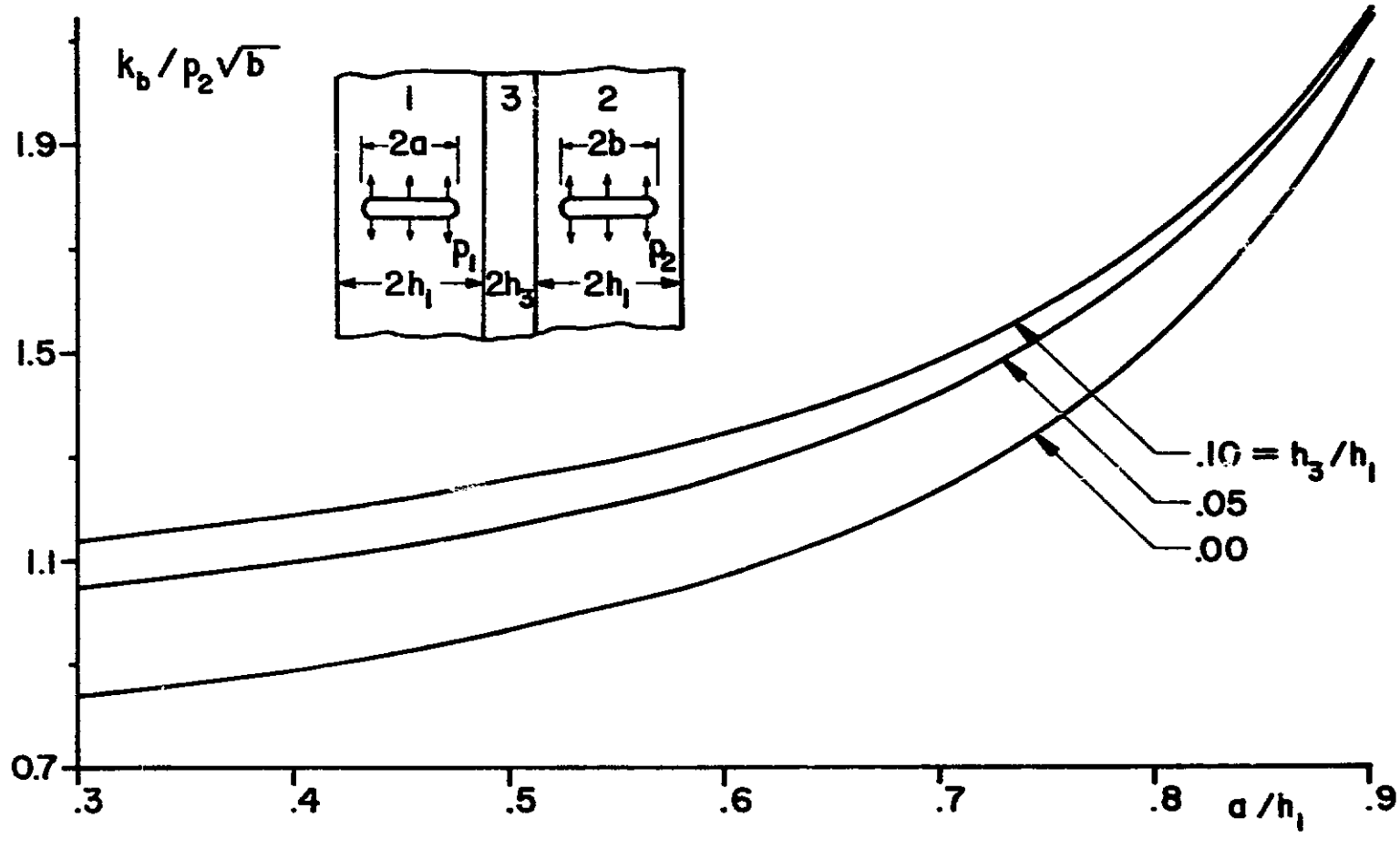

Figure 6. Variation of k_b with respect to a/h_1 for $b=0.8h_1$, plane stress case (Combination I).

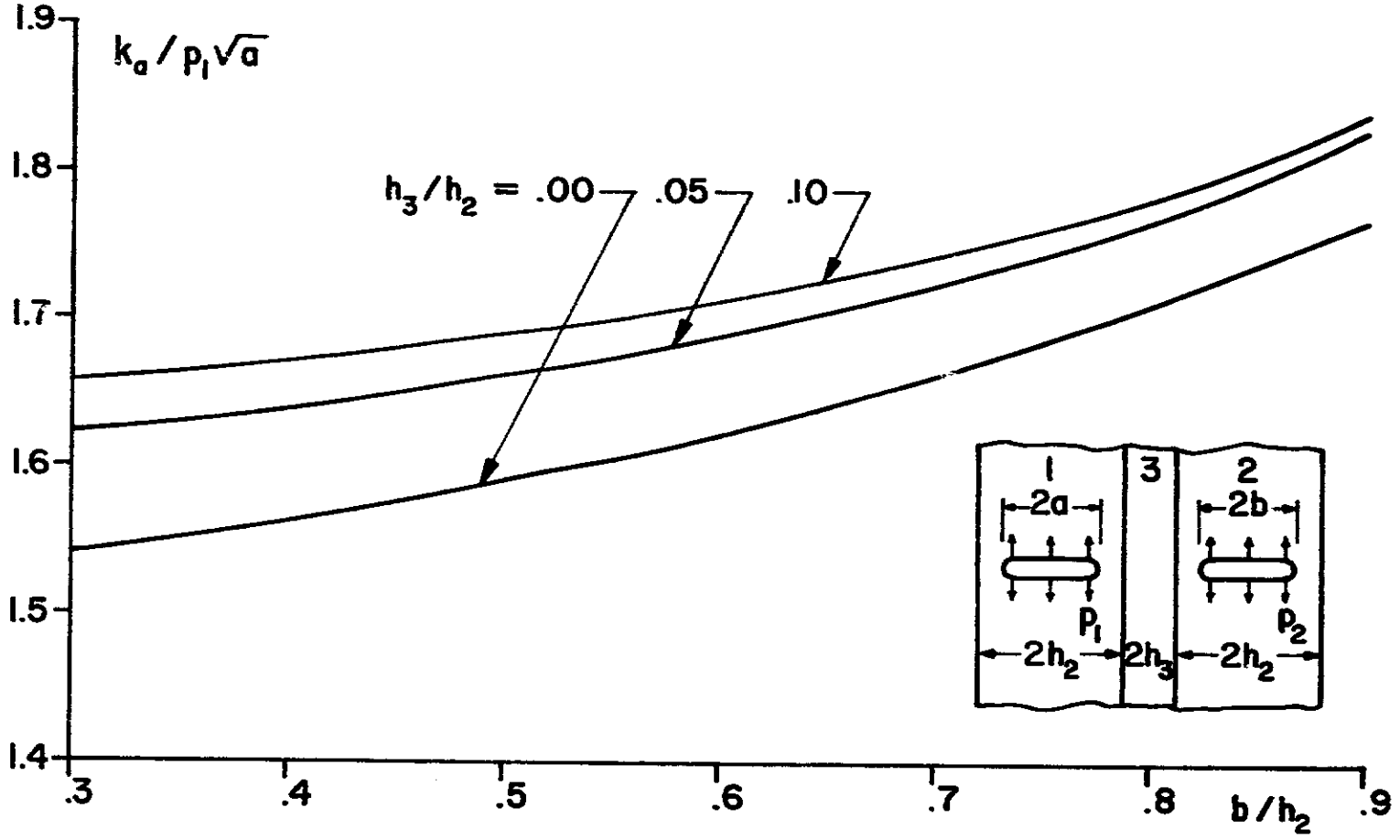

Figure 7. Variation of k_a with respect to b/h_2 for $a=0.8h_2$, plane stress case (Combination I).

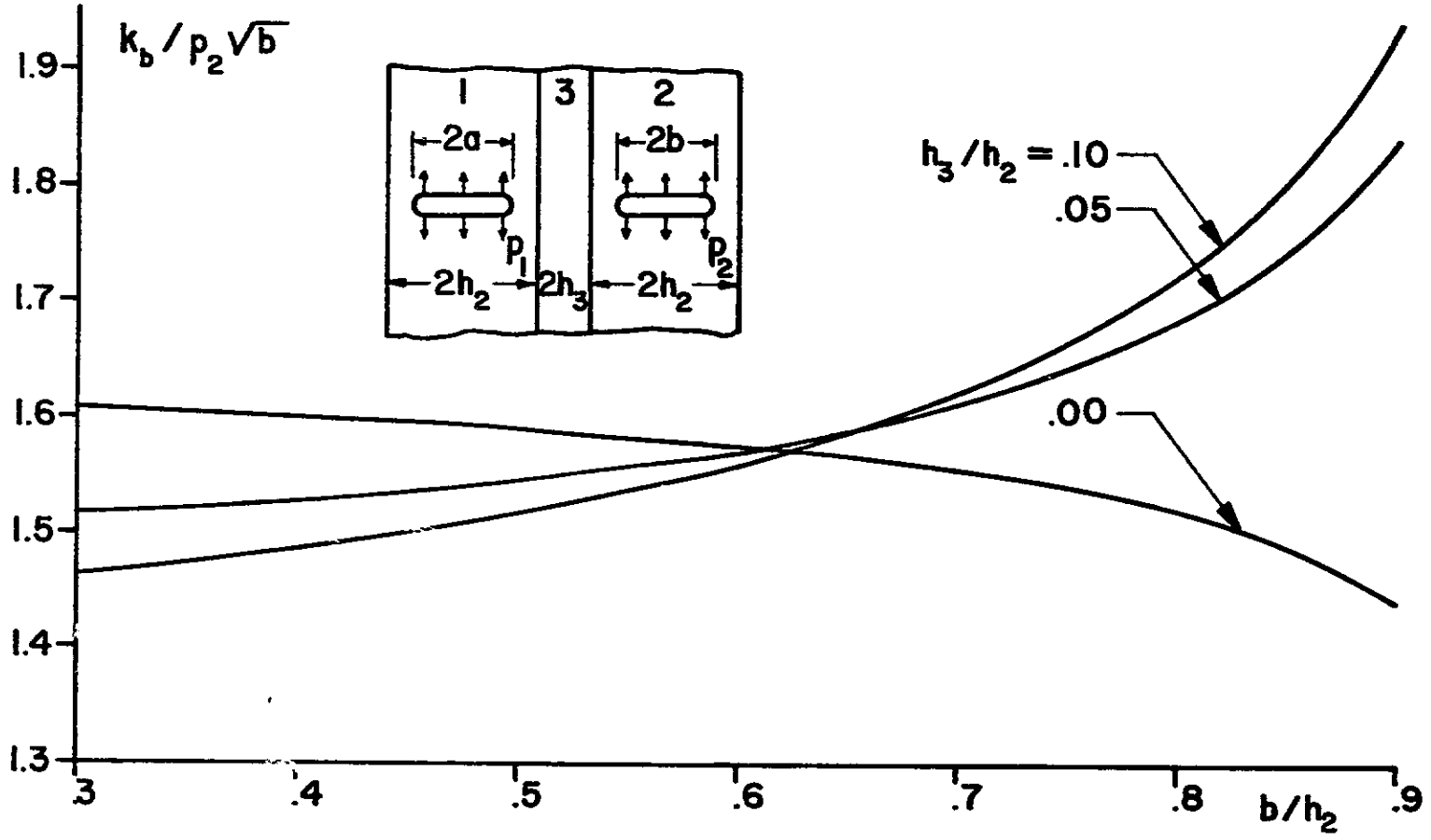

Figure 8. Variation of k_b with respect to b/h_2 for $a=0.8h_2$, plane stress case (Combination I).

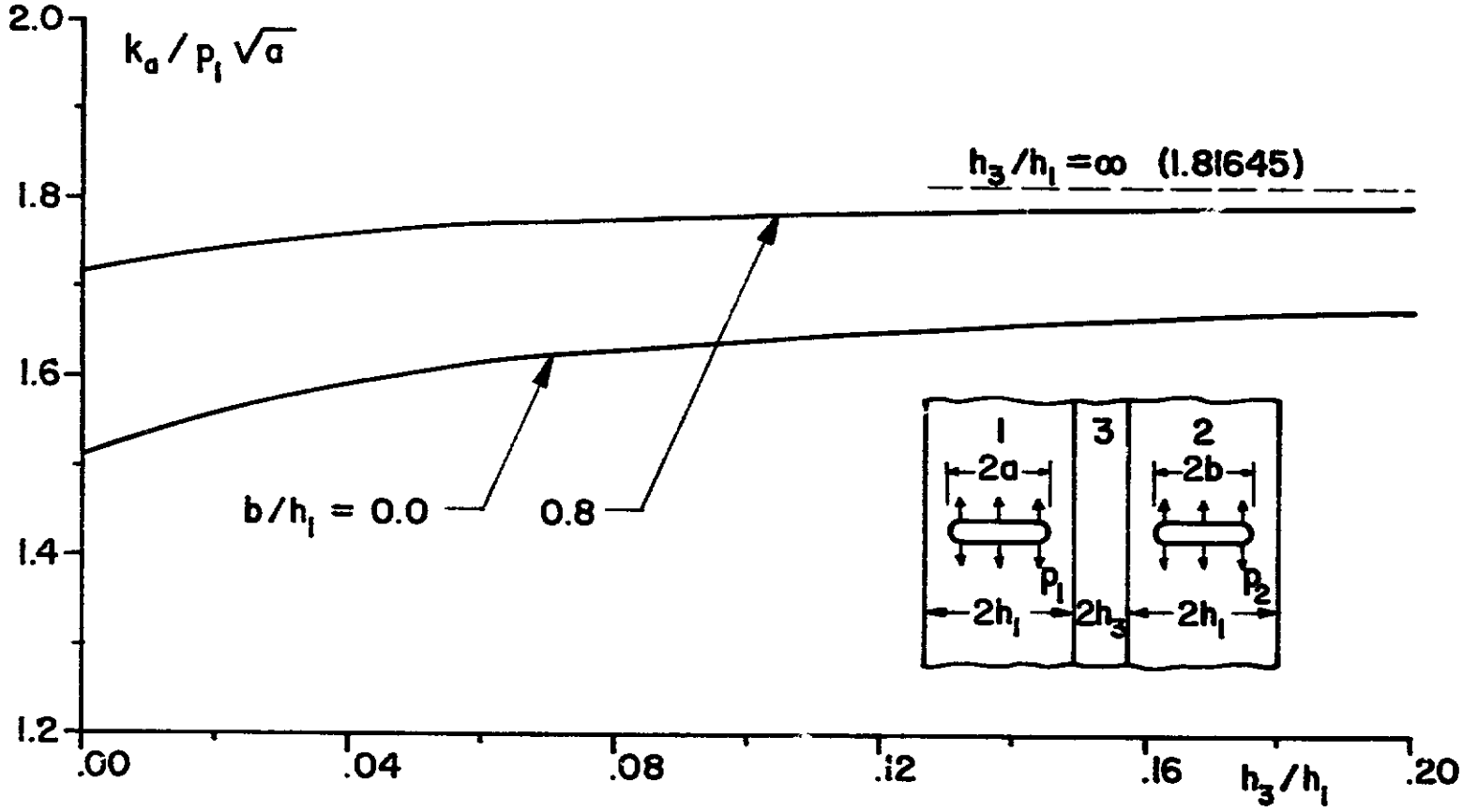

Figure 9. Variation of k_a with respect to h_3/h_1 for $a=0.8h_1$, plane stress case (Combination I).

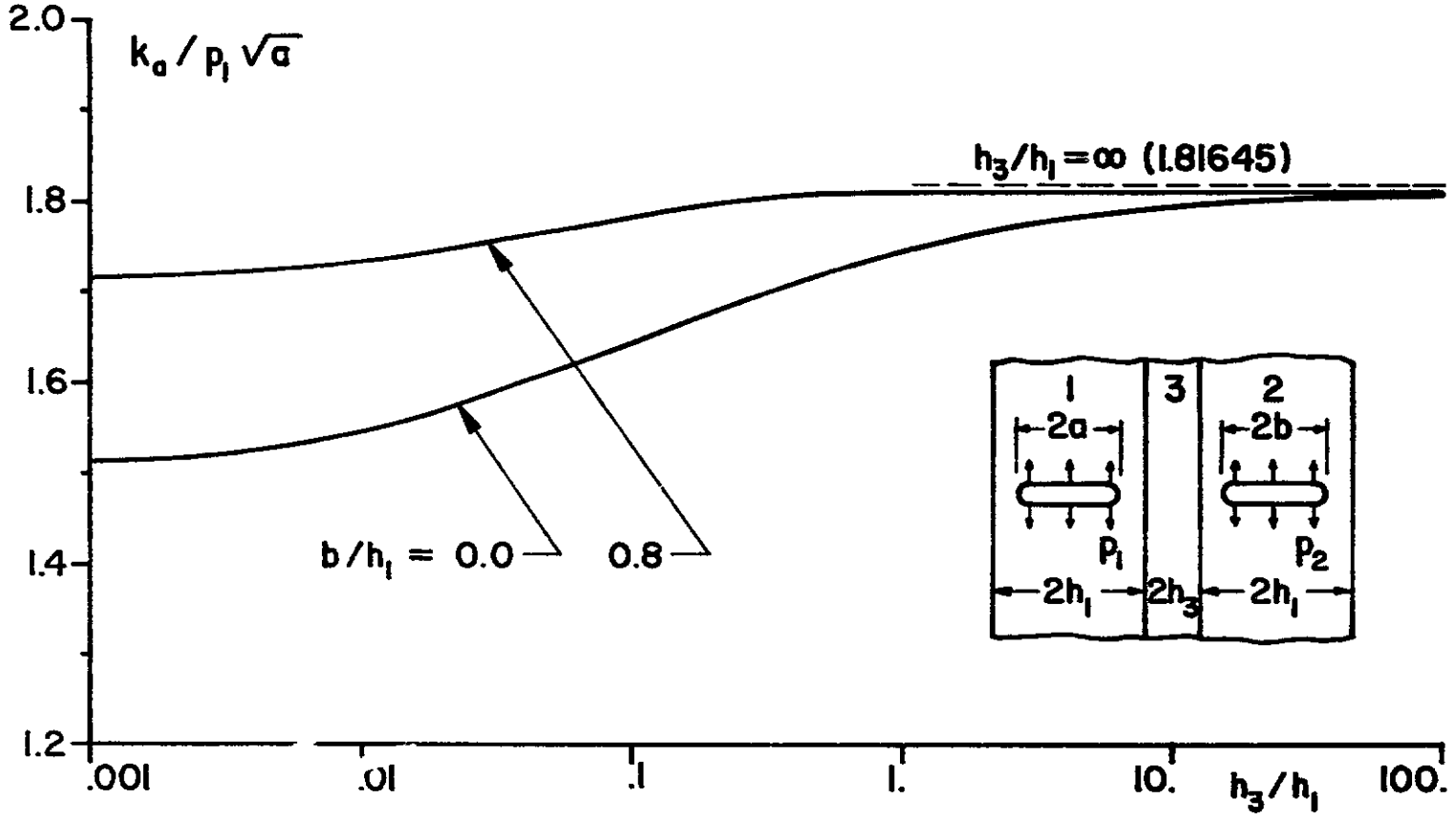

Figure 10. Variation of k_a with respect to (log) h_3/h_1 for $a=0.8h_1$, plane stress case (Combination I).

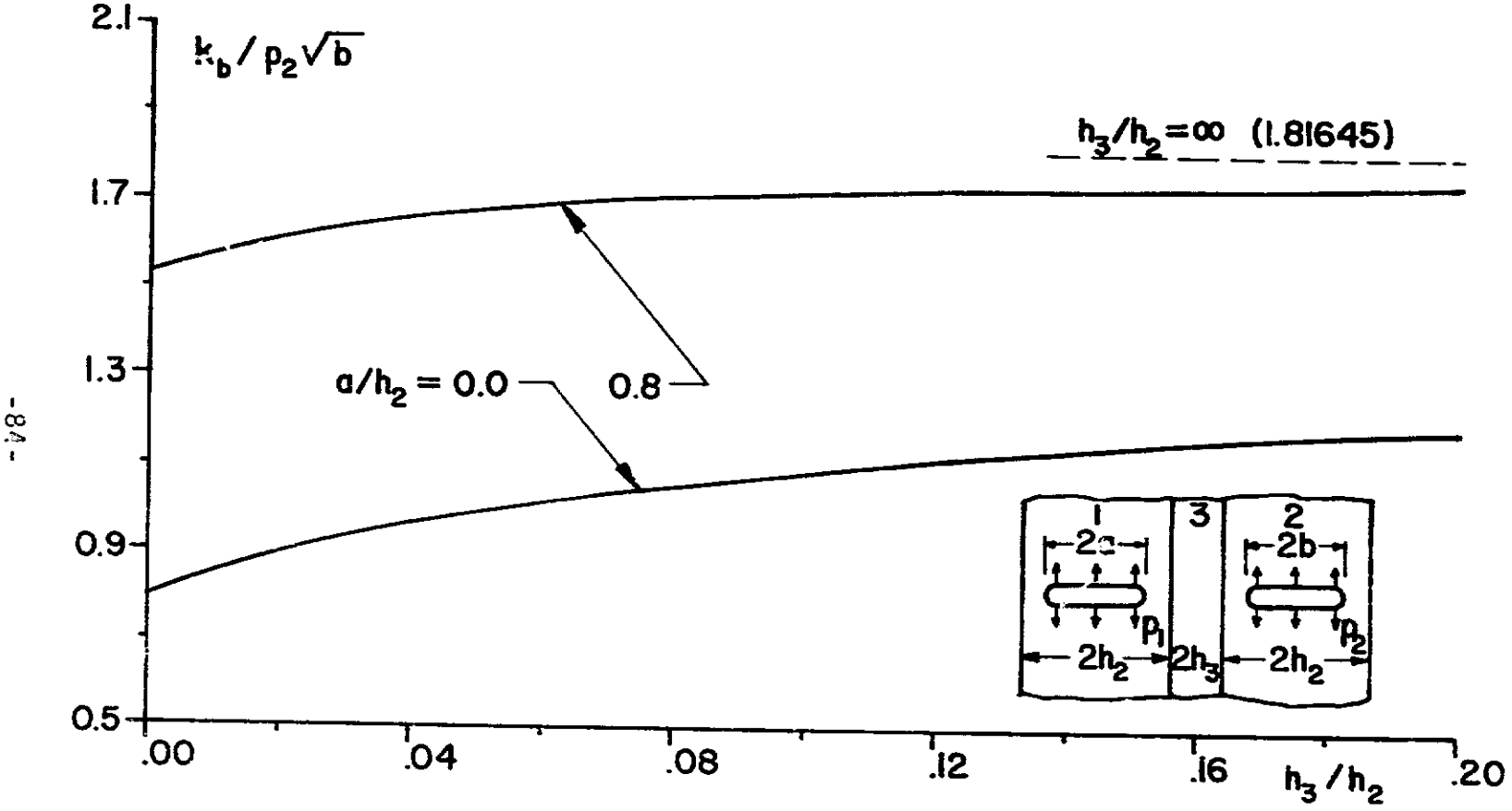

Figure 11. Variation of k_b with respect to h_3/h_2 for $b=0.8h_2$, plane stress case (Combination I).

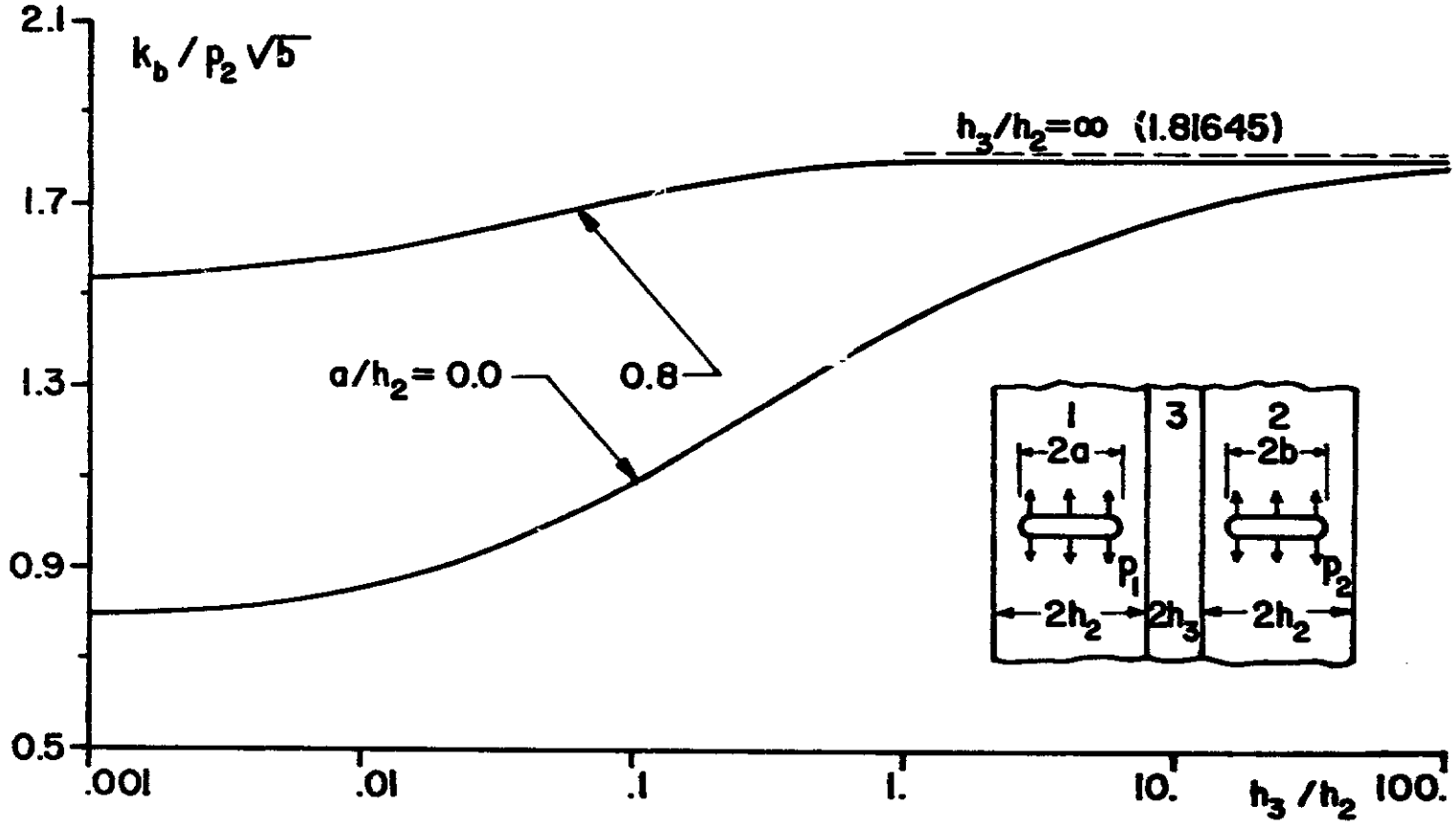

Figure 12. Variation of k_b with respect to (log) h_3/h_2 for $b=0.8h_2$, plane stress case (Combination I).

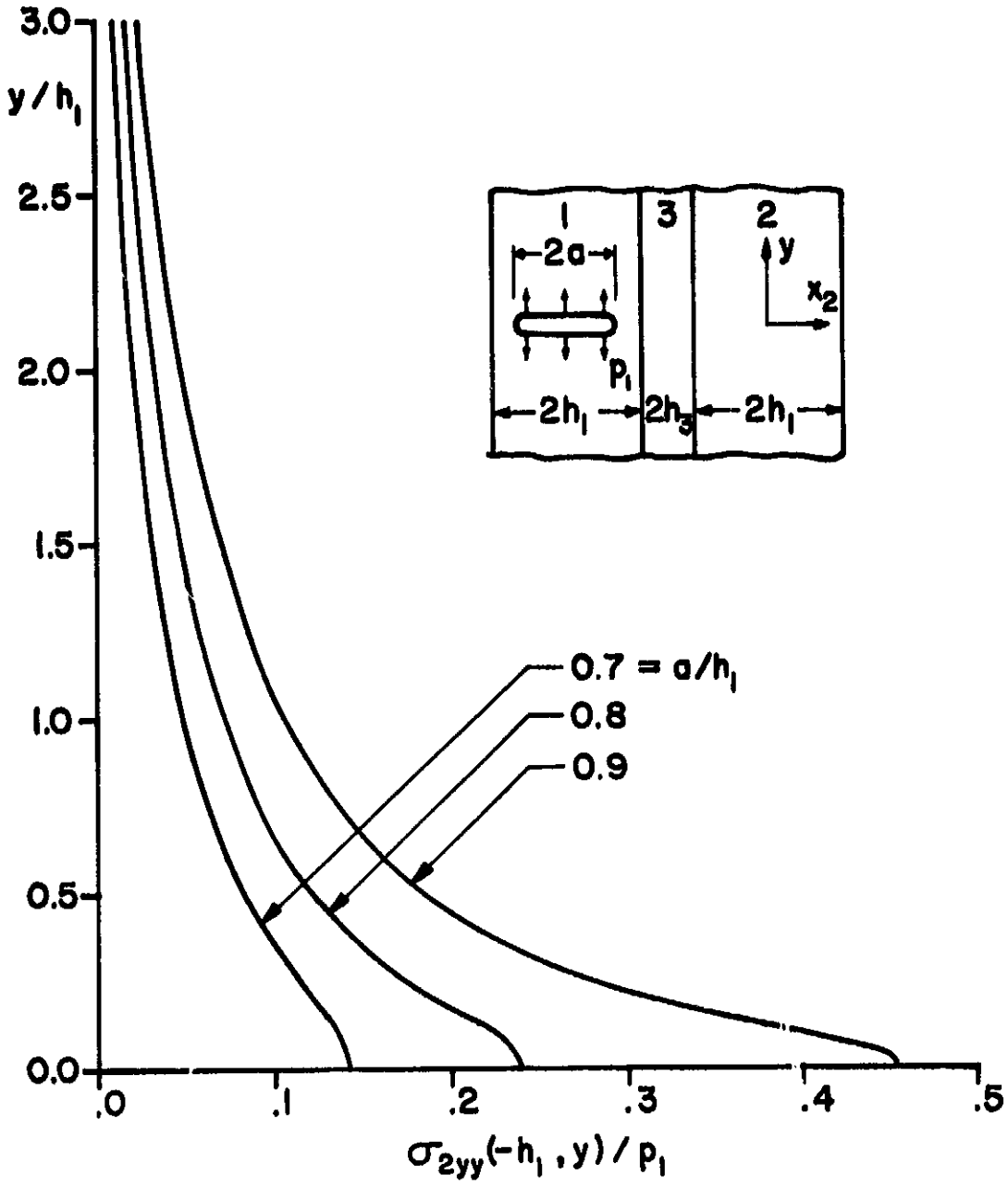

Figure 13. Distribution of the stress component σ_{2yy} at $x_2=-h_1$ for $h_3=.05h_1$, plane stress case (Combination I).

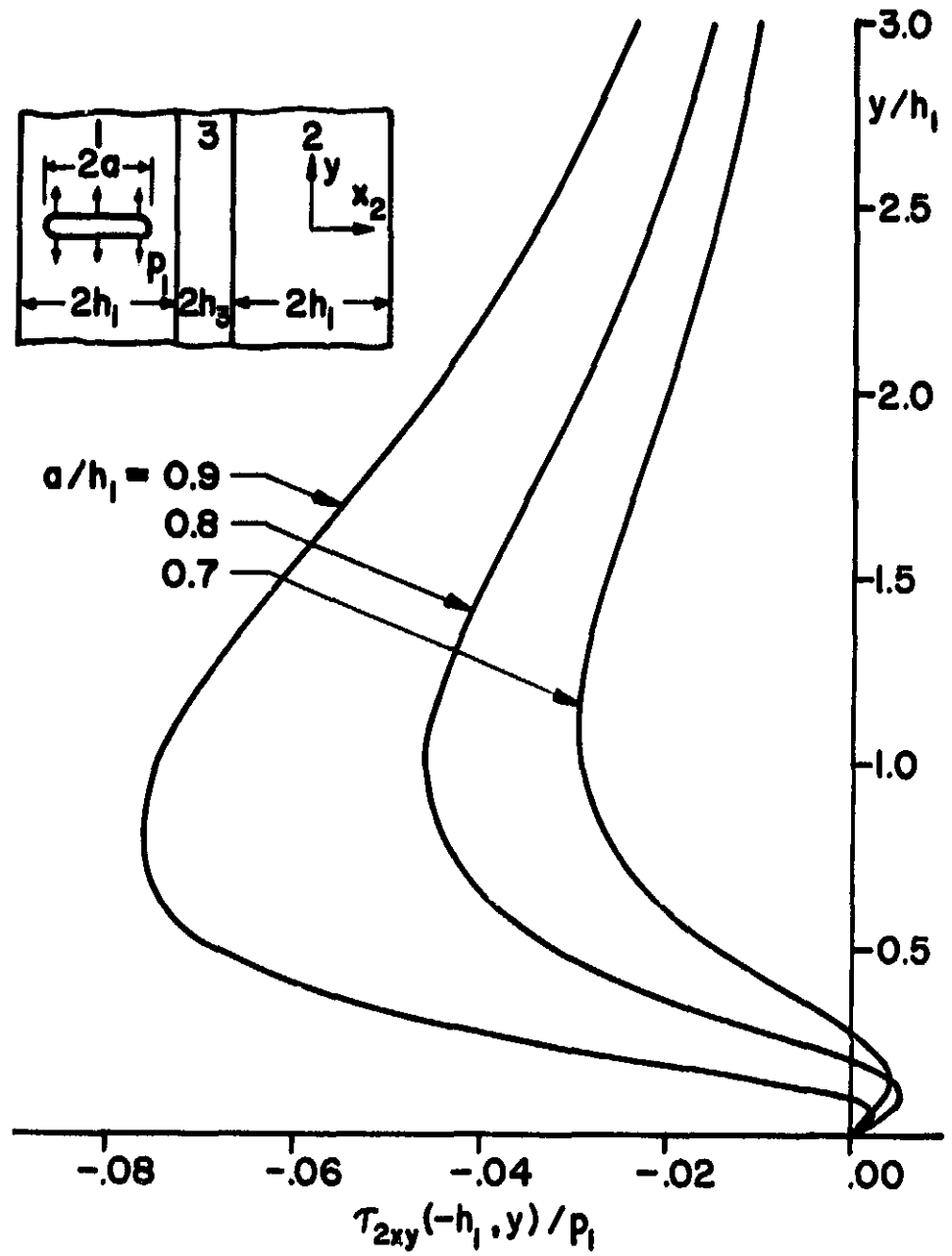

Figure 14. Distribution of the shear stress τ_{2xy} at $x_2=-h_1$ for $h_3=.05h_1$, plane stress case (Combination I).

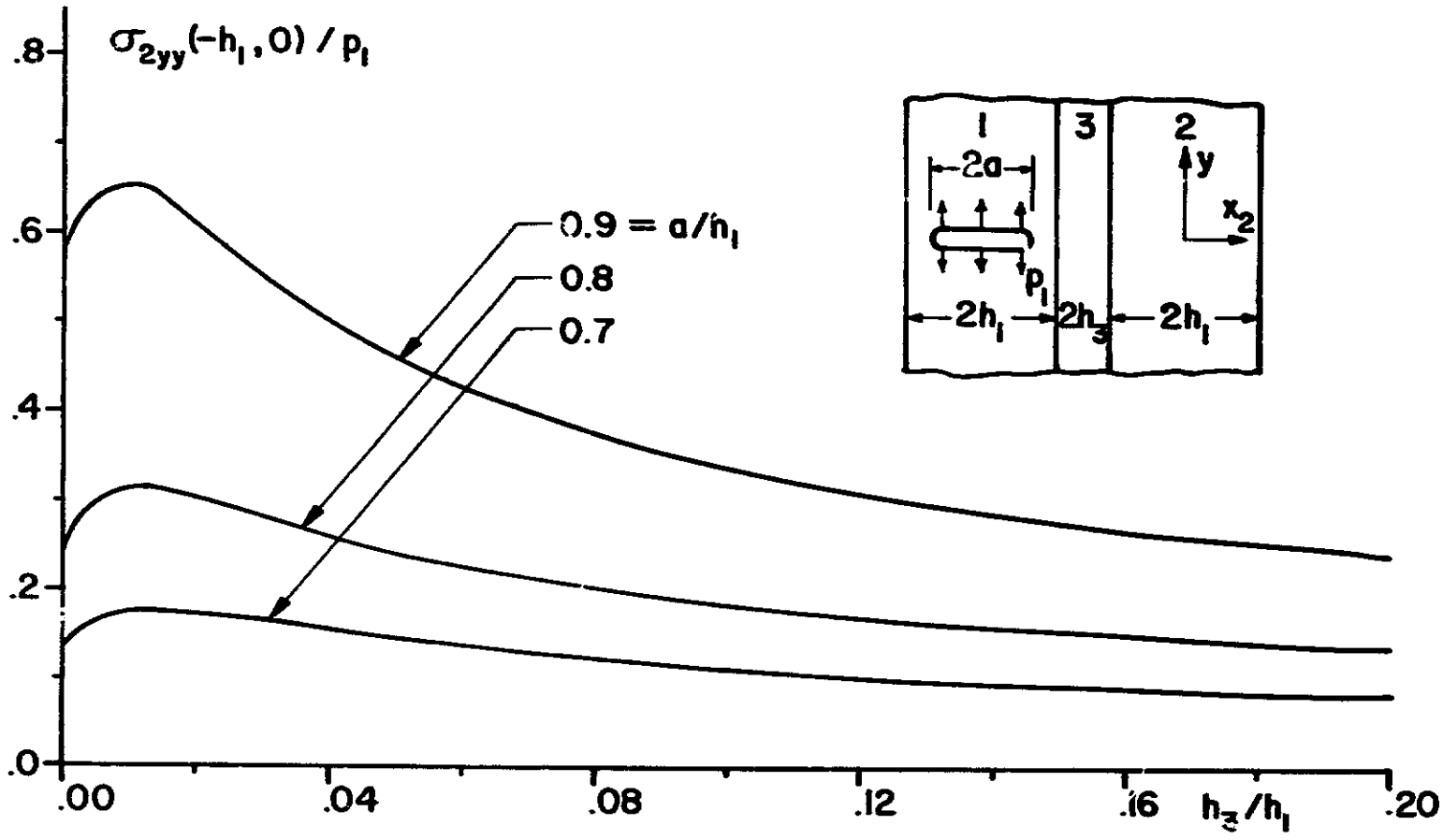

Figure 15. Variation of the cleavage stress $\sigma_{2yy}(-h_1,0)$ with h_3/h_1 for plane stress case (Combination I).

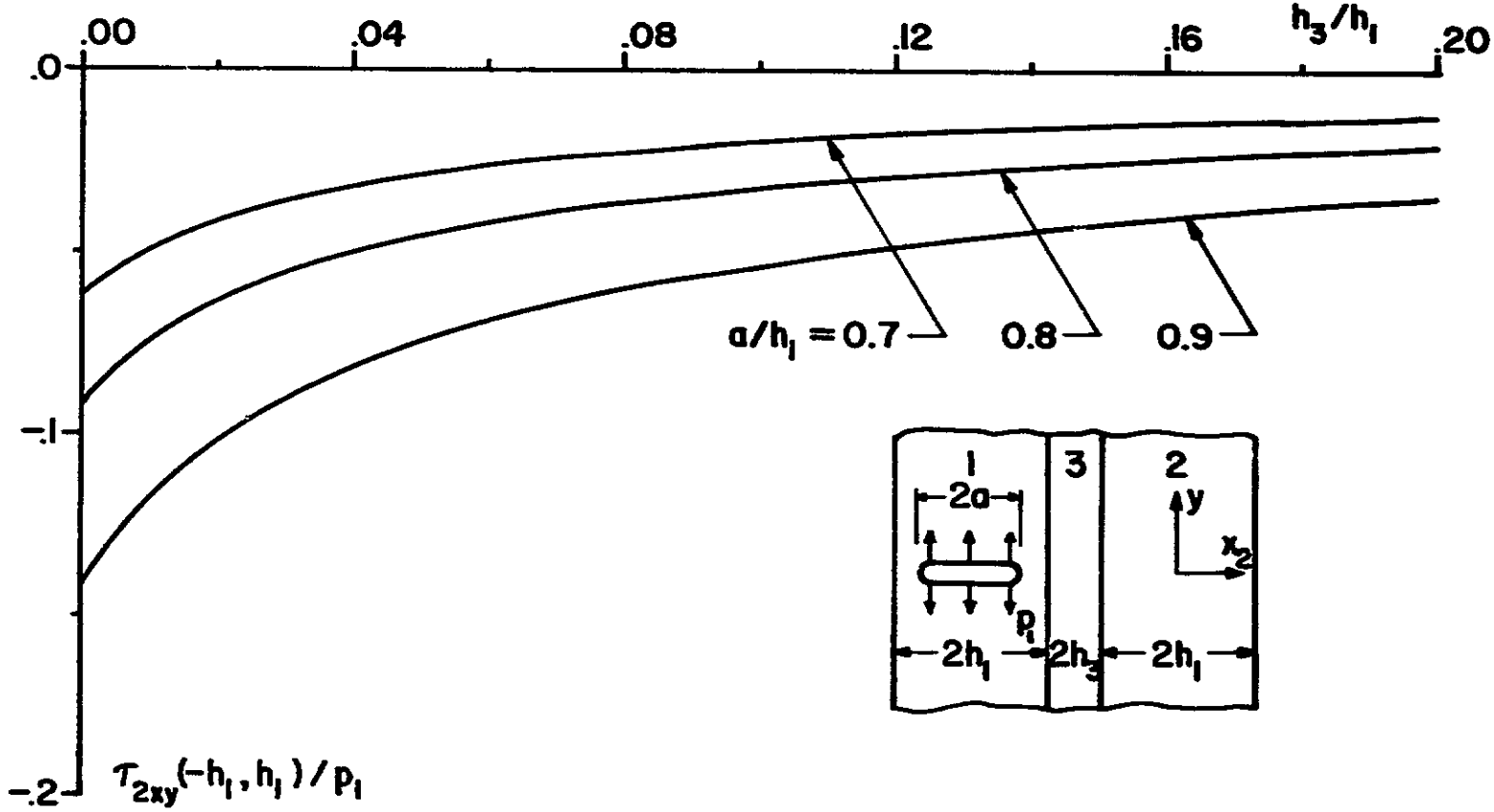

Figure 16. Variation of the shear stress $\tau_{2xy}(-h_1,h_1)$ with h_3/h_1 for plane stress case (Combination I).

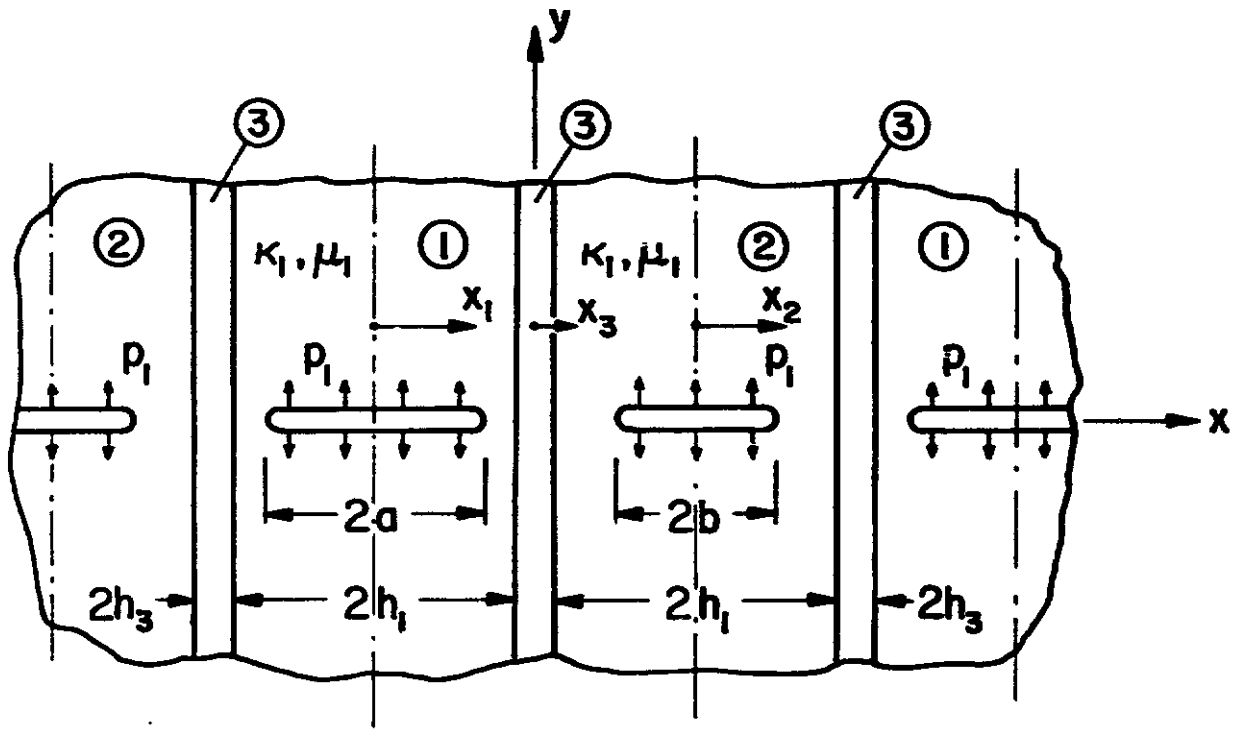

Figure 17. Configuration of the problem described in Chapter III.

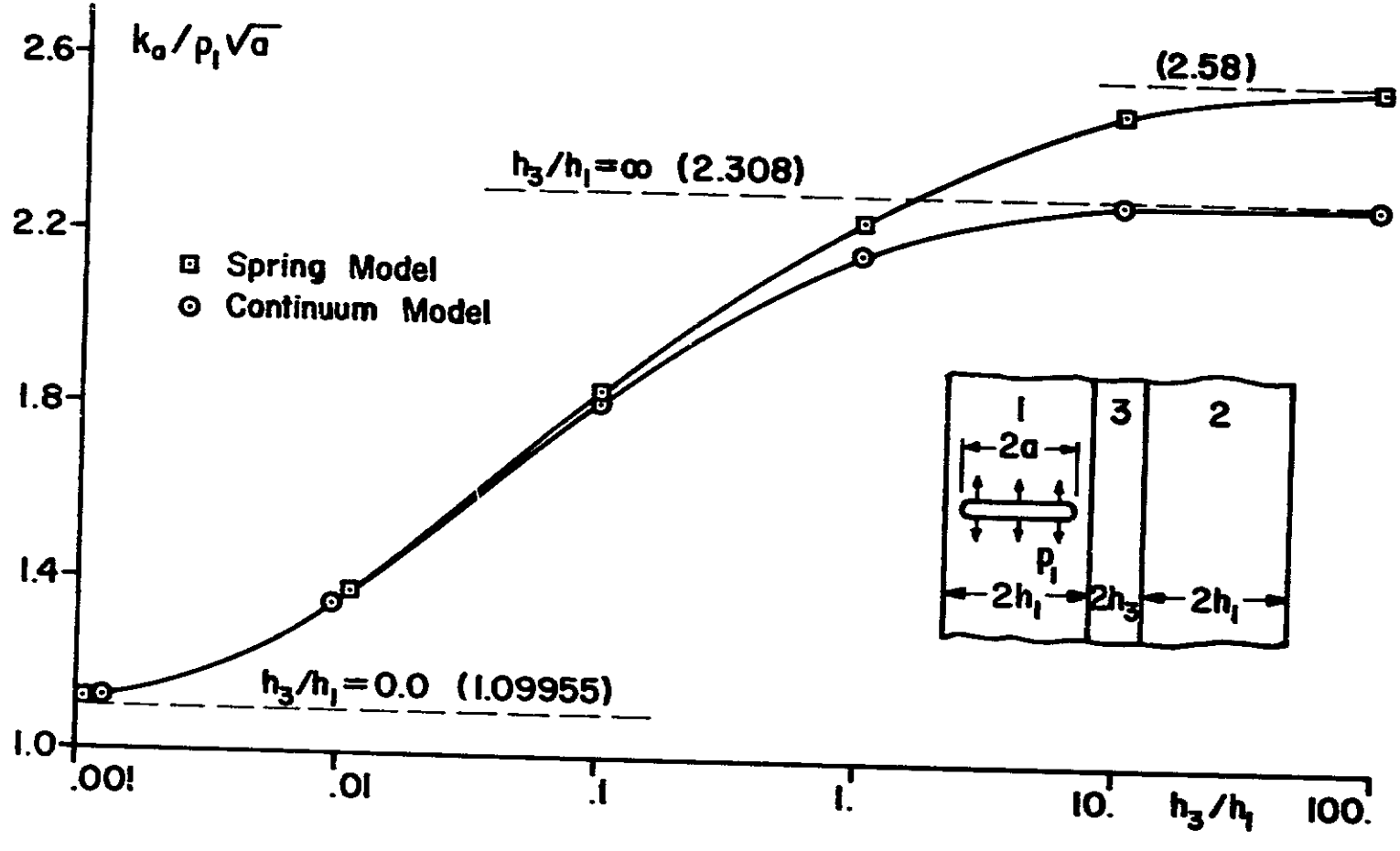

Figure 18. Comparison of two solutions for $a=0.9h_1$, plane stress case (Combination II).

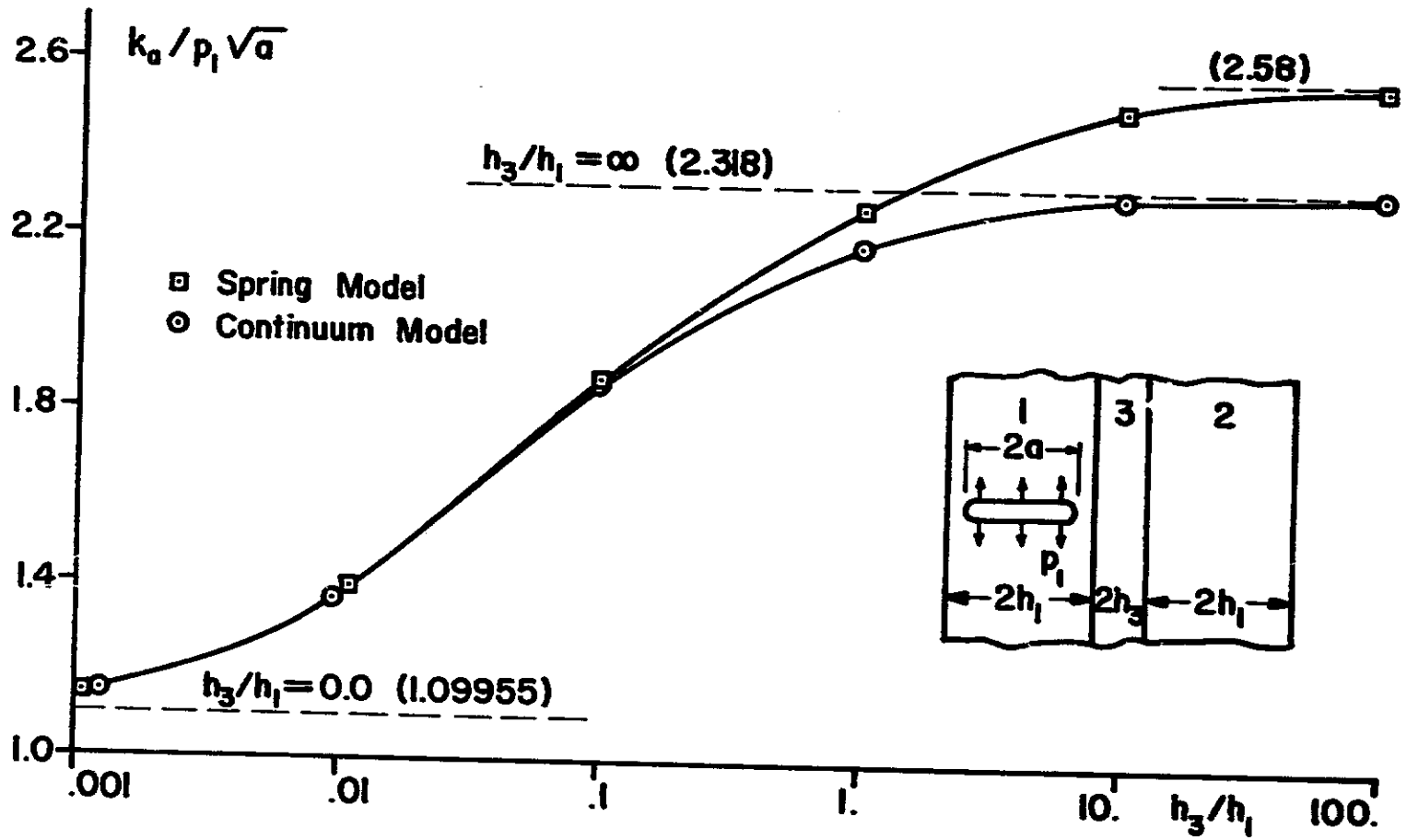

Figure 19. Comparison of two solutions for $a=0.9h_1$, plane strain case (Combination II).

C-2

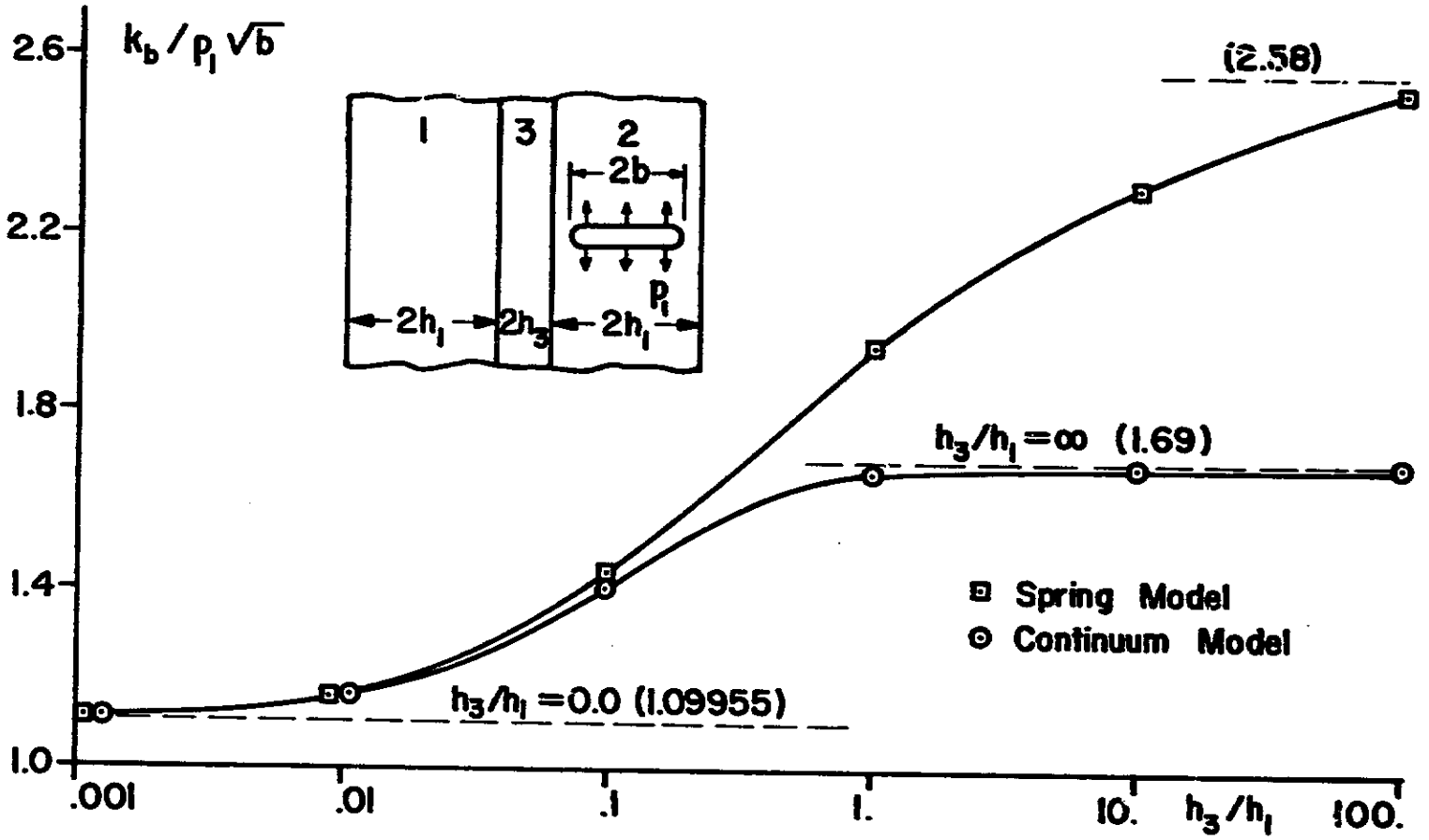

Figure 20. Comparison of two solutions for $b=0.9h_1$, plane stress case (Combination III).

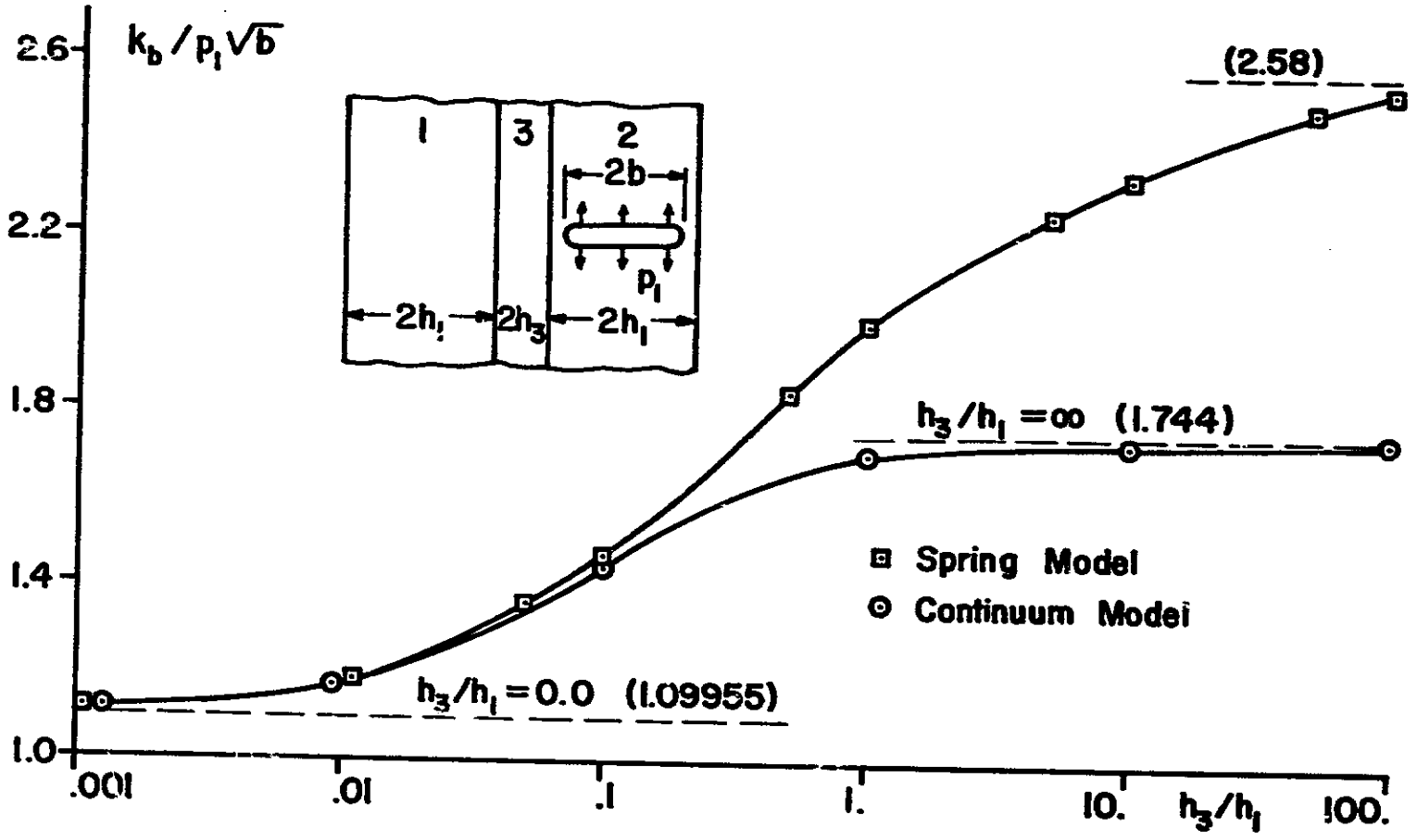

Figure 21. Comparison of two solutions for b=0.9h1, plane strain case (Combination III).

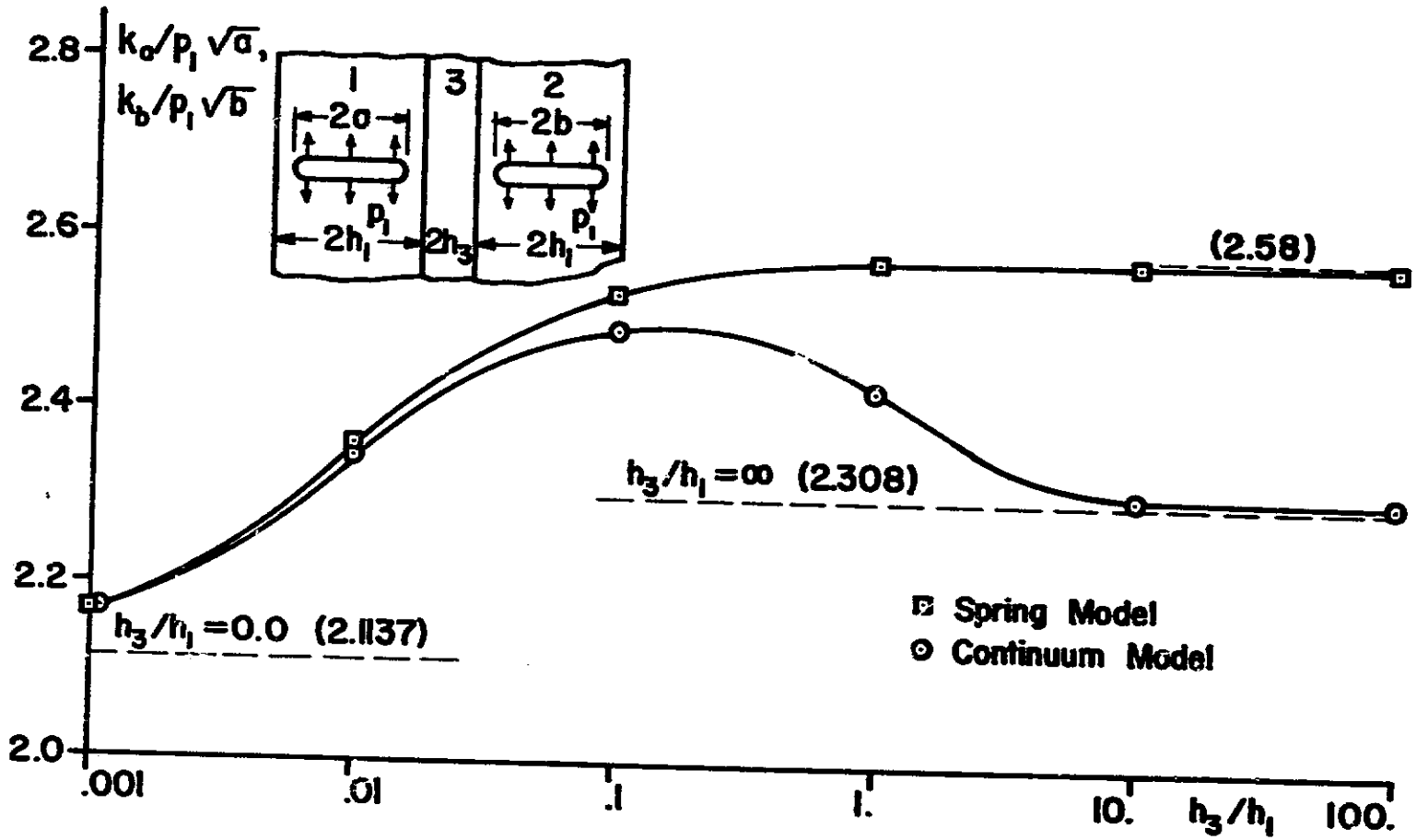

Figure 22. Comparison of two solutions for a=b=0.9h1, plane stress case (Combination II).

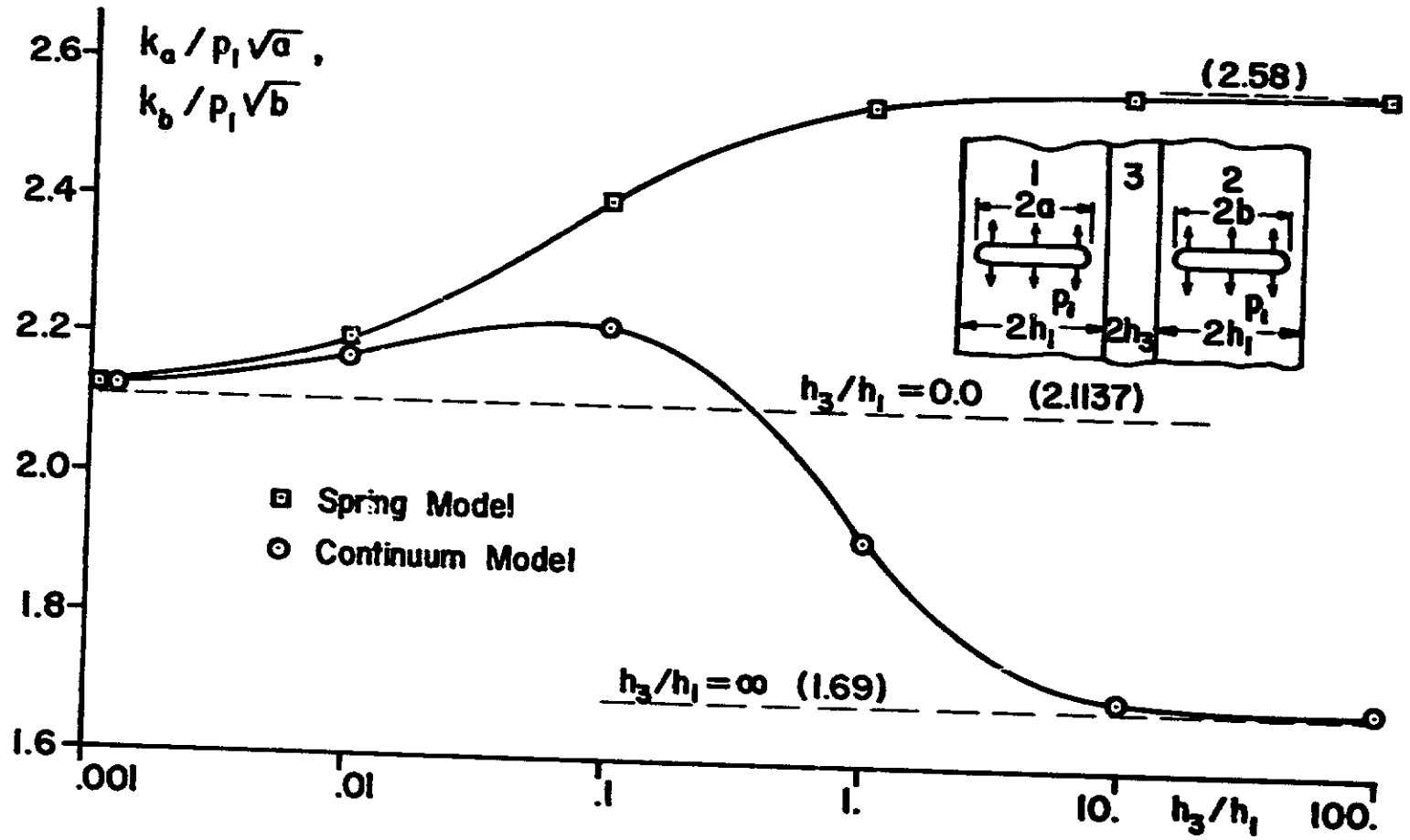

Figure 23. Comparison of two solutions for a=b=0.9h_1, plane stress case (Combination III).

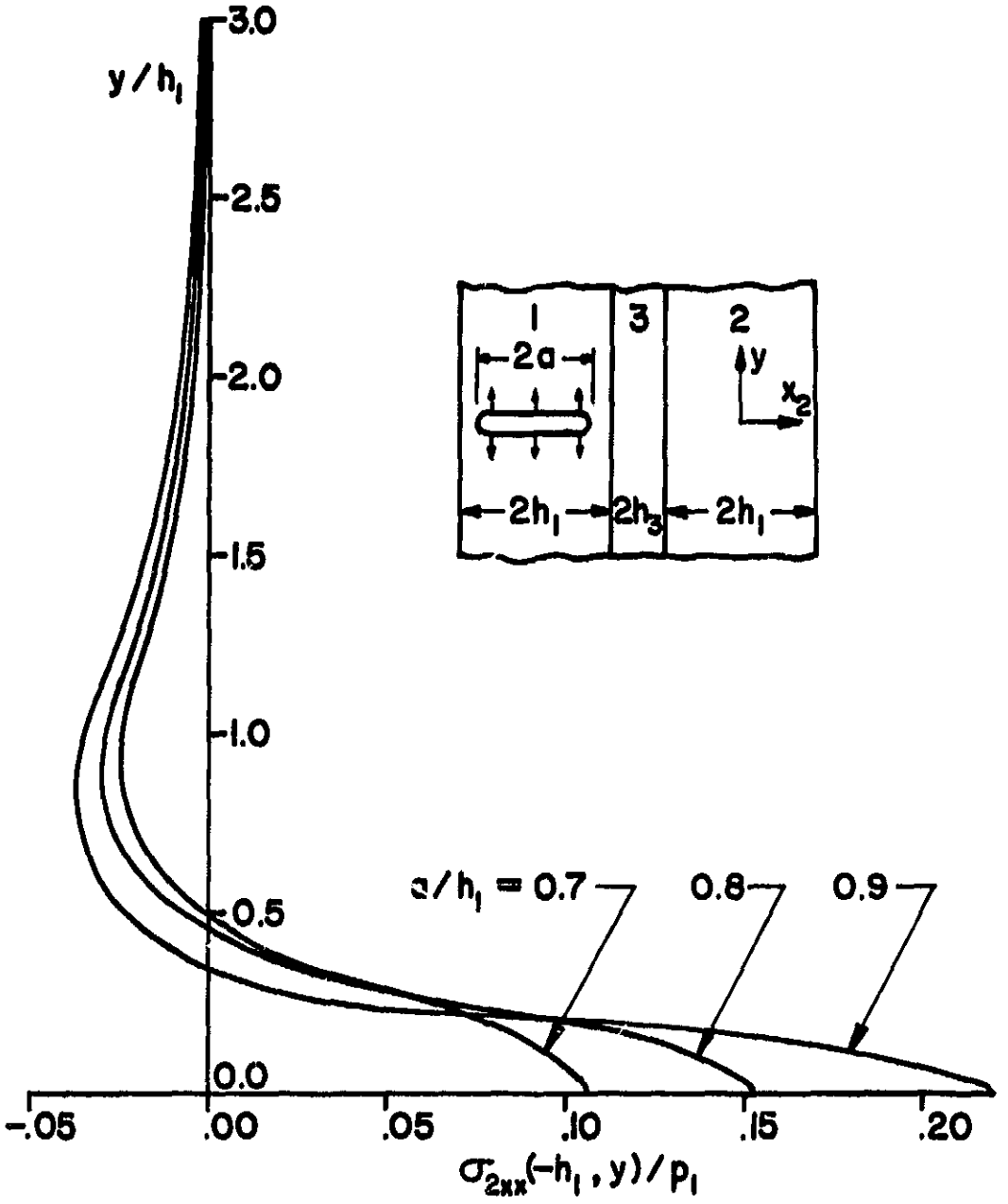

Figure 24. Distribution of the stress component σ_{2xx} at $x_2=-h_1$ for $h_3=0.05h_1$, plane stress case (Combination II).

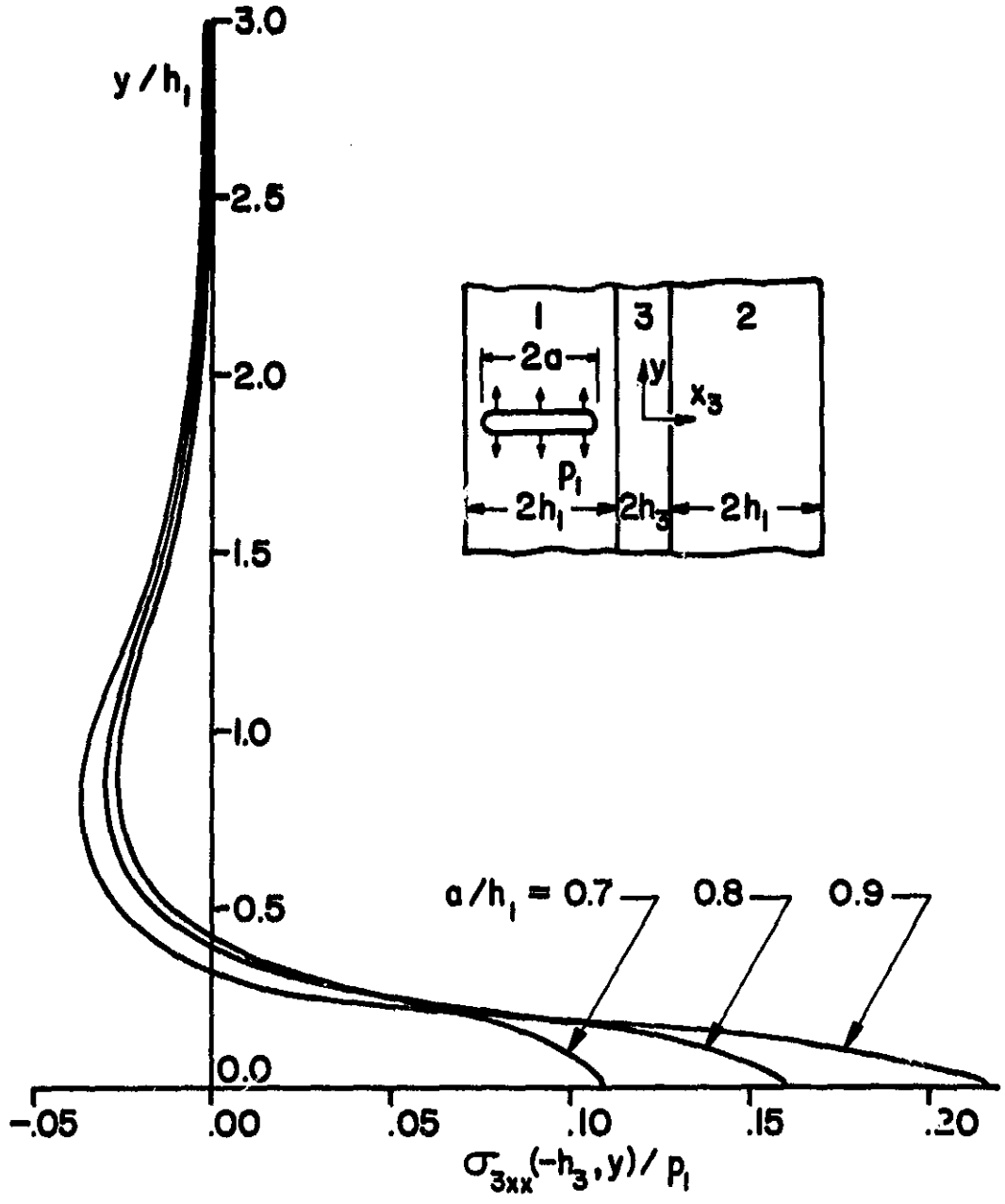

Figure 25. Distribution of the stress component σ_{3xx} at $x_3=-h_3$ for $h_3=0.05h_1$, plane stress case (Combination II).

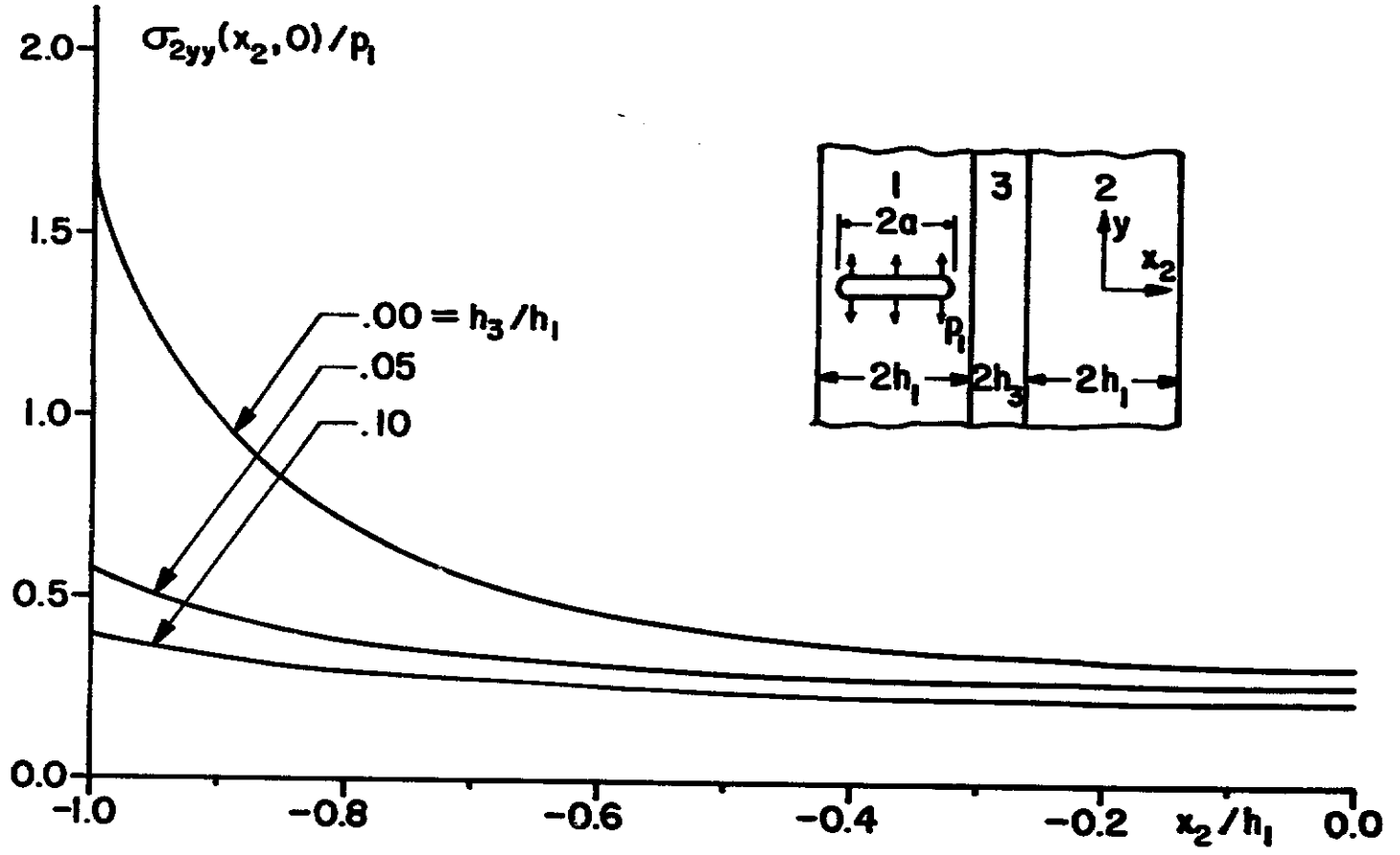

Figure 26. Distribution of the stress component σ_{2yy} on y=0 line for a=0.9h_1, plane stress case (Combination II).

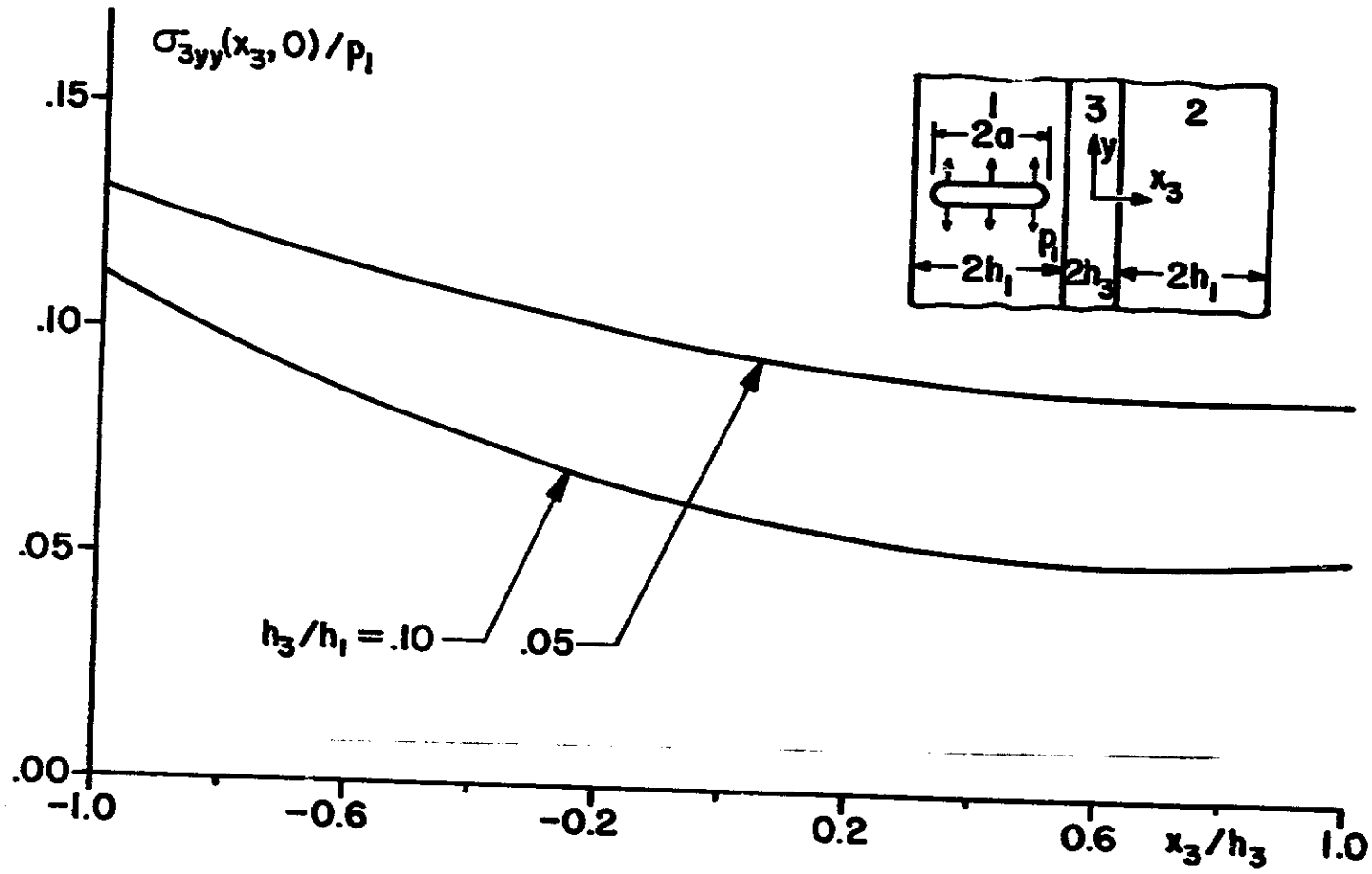

Figure 27. Distribution of the stress component σ_{3yy} at y=0 for a= $0.9h_1$, plane stress case (Combination II).

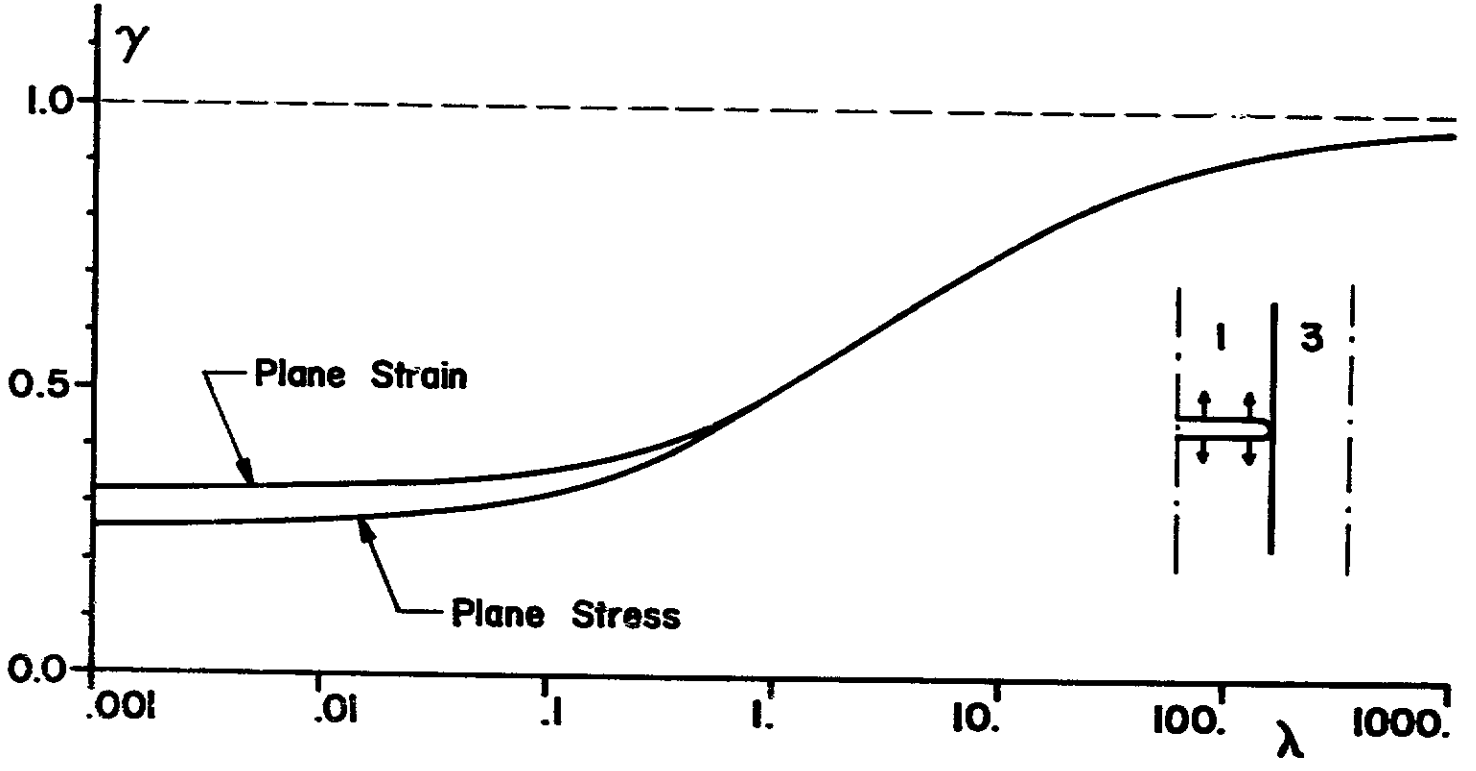

Figure 28. Variation of γ with $\lambda=\mu_1/\mu_3$ for $\nu_1=\nu_3=0.35$.

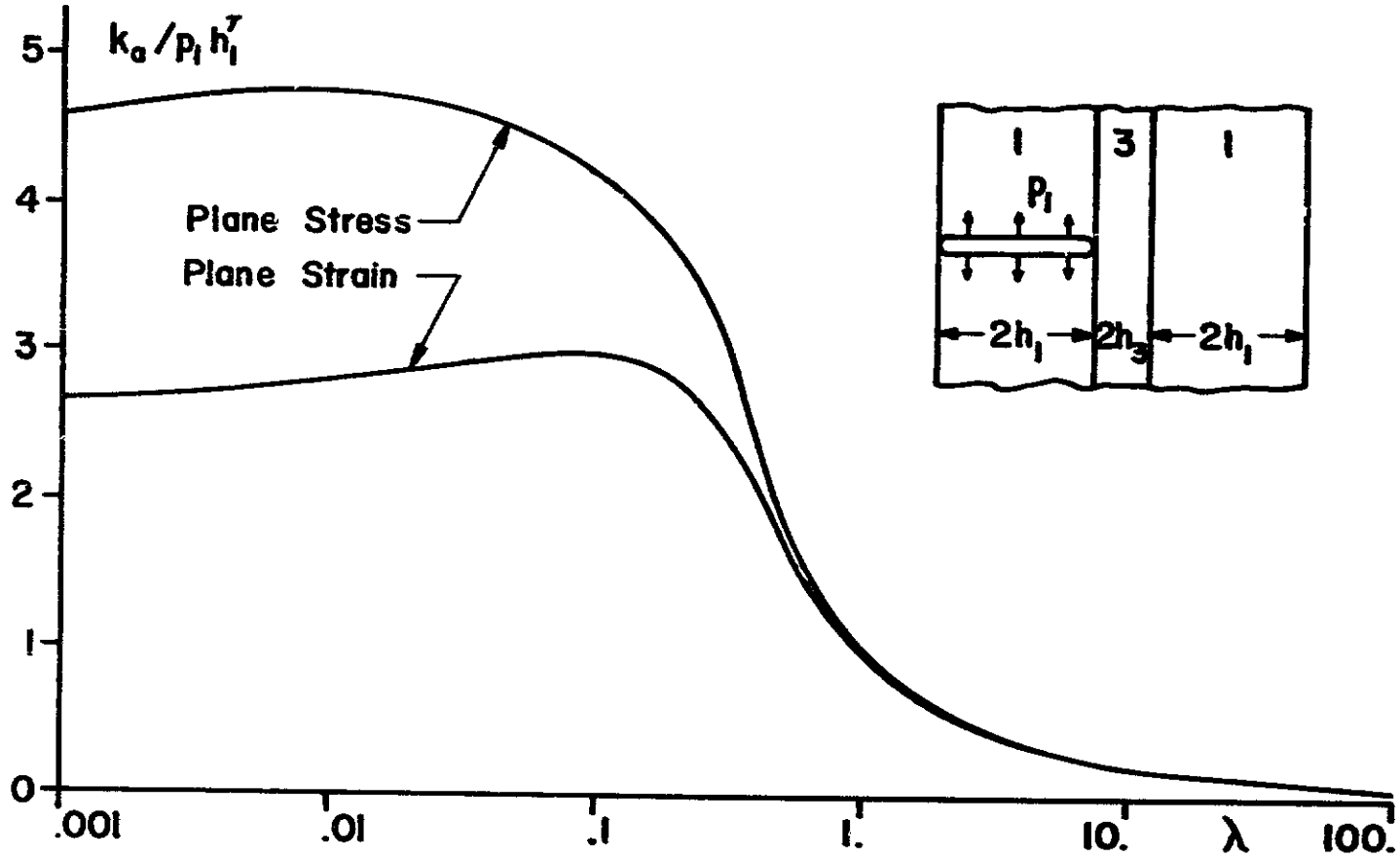

Figure 29. Variation of the stress intensity factor with $\lambda=\mu_1/\mu_3$ for $a=h_1$, $h_3=0.05h_1$, $\nu_1=\nu_3=0.35$.

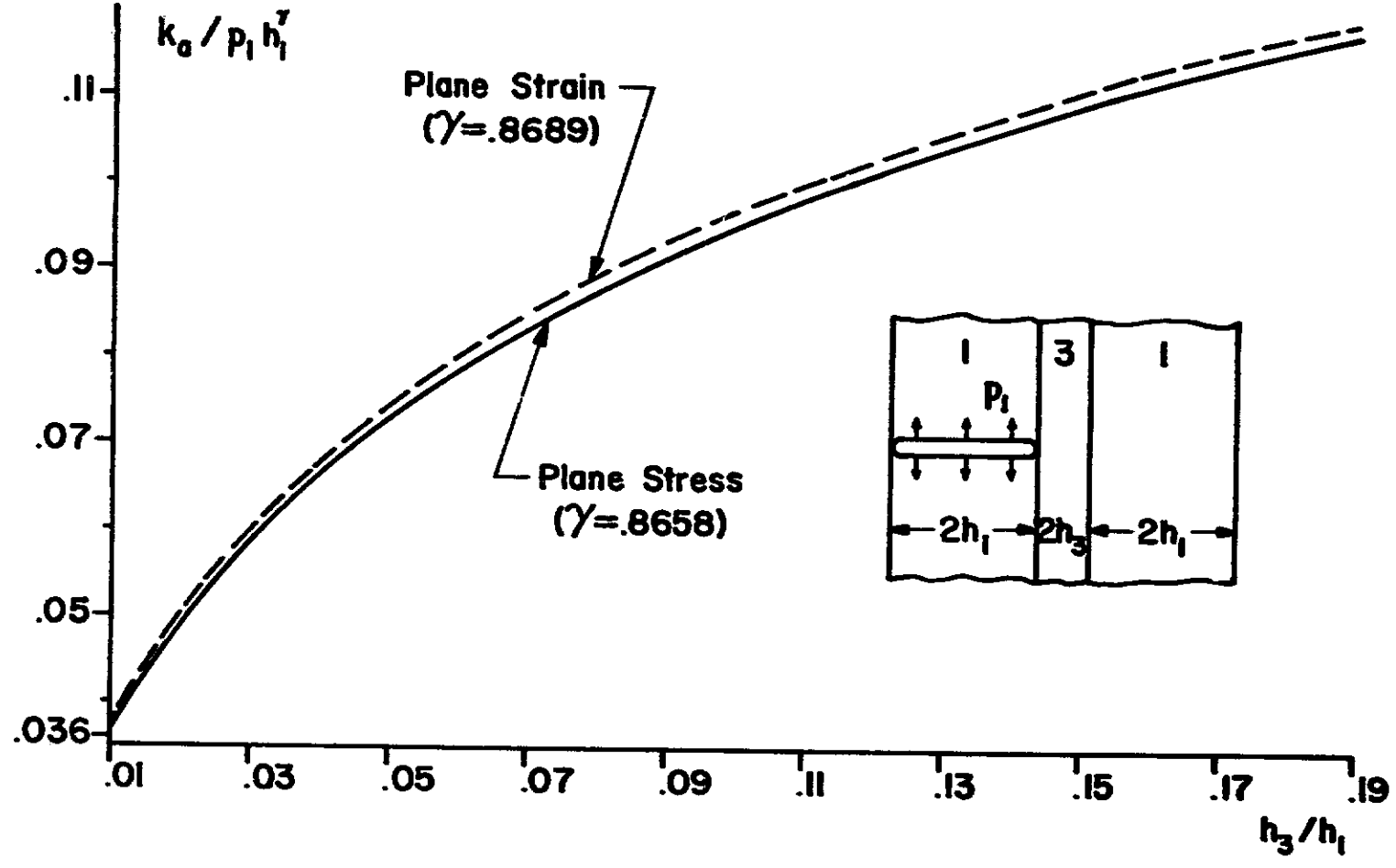

Figure 30. Variation of the stress intensity factor with h_3/h_1 for $a=h_1$ (Combination II).

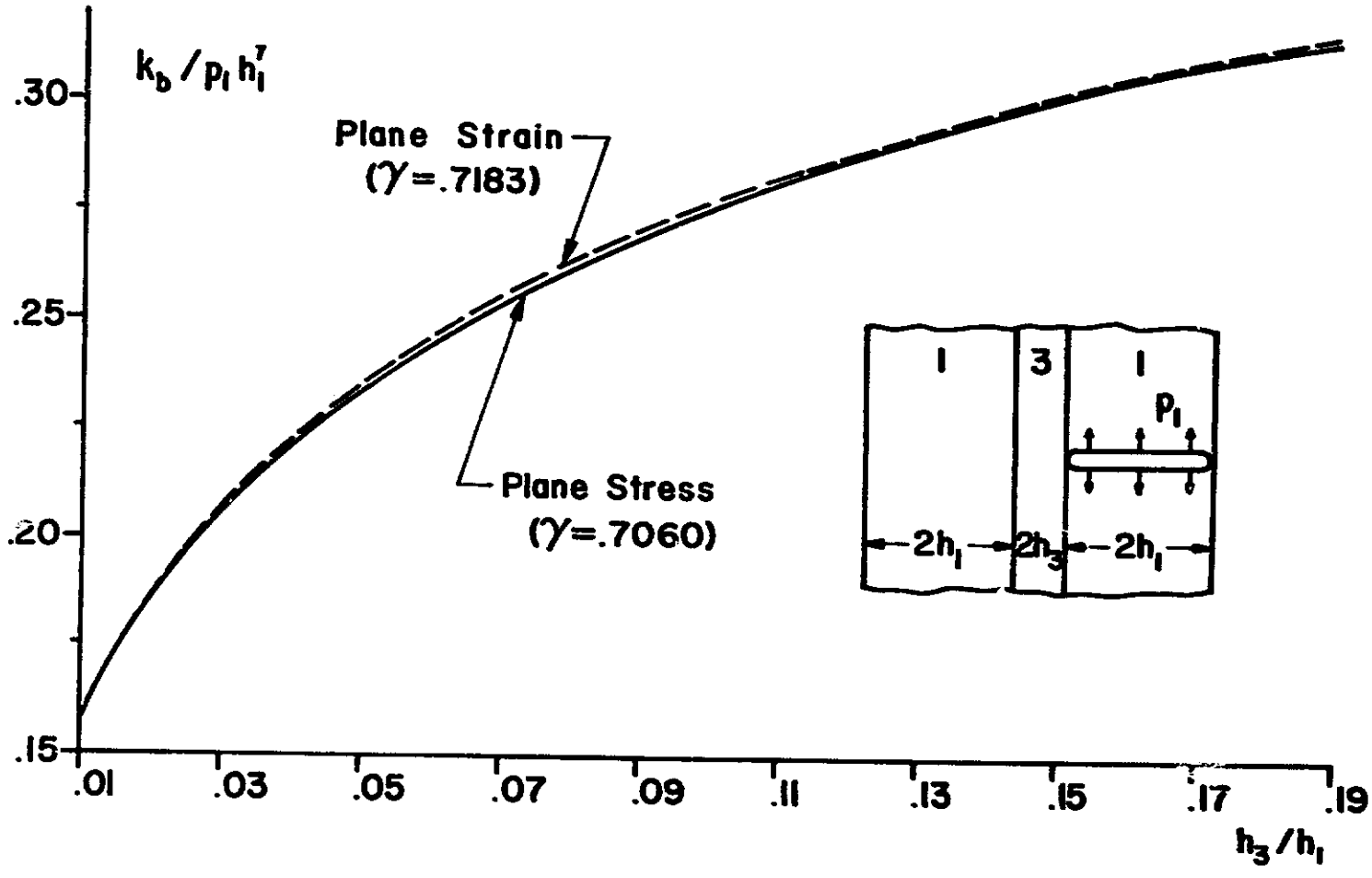

Figure 31. Variation of the stress intensity factor with h_3/h_1 for $a=h_1$ (Combination III).

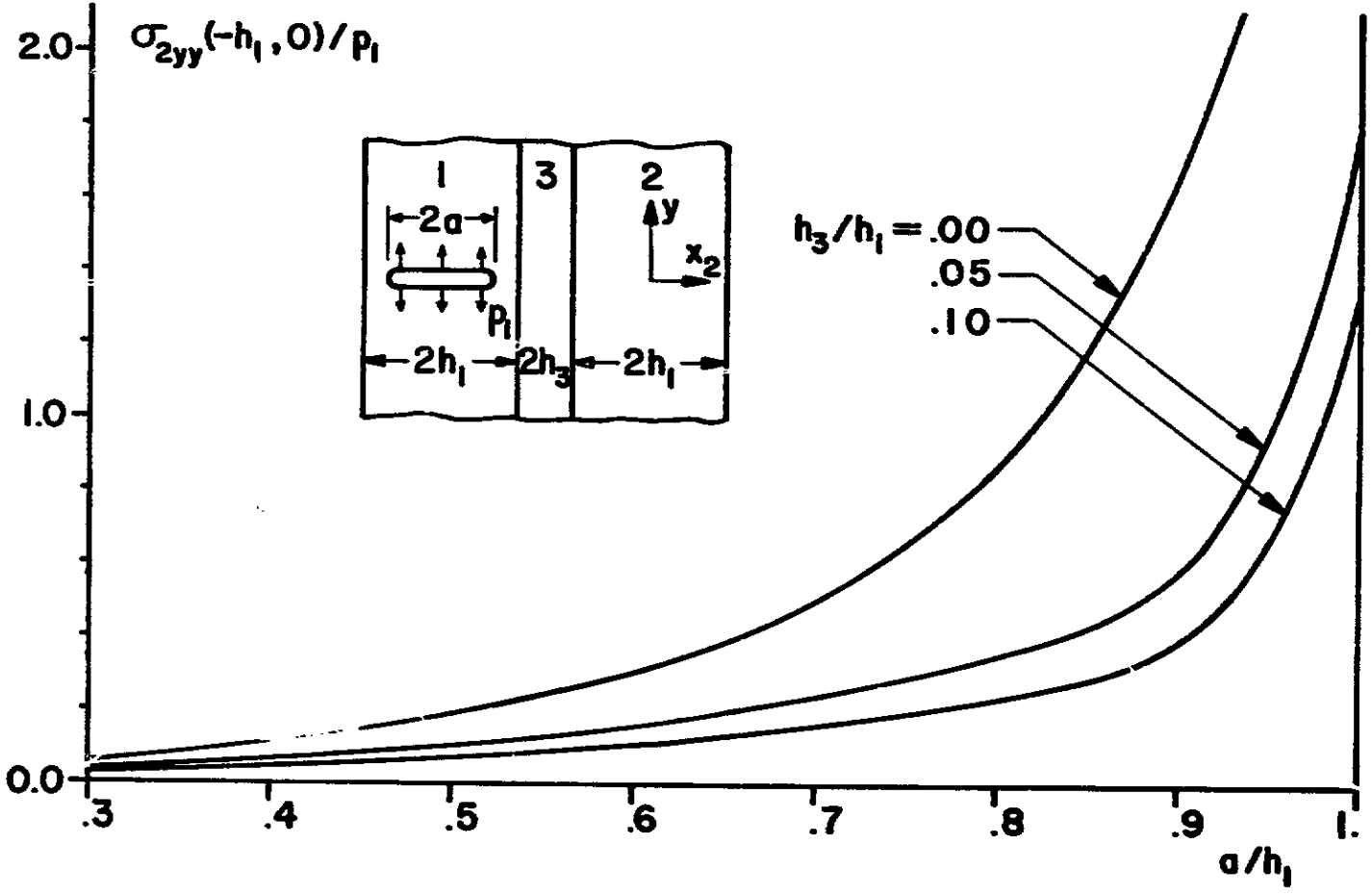

Figure 32. Variation of the cleavage stress $\sigma_{2yy}(-h_1,0)$ for plane stress case as the crack propagates (Combination II).

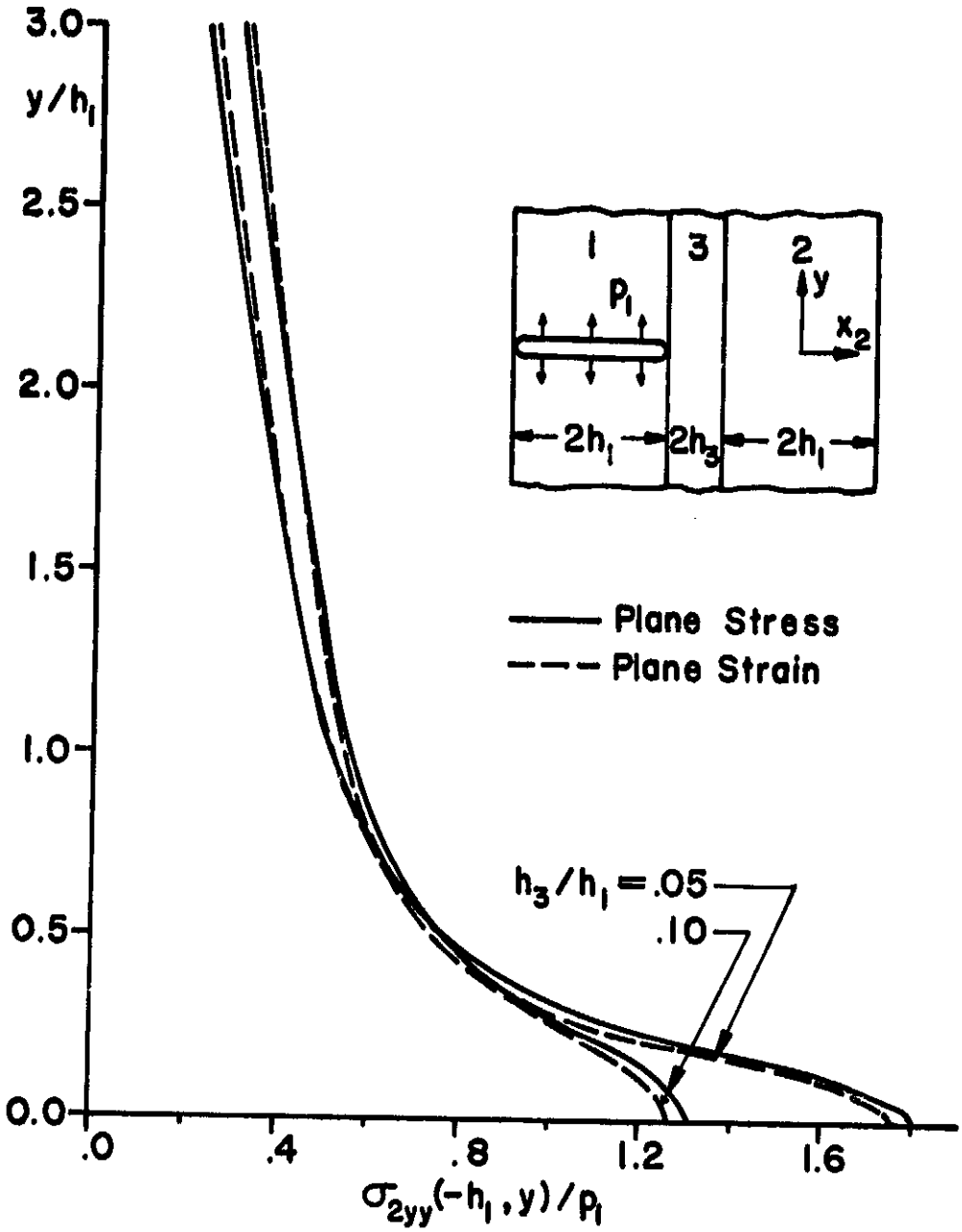

Figure 33. Variation of σ_{2yy} along the line $x_2=-h_1$ for $a=h_1$ (Combination II).

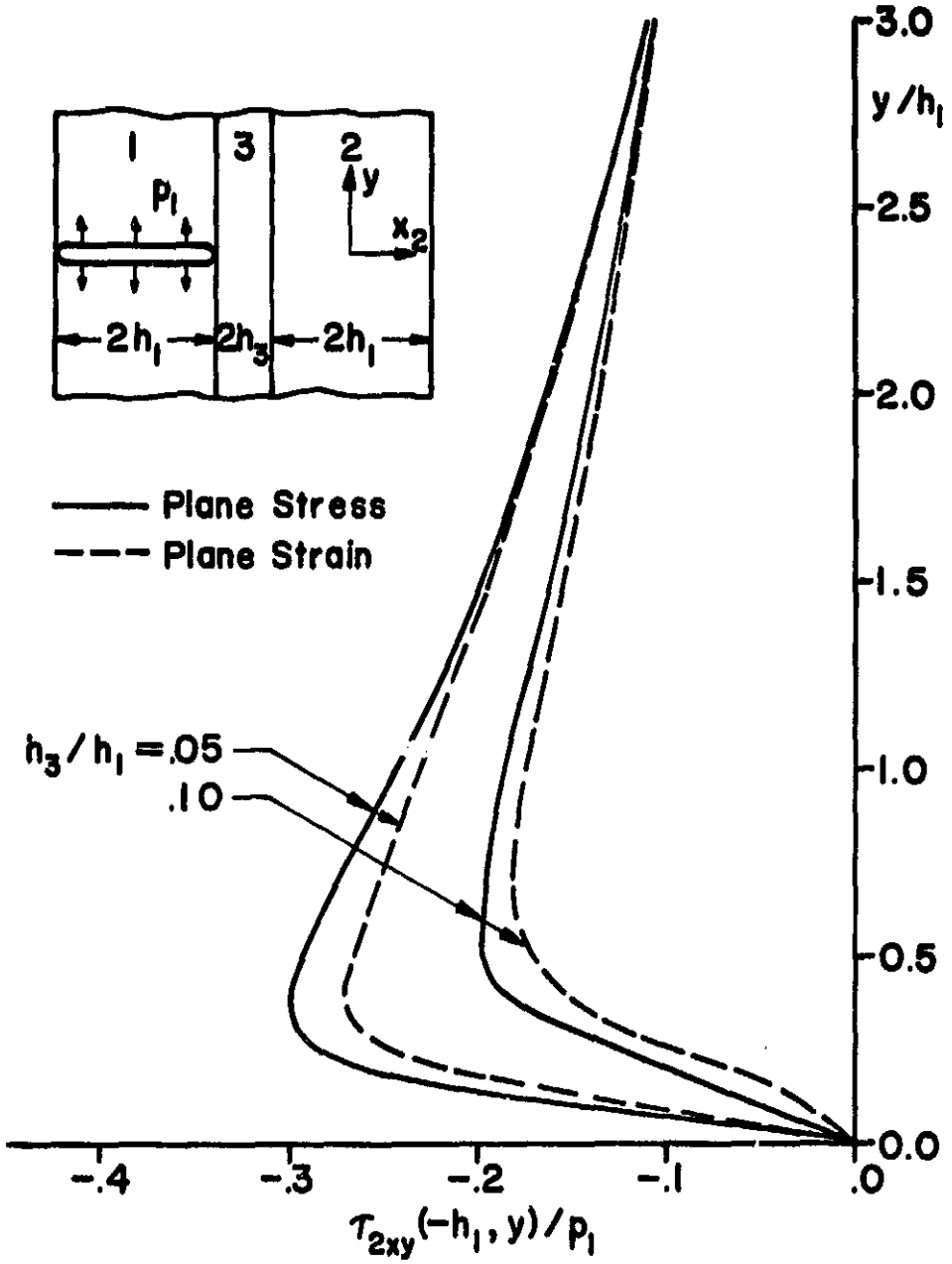

Figure 34. Variation of the shear stress τ_{2xy} along the line $x_2=-h_1$ for $a=h_1$ (Combination II).

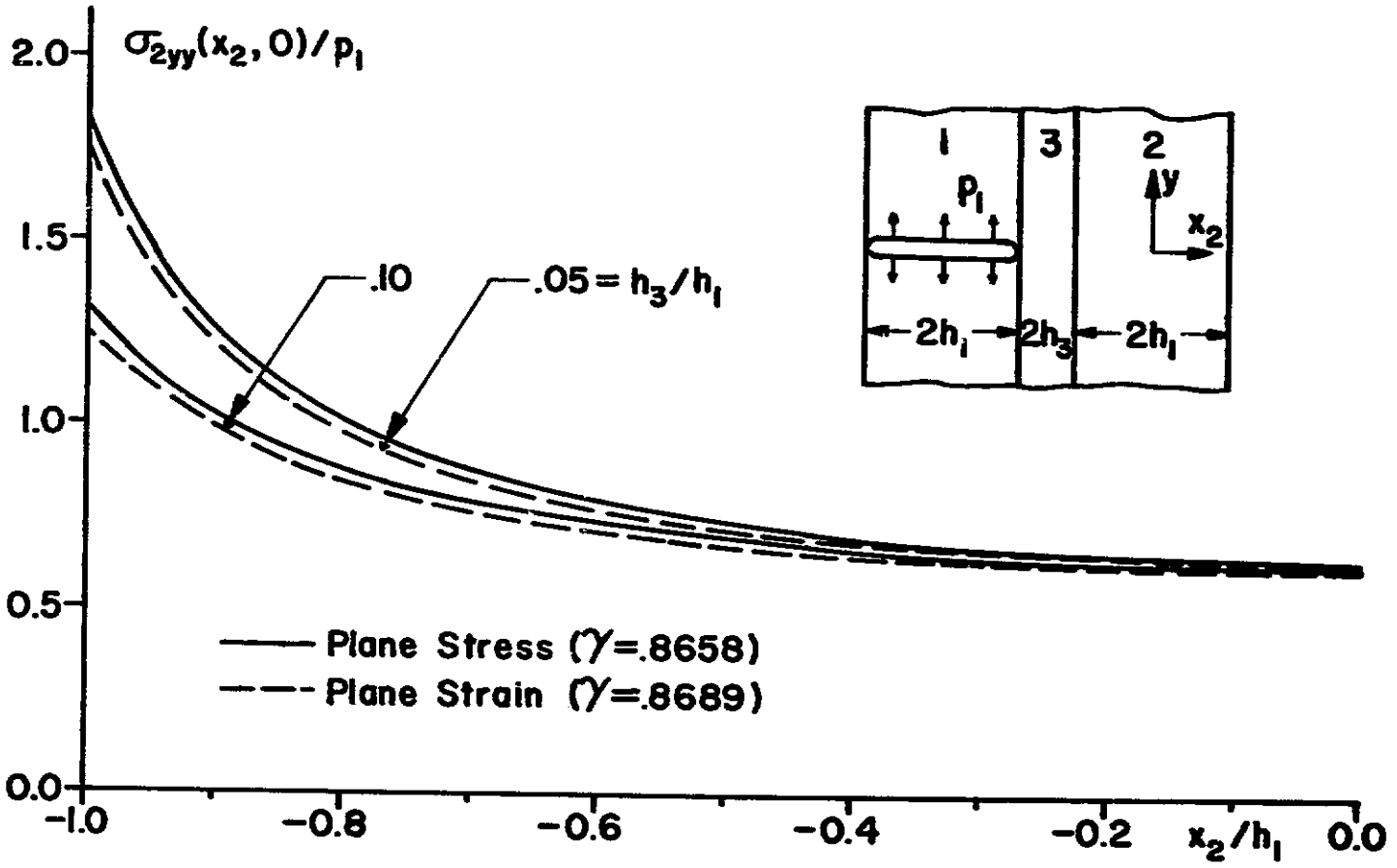

Figure 35. Distribution of the stress component σ_{2yy} at y=0 for a=h_1 (Combination II).

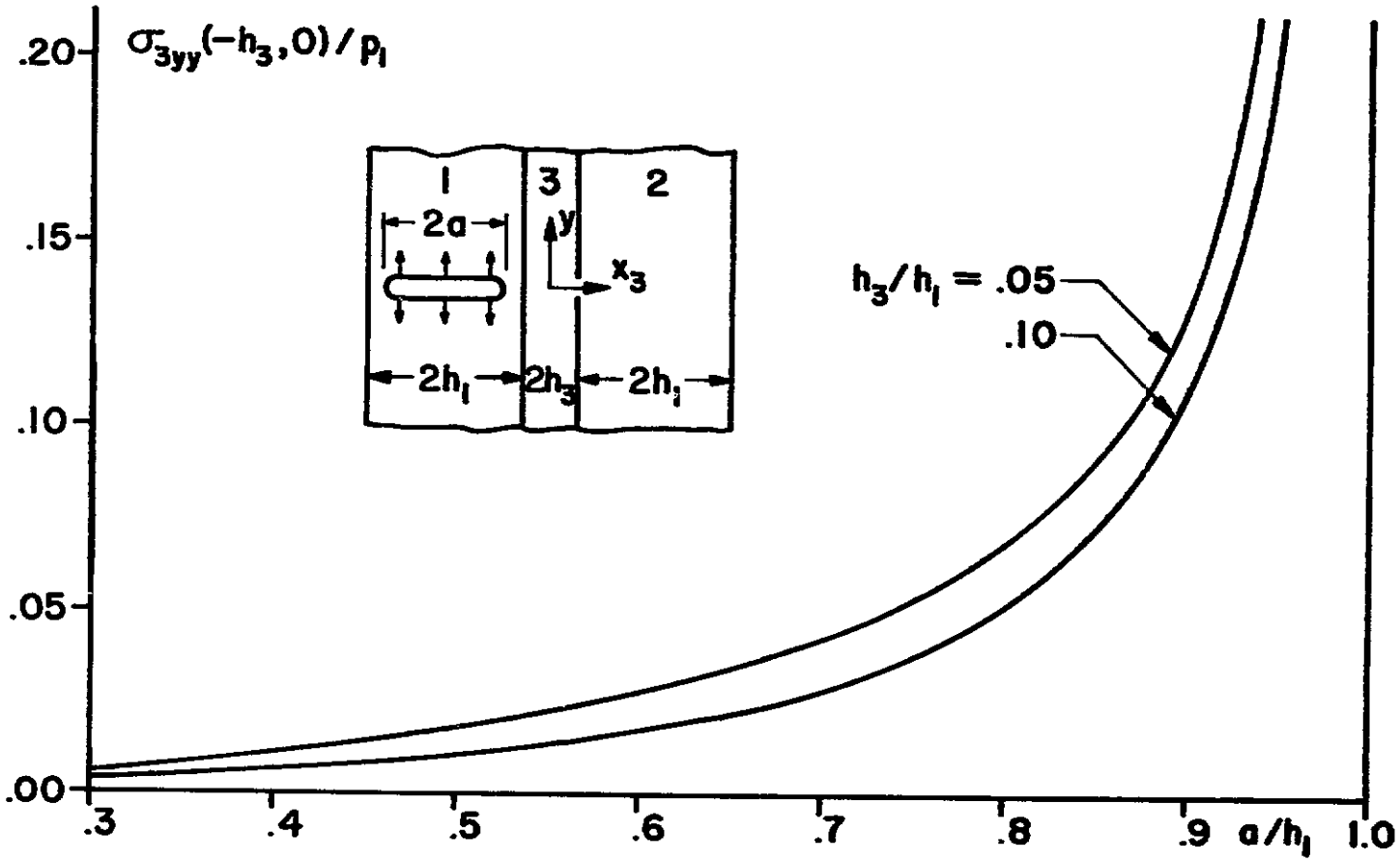

Figure 36. Variation of the cleavage stress in the adhesive layer as the crack approaches interface for plane stress case (Combination II).

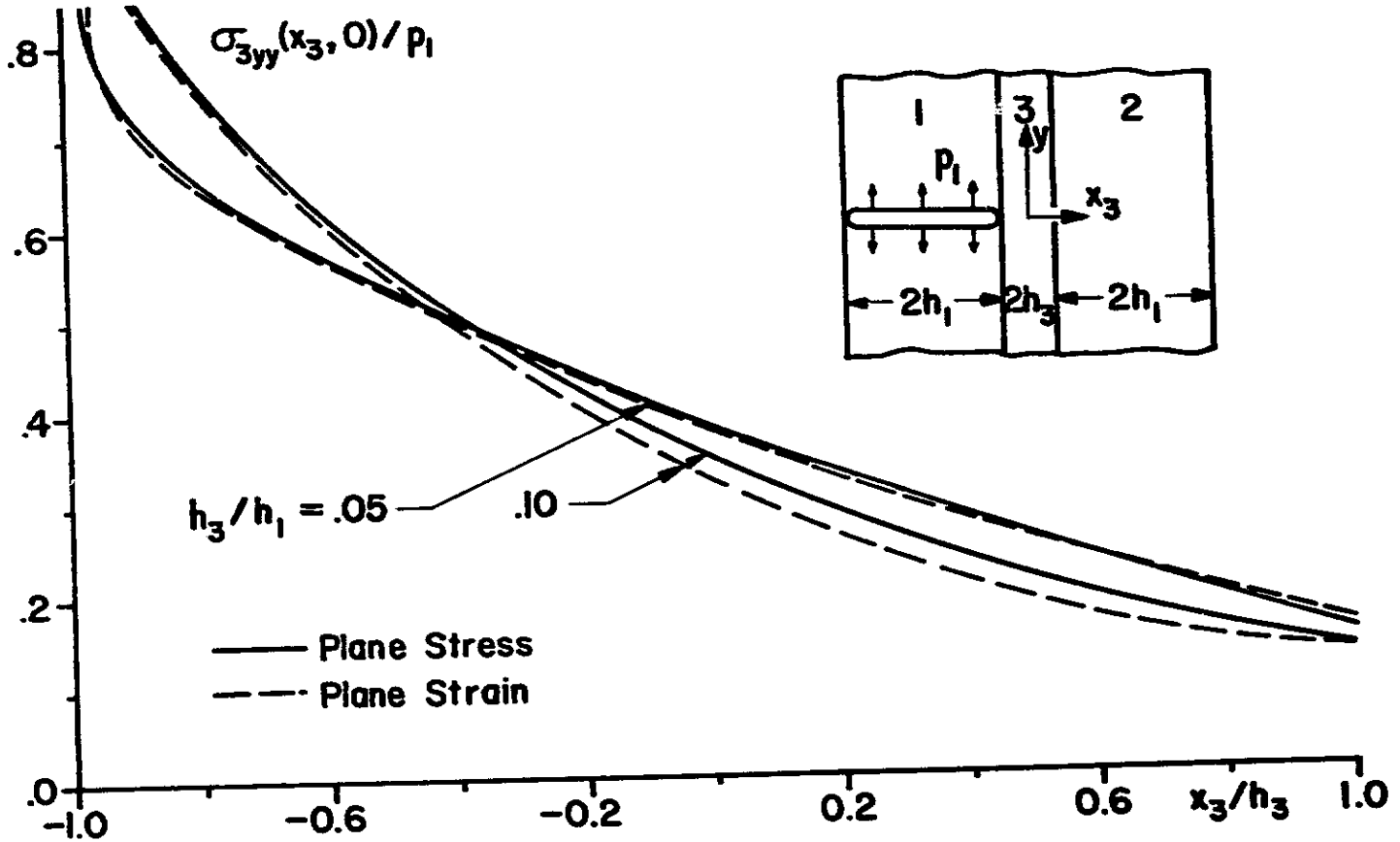

Figure 37. Distribution of the stress component σ_{3yy} at $y=0$ for $a=h_1$ (Combination II).

REFERENCES

1. Irwin, G. R., "Fracture Mechanics", in *Structural Mechanics*, Goodier and Hoff, ed., Pergamon Press, 1960.

2. Bennett, S. J., DeVries, K. L. and Williams, M. L., "Adhesive Fracture Mechanics", *Int. J. Fracture*, Vol. 10 (1974) p. 33.

3. Erdogan, F., "Approximate Solution of Systems of Singular Integral Equations", *SIAM J. Appl. Math.*, Vol. 17 (1969) p. 1041.

4. Erdogan, F., "Complex Function Technique", in *Treatise on Continuum Physics*, Eringen, A. C., ed., Vol. II, Ch. 2, Academic Press, 1974.

5. Erdogan, F. and Bakioglu, M., "Fracture of Composite Plates Containing Periodic Buffer Strips", NASA Technical Report, Grant NGR 39-007-011, Lehigh University, Oct. 1974.

6. Eisenmann, J. R. and Kaminski, B. E., "Fracture Control for Composite Structures", *Engng. Fracture Mech.*, Vol. 4 (1972) p. 907.

7. Delale, F. and Erdogan, F., "Fracture of Composite Orthotropic Plates Containing Periodic Buffer Strips", NASA Technical Report, Grant NGR 39-007-011, Lehigh University, Jan. 1976.

8. Erdogan, F. and Civelek, M. B., "Contact Problem for an Elastic Reinforcement Bonded to an Elastic Plate", *J. Appl Mech., Trans. ASME*, Vol. 41 (1974) p. 1014.

9. Erdogan, F. and Arin, K., "A Sandwich Plate with a Part-through and a Debonding Crack", *J. Engng. Frac. Mech.*, Vol. 4 (1972) p. 449.

10. Williams, M. L., "The Fracture Threshold for an Adhesive Interlayer", *J. Appl. Polym. Sci.*, Vol. 14 (1970) p. 1121.

11. Updike, D. P., "The Effect of Adhesive Layer Elasticity on the Fracture Mechanics of a Blister Test Specimen", NASA Technical Report, Grant NGR 39-007-011, Lehigh University, Sept. 1975.

12. Muskhelishvili, N. I., *Singular Integral Equations*, Groningen: Wolters-Noordhoff Publishing, 1958.

13. Timoshenko, S. P. and Goodier, J. N., *Theory of Elasticity*, 3rd ed., New York: McGraw-Hill, 1970.

14. Sneddon, I. N. and Srivastav, R. P., "The Stress Field in the Vicinity of a Griffith Crack in a Strip of Finite Width", *Int. J. Engng. Sci.*, Vol. 9 (1971) p. 479.

15. Isida, M., "Laurent Series Expansion for Internal Crack Problems", in *Methods of Analysis and Solutions of Crack Problems*, Sih, G. C., ed., Vol. 1, Leyden: Noordhoff Int. Publishing, 1972.

16. Bogy, D. B., "The Plane Elastostatic Solution for a Symmetrically Loaded Crack in a Strip Composite", *Int. J. Engng. Sci.*, Vol. 11 (1973) p. 985.

17. Erdogan, F., Gupta, G. D. and Cook, T. S., "Numerical Solution of Singular Integral Equations", in *Methods of Analysis and Solutions of Crack Problems*, Sih, G. C., ed., Vol. 1, Leyden: Noordhoff Int. Publishing, 1972.

18. Krenk, S., "A Note on the Use of the Interpolation Polynomial for Solutions of Singular Integral Equations", Technical Report, Lehigh University, Aug. 1973.

19. Davis, P. J. and Rabinowitz, P., *Numerical Integration*, Blaisdell Publishing Co., 1967.

20. Gupta, G. D. and Erdogan, F., "The Problem of Edge Cracks in an Infinite Strip", *J. Appl. Mech., Trans. ASME*, Vol. 41 (1974) p. 1001.

21. Gupta, G. D., "A Layered Composite with a Broken Laminate", *Int. J. Solids, Structures*, Vol. 10 (1973) p. 1141.

22. Erdogan, F. and Biricikoglu, V., "Two Bonded Half Planes with a Crack Going through the Interface", *Int. J. Engng. Sci.*, Vol. 11 (1973) p. 745.

23. Cook, T. S. and Erdogan, F., "Stresses in Bonded Materials with a Crack Perpendicular to the Interface", *Int. J. Engng. Sci.*, Vol. 10 (1972) p. 677.

24. Conte, S. D. and DeBoor, C., *Elementary Numerical Analysis*, 2nd ed., New York: McGraw-Hill, 1972.

25. Erdelyi, A., ed. *Tables of Integral Transforms*, Vol. 1, New York: McGraw-Hill, 1953.

APPENDIX A

Evaluation of some integrals [21], [25]:

$$\int_0^\infty e^{-ry}\cos(ys)dy = \frac{r}{r^2+s^2} \quad , \quad r>0 \quad ,$$

$$\int_0^\infty e^{-ry}\sin(ys)dy = \frac{s}{r^2+s^2} \quad , \quad r>0 \quad , \qquad \text{(A.1a-d)}$$

$$\int_0^\infty ye^{-ry}\cos(ys)dy = \frac{r^2-s^2}{(r^2+s^2)^2} \quad , \quad r>0 \quad ,$$

$$\int_0^\infty ye^{-ry}\sin(ys)dy = \frac{2rs}{(r^2+s^2)^2} \quad , \quad r>0 \quad .$$

$$\int_0^\infty \frac{1}{r(r^2+s^2)}\sin(ry)dr = \frac{\pi}{2s^2}(1-e^{-sy}) \quad ,$$

$$\int_0^\infty \frac{r}{(r^2+s^2)^2}\sin(ry)dr = \frac{\pi}{4s}ye^{-sy} \quad ,$$

$$\int_0^\infty \frac{1}{r^2+s^2}\cos(ry)dr = \frac{\pi}{2s}e^{-sy} \quad , \qquad \text{(A.2a-e)}$$

$$\int_0^\infty \frac{s^2}{(r^2+s^2)^2}\cos(ry)dr = \frac{\pi}{4s}(1+sy)e^{-sy}$$

$$\int_0^\infty \frac{r^2}{(r^2+s^2)^2}\cos(ry)dr = \frac{\pi}{4s}(1-sy)e^{-sy} \quad .$$

APPENDIX B

Expressions of the functions used in Eqs. (2.16) and (2.17):

$$F_{i1}(s) = \frac{2s}{\pi}\int_0^\infty m_i(r)\left[2s^2 + \frac{\kappa_i - 3}{2}(r^2+s^2)\right]\frac{\sin(h_i r)}{(r^2+s^2)^2}\,dr \ ,$$

$$F_{i2}(s) = \frac{2s^2}{\pi}\int_0^\infty m_i(r)\left[2r^2 + \frac{\kappa_i + 1}{2}(r^2+s^2)\right]\frac{\cos(h_i r)}{r(r^2+s^2)^2}\,dr \ ,$$

(B.1a-d)

$$F_{i3}(s) = \frac{4s^2}{\pi}\int_0^\infty m_i(r) r\,\frac{\cos(h_i r)}{(r^2+s^2)^2}\,dr \ ,$$

$$F_{i4}(s) = \frac{4s}{\pi}\int_0^\infty m_i(r) r^2\,\frac{\sin(h_i r)}{(r^2+s^2)^2}\,dr \ , \quad (i=1,2) \ .$$

The forms of the functions a_{ij}, b_{ij}, c_{ij}, d_{ij}, $(i=1,2; j=1\text{-}4)$ appearing in Eqs. (2.17) are as follows:

$$c_{11} = (q_5 q_{32} q_{35} + q_{31} q_{34})/D \ ,$$

$$c_{12} = (q_{31} q_{37} - q_5 q_{32} q_{38})/D \ ,$$

$$c_{13} = (q_{32} q_{39} - q_{31} q_{37})/D \ ,$$

$$c_{14} = (q_{31} q_{34} + q_{32} q_{40})/D \ ,$$

$$c_{21} = -(q_5 q_{30} q_{35} + q_{33} q_{34})/D \ ,$$

$$c_{22} = (q_5 q_{30} q_{38} - q_{33} q_{37})/D \ ,$$

$$c_{23} = (q_{33} q_{37} - q_{30} q_{39})/D \ ,$$

$$c_{24} = -(q_{30} q_{40} + q_{33} q_{34})/D \ ,$$

$$d_{11} = c_{11} \quad , \quad d_{12} = -c_{12} \quad ,$$

$$d_{13} = (q_{31}q_{41} - q_{32}q_{42})/D \quad ,$$

$$d_{14} = (q_{31}q_{43} + q_{32}q_{44})/D \quad ,$$

$$d_{21} = c_{21} \quad , \quad d_{22} = -c_{22} \quad ,$$

$$d_{23} = (q_{30}q_{42} - q_{33}q_{41})/D \quad ,$$

$$d_{24} = -(q_{30}q_{44} + q_{33}q_{43})/D \quad ,$$

$$a_{21} = -(\lambda_1 q_{27}c_{11} + q_{36}c_{21})/q_5 \quad ,$$

$$a_{22} = -(\lambda_1 q_{27}c_{12} + q_{36}c_{22})/q_5 \quad ,$$

$$a_{23} = (\lambda_1 q_1 - \lambda_1 q_{27}c_{13} - q_{36}c_{23})/q_5 \quad ,$$

$$a_{24} = (\lambda_1 q_2 - \lambda_1 q_{27}c_{14} - q_{36}c_{24})/q_5 \quad ,$$

$$b_{21} = a_{21} \quad , \quad b_{22} = -a_{22} \quad ,$$

$$b_{23} = -(q_1 + \lambda_1 q_{27}d_{13} + q_{36}d_{23})/q_5 \quad ,$$

$$b_{24} = (q_2 - \lambda_1 q_{27}d_{14} - q_{36}d_{24})/q_5 \quad ,$$

$$a_{11} = (\lambda_2 q_4 a_{21} - sh_1 q_1 c_{11} + \lambda_2 sh_2 q_3 c_{21})/q_2 \quad ,$$

$$a_{12} = (\lambda_2 q_4 a_{22} - sh_1 q_1 c_{12} + \lambda_2 sh_2 q_3 c_{22})q_2^{-1} \quad ,$$

$$a_{13} = (-1 + \lambda_2 q_4 a_{23} - sh_1 q_1 c_{13} + \lambda_2 sh_2 q_3 c_{23})/q_2 \quad ,$$

$$a_{14} = (\lambda_2 q_4 a_{24} - sh_1 q_1 c_{14} + \lambda_2 sh_2 q_3 c_{24})/q_2 \quad ,$$

$$b_{11} = a_{11} \ , \quad b_{12} = -a_{12} \ ,$$

$$b_{13} = (\lambda_2 + \lambda_2 q_4 b_{23} - sh_1 q_1 d_{13} + \lambda_2 sh_2 q_3 d_{23})/q_2 \ ,$$

$$b_{14} = (\lambda_2 q_4 b_{24} - sh_1 q_1 d_{14} + \lambda_2 sh_2 q_3 d_{24})/q_2 \ , \qquad (B.2)$$

where

$$D = q_{30} q_{31} - q_{32} q_{33} \ , \qquad (B.3)$$

$$q_1 = (1-e^{-2sh_1})/2 \ , \quad q_2 = (1+e^{-2sh_1})/2 \ ,$$

$$q_3 = (1-e^{-2sh_2})/2 \ , \quad q_4 = (1+e^{-2sh_2})/2 \ ,$$

$$q_5 = [1-e^{-2s(h_1+h_2)}]/2 \ , \quad q_6 = [1+e^{-2s(h_1+h_2)}]/2 \ ,$$

$$q_7 = (e^{-2sh_2}-e^{-2sh_1})/2 \ , \quad q_8 = (e^{-2sh_1}+e^{-2sh_2})/2 \ ,$$

$$q_9 = (1-e^{-4sh_1})/2 \ , \quad q_{10} = (1+e^{-4sh_1})/2 \ ,$$

$$q_{11} = (1-e^{-4sh_2})/2 \ , \quad q_{12} = (1+e^{-4sh_2})/2 \ ,$$

$$q_{13} = (1+\kappa_1)(\lambda_2-1)q_7/2 \ ,$$

$$q_{14} = (1+\kappa_1)\lambda_2 sh_o(\lambda_4 q_2 q_4 - \lambda_3 q_1 q_3) \ ,$$

$$q_{15} = (1+\kappa_2) q_5 q_7/2 \ ,$$

$$q_{16} = 2s^2 h_o h_2 (\lambda_3 q_1^2 - \lambda_4 q_2^2) \ ,$$

$$q_{17} = -\lambda_3 sh_o q_1 q_3 \ , \quad q_{18} = \kappa_2 q_5 - q_7 \ ,$$

$$q_{19} = -\lambda_4 sh_o q_2 q_4 \ , \quad q_{20} = -\kappa_2 q_5 - q_7 \ ,$$

$$q_{21} = (1+\kappa_1)sh_0q_5[(\lambda_3-\lambda_4)e^{-2sh_1}-(\lambda_3+\lambda_4)q_{10}]/2 \ ,$$

$$q_{22} = (\kappa_2+\lambda_2)(1-\lambda_2)q_{11}/2 \ ,$$

$$q_{23} = (1+\kappa_2)\lambda_2sh_0[(\lambda_3-\lambda_4)e^{-2sh_2}-(\lambda_3+\lambda_4)q_{12}]/2 \ ,$$

$$q_{24} = sh_2e^{-2sh_2+q_{11}/2} \ , \quad q_{25} = (1-\lambda_1)sh_1q_5 \ ,$$

$$q_{26} = -(\kappa_1+\lambda_1)q_5q_9/2 \ , \quad q_{27} = sh_1e^{-2sh_1+q_9/2} \ ,$$

$$q_{28} = 4\lambda_3\lambda_4s^2h_0^2q_5 \ ,$$

$$q_{29} = 2\lambda_1sh_0(\lambda_3q_1q_3 + \lambda_4q_2q_4) \ ,$$

$$q_{30} = q_{13} + q_{14} \ ,$$

$$q_{31} = q_{15} + q_{16}e^{-2sh_2} + q_{17}q_{18} + q_{19}q_{20} \ ,$$

$$q_{32} = (1-\lambda_2)^2sh_2e^{-2sh_2} - q_{22} + q_{23} - 4\lambda_2^2\lambda_3\lambda_4s^2h_0^2q_{24} \ ,$$

$$q_{33} = q_{25}e^{-2sh_1} + q_{21} - q_{27}(q_{28}+q_{29}) + q_{26} \ ,$$

$$q_{34} = (\lambda_2-1)q_4 - 2\lambda_2\lambda_3sh_0q_3 \ ,$$

$$q_{35} = q_2 + 2\lambda_3sh_0q_1 \ ,$$

$$q_{36} = sh_2q_6 + (q_5-q_7)/2 \ ,$$

$$q_{37} = (\lambda_2-1)q_3 - 2\lambda_2\lambda_4sh_0q_4 \ ,$$

$$q_{38} = q_1 + 2\lambda_4sh_0q_1 \ ,$$

$$q_{39} = q_1q_{29} + 2\lambda_4sh_0q_2q_5 + (\lambda_1+4\lambda_3\lambda_4s^2h_0^2)q_1q_5 \ ,$$

$$q_{40} = q_2q_{29} + 2\lambda_3 sh_o q_1 q_5 + (\lambda_1+4\lambda_3\lambda_4 s^2h_o^2)q_2q_5 \quad ,$$

$$q_{41} = \lambda_2\{[\lambda_2(1-4\lambda_3\lambda_4 s^2h_o^2)-1]q_3 - 2\lambda_4 sh_o q_4\} \quad ,$$

$$q_{42} = q_1(q_5+\lambda_2 q_{29}) \quad ,$$

$$q_{43} = \lambda_2\{[\lambda_2(1-4\lambda_3\lambda_4 s^2h_o^2)-1]q_4 - 2\lambda_3 sh_o q_3\} \quad ,$$

$$q_{44} = q_2(q_5+\lambda_2 q_{29}) \quad . \qquad \text{(B.4)}$$

The expressions for the functions $K_{ij}(x_i,t,s)$, $(i,j=1,2)$ which appear in Eq. (2.33) are

$$\pi K_{11}(x_i,t,s) = \sum_{k=1}^{4} N_{1k}(s,t)[(a_{ik}+2c_{ik})\cosh(x_i s) + c_{ik} s x_i \sinh(x_i s)]e^{-sh_i} \quad ,$$

$$\pi K_{12}(x_i,t,s) = \sum_{k=1}^{4} N_{2k}(s,t)[(b_{ik}+2d_{ik})\cosh(x_i s) + d_{ik} s x_i \sinh(x_i s)]e^{-sh_i} \quad ,$$

$$(i=1,2) \quad . \qquad \text{(B.5)}$$

APPENDIX C

Derivation of the stress intensity factors defined by Eqs. (2.60) and (2.73) as:

$$k_a = \lim_{x_1 \to a} \sqrt{2(x_1-a)}\, \sigma_{1yy}(x_1,0) \quad , \quad a<h_1 \tag{2.60}$$

$$k_b = \lim_{x_2 \to b} \sqrt{2(x_2-b)}\, \sigma_{2yy}(x_2,0) \quad , \quad b<h_2 \, . \tag{2.73}$$

From Eq. (2.31) we can write

$$\sigma_{jyy}(x_j,0) = \frac{4\mu_j}{1+\kappa_j} \frac{1}{\pi} \int_{-a_j}^{a_j} \frac{G_j(t)}{t-x_j}\, dt + \sigma_{jyyb}(x_j,0) \quad , \tag{C.1}$$

where $\sigma_{jyyb}(x_j,0)$, $(j=1,2)$ are the bounded parts of the cleavage stresses, $\sigma_{jyy}(x_j,0)$. Consider Eqs. (2.49) and (2.62):

$$G_j(t) = \frac{\phi_j(t)}{\sqrt{a_j^2-t^2}} = \frac{\phi_j(t)e^{i\pi/2}}{(t-a_j)^{1/2}(t+a_j)^{1/2}} \quad , \quad (j=1,2;a_1=a,a_2=b) \quad . \tag{C.2}$$

Define the sectionally holomorphic functions,

$$X_j(z) = \frac{1}{\pi} \int_{-a_j}^{a_j} \frac{G_j(t)}{t-z}\, dt \quad , \quad (j=1,2) \quad . \tag{C.3}$$

Following Muskhelishvili [12, Chapter 4] and using Eq. (C.2) we obtain

$$X_j(z) = \frac{\phi_j(-a_j)e^{i\pi/2}}{\sqrt{2a_j}\,\sqrt{z+a_j}} - \frac{\phi_j(a_j)}{\sqrt{2a_j}\,\sqrt{z-a_j}} + X_{jo}(z) \tag{C.4}$$

and

$$X_j(x_j) = - \frac{\phi_j(a_j)}{\sqrt{2a_j}\,\sqrt{x_j - a_j}} + X_{j1}(x_j) \quad , \quad (j=1,2) \qquad (C.5)$$

where $X_{jo}(z)$ and $X_{j1}(x_j)$ are bounded functions for $-a_j<x_j<a_j$. Now with Eqs. (C.1), (C.3), (C.5), Eqs. (2.60) and (2.73) become

$$k_a = - \frac{4\mu_1}{1+\kappa_1} \lim_{x_1 \to a} \frac{\phi_1(a)}{\sqrt{a}} \quad , \quad a<h_1$$

$$k_b = - \frac{4\mu_2}{1+\kappa_2} \lim_{x_2 \to b} \frac{\phi_2(b)}{\sqrt{b}} \quad , \quad b<h_2 \qquad (C.6a,b)$$

Using Eq. (C.?) we can rewrite Eqs. (C.6) as

$$k_a = - \frac{4\mu_1}{1+\kappa_1} \lim_{x_1 \to a} \sqrt{2(a-x_1)}\, G_1(x_1) \quad , \quad a<h_1$$

$$k_b = - \frac{4\mu_2}{1+\kappa_2} \lim_{x_2 \to b} \sqrt{2(b-x_2)}\, G_2(x_2) \quad , \quad b<h_2 \qquad (C.7a,b)$$

or with th: definitions (2.53) and (2.66)

$$k_a = - \sqrt{a}\, p_1\, \theta_1(1) \quad , \quad a<h_1$$

$$k_b = - \sqrt{b}\, p_2\, \theta_2(1) \quad , \quad b<h_2 \qquad (C.8a,b)$$

are obtained.

APPENDIX D

Expressions of the functions appearing in Eqs. (3.5) and (3.6):

$$F_{i1}(s) = \frac{2s}{\pi}\int_0^\infty m_i(r)[2s^2+\frac{\kappa_1-3}{2}(r^2+s^2)]\frac{\sin(h_1 r)}{(r^2+s^2)^2}\,dr\ ,$$

$$F_{i2}(s) = \frac{2s^2}{\pi}\int_0^\infty m_i(r)[2r^2+\frac{\kappa_1+1}{2}(r^2+s^2)]\frac{\cos(h_1 r)}{r(r^2+s^2)^2}\,dr\ ,$$

$$F_{i3}(s) = \frac{4s^2}{\pi}\int_0^\infty m_i(r) r\frac{\cos(h_1 r)}{(r^2+s^2)^2}\,dr\ , \qquad (D.1a\text{-}d)$$

$$F_{i4}(s) = \frac{4s}{\pi}\int_0^\infty m_i(r) r^2\frac{\sin(h_1 r)}{(r^2+s^2)^2}\,dr\ ,\quad (i=1,2)\ .$$

Functions a_{ij}, b_{ij}, c_{ij}, d_{ij}, $(i,j=1\text{-}4)$ used in Eqs. (3.6):

$$a_{31} = q_{34}/D_1\ ,\quad a_{32} = q_{35}/D_1\ ,$$

$$a_{33} = \lambda q_{29}/D_1\ ,\quad a_{34} = \lambda q_{25}/D_1\ ,$$

$$b_{3j} = a_{3j}\ ,\quad (j=1\text{-}4)\ ,$$

$$c_{31} = q_{32}/D_1\ ,\quad c_{32} = q_{33}/D_1\ ,$$

$$c_{33} = -\lambda q_{28}/D_1\ ,\quad c_{34} = -\lambda q_{24}/D_1\ ,$$

$$d_{3j} = c_{3j}\ ,\quad (j=1\text{-}4)\ ,$$

$$a_{41} = q_{36}/D_2\ ,\quad a_{42} = q_{37}/D_2\ ,$$

$$a_{43} = -\lambda q_{31}/D_2\ ,\quad a_{44} = -\lambda q_{27}/D_2\ ,$$

$$b_{4j} = -a_{4j} \quad , \quad (j=1\text{-}4) \quad ,$$

$$c_{41} = q_{38}/D_2 \quad , \quad c_{42} = q_{39}/D_2 \quad ,$$

$$c_{43} = \lambda q_{30}/D_2 \quad , \quad c_{44} = \lambda q_{26}/D_2 \quad ,$$

$$d_{4j} = -c_{4j} \quad , \quad (j=1\text{-}4) \quad ,$$

$$c_{11} = -(q_2 + q_{41}c_{31} + q_{42}a_{41})/q_{40} \quad ,$$

$$c_{12} = (q_1 - q_{41}c_{32} - q_{42}a_{42})/q_{40} \quad ,$$

$$c_{13} = -(\lambda q_1 + q_{41}c_{33} + q_{42}a_{43})/q_{40} \quad ,$$

$$c_{14} = -(\lambda q_2 + q_{41}c_{34} + q_{42}a_{44})/q_{40} \quad ,$$

$$d_{1j} = -(q_{41}d_{3j} + q_{42}b_{4j})/q_{40} \quad , \quad (j=1\text{-}4) \quad ,$$

$$a_{11} = q_{43}c_{11} + q_{44}c_{31} + q_{45}a_{41} \quad ,$$

$$a_{12} = q_{43}c_{12} + q_{44}c_{32} + q_{45}a_{42} + 1/(\lambda-1)q_2 \quad ,$$

$$a_{13} = q_{43}c_{13} + q_{44}c_{33} + q_{45}a_{43} - \lambda/(\lambda-1)q_2 \quad ,$$

$$a_{14} = q_{43}c_{14} + q_{44}c_{34} + q_{45}a_{44} \quad ,$$

$$b_{1j} = q_{43}d_{1j} + q_{44}c_{3j} - q_{45}a_{4j} \quad , \quad (j=1\text{-}4) \quad ,$$

$$a_{2j} = b_{1j} \quad , \quad (j=1\text{-}4) \quad ,$$

$$b_{2j} = a_{1j} \quad , \quad (j=1\text{-}4) \quad ,$$

$$c_{2j} = d_{1j} \quad , \quad (j=1\text{-}4) \quad ,$$

$$d_{2j} = c_{1j} \quad , \quad (j=1\text{-}4) \tag{D.2}$$

where

$$D_1 = 2(1-\lambda)[(1-\lambda)sh_3 e^{-2sh_3} + (1+\lambda\kappa_3)q_3q_4]q_{21}$$
$$+ (1+\kappa_1)\lambda[(\lambda-1)sh_3q_5e^{-2sh_3} - \kappa_3\lambda q_5q_7/2 - \kappa_3q_{11}^2/2 - q_9^2/2] \quad ,$$

$$D_2 = 2(\lambda-1)[(1-\lambda)sh_3 e^{-2sh_3} - (1+\lambda\kappa_3)q_3q_4]q_{21}$$
$$+ (1+\kappa_1)\lambda[(1-\lambda)sh_3q_5e^{-2sh_3} - \kappa_3\lambda q_5q_7/2 - \kappa_3q_{12}^2/2 - q_{10}^2/2] \quad , \tag{D.3}$$

$$q_1 = (1-e^{-2sh_1})/2 \quad , \quad q_2 = (1+e^{-2sh_1})/2 \quad ,$$

$$q_3 = (1-e^{-2sh_3})/2 \quad , \quad q_4 = (1+e^{-2sh_3})/2 \quad ,$$

$$q_5 = (1-e^{-4sh_1})/2 \quad , \quad q_6 = (1+e^{-4sh_1})/2 \quad ,$$

$$q_7 = (1-e^{-4sh_3})/2 \quad , \quad q_8 = (1+e^{-4sh_3})/2 \quad ,$$

$$q_9 = [1-e^{-2(h_1+h_3)s}]/2 \quad , \quad q_{10} = [1+e^{-2(h_1+h_3)s}]/2 \quad ,$$

$$q_{11} = (e^{-2sh_3} - e^{-2h_1s})/2 \quad , \quad q_{12} = [e^{-2h_1s} + e^{-2h_3s}]/2 \quad ,$$

$$q_{13} = -(1+\kappa_1)\lambda q_2/2 \quad , \quad q_{14} = (\lambda-1)q_4 \quad ,$$

$$q_{15} = (\lambda-1)sh_3q_3 + (1+\kappa_3)\lambda q_4/2 \quad ,$$

$$q_{16} = (1-\lambda)sh_3q_4 - (1+\kappa_3)\lambda q_3/2 \quad ,$$

$$q_{17} = (1-\lambda)q_3 \quad , \quad q_{18} = (1+\kappa_1)\lambda q_1/2 \quad ,$$

$$q_{19} = [1 - (1-\kappa_3)\lambda/2]q_3 + (1-\lambda)sh_3q_4 \quad ,$$

$$q_{20} = (\lambda-1)sh_3q_3 - [1 - (1-\kappa_3)\lambda/2]q_4 \ ,$$

$$q_{21} = sh_1e^{-2sh_1} - \kappa_1q_1q_2 \ ,$$

$$q_{22} = q_9/2 + sh_3q_{10} + \kappa_3q_{11}/2 \ ,$$

$$q_{23} = -sh_3q_9 - q_{10}/2 + \kappa_3q_{12}/2 \ ,$$

$$q_{24} = q_{14}q_{21} - q_9q_{13} \ , \quad q_{25} = q_{15}q_{21} - q_{13}q_{22} \ ,$$

$$q_{26} = q_{16}q_{21} - q_{13}q_{23} \ , \quad q_{27} = q_{17}q_{21} + q_{10}q_{13} \ ,$$

$$q_{28} = q_{17}q_{21} - q_9q_{18} \ , \quad q_{29} = q_{19}q_{21} - q_{18}q_{22} \ ,$$

$$q_{30} = q_{20}q_{21} - q_{18}q_{23} \ , \quad q_{31} = q_{14}q_{21} + q_{10}q_{18} \ ,$$

$$q_{32} = (1-\lambda)\lambda q_4q_{21} + (1+\kappa_1)\lambda(q_{11}-2\lambda q_1q_4)q_2/2 \ ,$$

$$q_{33} = (1-\lambda)\lambda q_3q_{21} - (1+\kappa_1)\lambda(q_{11}+2\lambda q_2q_3)q_1/2 \ ,$$

$$q_{34} = \lambda[(\lambda-1)sh_3q_3 + (1+\kappa_3)\lambda q_4/2]q_{21}$$
$$+ (1+\kappa_1)\lambda[(q_{12}+2\lambda q_1q_3)sh_3 + (1+\kappa_3)\lambda q_1q_4 + q_2q_3]q_2/2 \ ,$$

$$q_{35} = \lambda\{(\lambda-1)sh_3q_4 - [1-(1-\kappa_3)\lambda_2/2]q_3\}q_{21}$$
$$- (1+\kappa_1)\lambda[(q_{12}-2\lambda q_2q_4)sh_3 - (1-\kappa_3)\lambda q_2q_3 + q_2q_3]q_1 \ ,$$

$$q_{36} = \lambda(\lambda-1)q_3q_{21} + (1+\kappa_1)\lambda(q_{12}+2\lambda q_1q_3)q_2/2 \ ,$$

$$q_{37} = \lambda(\lambda-1)q_4q_{21} - (1+\kappa_1)\lambda(q_{12}-2\lambda q_2q_4)q_1/2 \ ,$$

$$q_{38} = \lambda[(1-\lambda)sh_3q_4 - (1+\kappa_3)\lambda q_3/2]q_{21}$$
$$+ (1+\kappa_1)\lambda[[q_{11}-2\lambda q_1q_4)sh_3 - (1+\kappa_3)\lambda q_1q_3 - q_2q_4]q_2/2 \ ,$$

$$q_{39} = \lambda\{(1-\lambda)sh_3q_3 + [1-(1-\kappa_3)\lambda/2]q_4\}q_{21}$$

$$+ (1+\kappa_1)\lambda[-(q_{11}+2\lambda q_2q_3)sh_3 - (1-\kappa_3)\lambda q_2q_4+q_2q_4]q_1/2 \ ,$$

$$q_{40} = (1-\lambda)sh_1e^{-2sh_1}-(\lambda+\kappa_1)q_1q_2 \ ,$$

$$q_{41} = (1+\kappa_3)q_{11}/2 \ , \quad q_{42} = (1+\kappa_3)q_{12}/2 \ ,$$

$$q_{43} = -sh_1\tanh(sh_1) + (1+\kappa_1)/2(\lambda-1) \ ,$$

$$q_{44} = -(1+\kappa_3)q_4/2(\lambda-1)q_2 \ ,$$

$$q_{45} = (1+\kappa_3)q_3/2(\lambda-1)q_2 \ . \qquad (D.4)$$

The functions $K_{ij}(x_i,t,s)$, $(i,j=1,2)$ appearing in Eq. (3.10):

$$\pi K_{i1}(x_i,t,s) = \sum_{k=1}^{4} N_{1k}(s,t)[(a_{ik}+2c_{ik})\cosh(x_is) + c_{ik}sx_i\sinh(x_is)]e^{-sh_1} \ ,$$

$$\pi K_{i2}(x_i,t,s) = \sum_{k=1}^{4} N_{1k}(s,t)[(b_{ik}+2d_{ik})\cosh(x_is) + d_{ik}sx_i\sinh(x_is)]e^{-sh_1} \ ,$$

$$(i=1,2) \ . \qquad (D.5)$$

APPENDIX E

Derivation of the stress intensity factor for $a=h_1$, $b=0$ in section 3.4.3:

Define

$$k_a = \lim_{x_3 \to -h_3} \sqrt{2}\,(x_3+h_3)^{\gamma}\sigma_{3yy}(x_3,0) \quad , \quad a=h_1 \quad . \tag{3.40}$$

From Eq. (3.47a) we can write

$$\sigma_{3yy}(x_3,0) = \frac{4\mu_3}{\kappa_1+1}\frac{1}{\pi}\int_{-h_1}^{h_1} k_{31s}(x_3,t)G_1(t)dt + \sigma_{30b}(x_3) \quad , \tag{E.1}$$

for $a=h_1$ where $\sigma_{30b}(x_3)$ is bounded and

$$k_{31s}(x_3,t) = \int_0^{\infty} K_{31s}(x_3,t,s)e^{-s(h_1-t)}ds \quad , \tag{E.2}$$

in which

$$K_{31s}(x_3,t,s) = \lim_{s\to\infty} K_{31}(x_3,t,s) \quad . \tag{E.3}$$

From Eq. (3.49) by using Eqs. (2.27) and (D.2)

$$K_{31s}(x_3,t,s) = -\frac{\lambda}{2}(\kappa_1+1)\left[\frac{1-2(h_1-t)s}{\lambda+\kappa_1} + \frac{3-2(h_3+x_3)s}{1+\lambda\kappa_3}\right]e^{-s(h_3+x_3)} \tag{E.4}$$

can be written with which (E.2) gives

$$k_{31s}(x_3,t) = -\frac{\lambda}{2}(\kappa_1+1)\left[Q_5(h_3+x_3)\frac{d}{dx_3}+Q_6\right]\left[t-(h_1+h_3+x_3)\right]^{-1} \tag{E.5}$$

where

$$Q_5 = 2[(\lambda+\kappa_1)^{-1} - (1+\lambda\kappa_3)^{-1}] \ ,$$

$$Q_6 = [(\lambda+\kappa_1)^{-1} - 3(1+\lambda\kappa_3)^{-1}] \ . \qquad \text{(E.6)}$$

Substituting (E.5) into (E.1) we obtain

$$\sigma_{3yy}(x_3,0) = -2\mu_1 \frac{1}{\pi} \int_{h_1}^{h_1} [Q_5(h_3+x_3) \frac{d}{dx_3} + Q_6][t-(h_1+h_3+x_3)]^{-1} G(t)dt + \sigma_{30b}(x_3) \ . \qquad \text{(E.7)}$$

The integral in the last expression can be evaluated by following the procedure followed in section 3.4.2. Hence one can get

$$\sigma_{3yy}(x_3,0) = -2Q_4 \frac{\phi_1(h_1)}{(2h_1)^\gamma} \frac{1}{(h_3+x_3)^\gamma} + \sigma_{31b}(x_3) \ , \qquad \text{(E.8)}$$

where

$$Q_4 = \mu_1(Q_5\gamma - Q_6)/\sin\pi\gamma \qquad \text{(E.9)}$$

and $\sigma_{31b}(x_3)$ is again bounded.

Now substituting (E.8) into Eq. (3.40)

$$k_a = -2Q_4 \sqrt{2} \frac{\phi_1(h_1)}{(2h_1)^\gamma} \ ,$$

$$= -2Q_4 \lim_{x_1 \to h_1} \sqrt{2} \ (h_1-x_1)^\gamma G_1(x_1)$$

$$= -Q_3(h_1)^\gamma p_1 \theta_1(1) \qquad \text{(E.10)}$$

is obtained. Here

$$Q_3 = Q_4(2)^{-(\gamma+.5)(\kappa_1+1)/\mu_1} \quad . \tag{E.11}$$